8-2022

Just Around the Corner: The Impact of Instruction Method and Corner Geometry on Teleoperation of Virtual Unmanned Ground Vehicles

Hannah Solini
Clemson University, hsolini@g.clemson.edu

JUST AROUND THE CORNER: THE IMPACT OF INSTRUCTION METHOD AND CORNER GEOMETRY ON TELEOPERATION OF VIRTUAL UNMANNED GROUND VEHICLES

A Dissertation
Presented to
the Graduate School of
Clemson University

In Partial Fulfillment
of the Requirements for the Degree
Doctor of Philosophy
Human Factors Psychology

---

by
Hannah Solini
August 2022

Dr. Chris Pagano, committee chair
Dr. Rick Tyrrell
Dr. Patrick Rosopa
Dr. Sabarish Babu

ABSTRACT

Teleoperated robots have proven useful across various domains, as they can more readily search for survivors, survey collapsed and structurally unsound buildings, map out safe routes for rescue workers, and monitor rescue environments. A significant drawback of these robots is that they require the operator to perceive the environment indirectly. As such, camera angles, uneven terrain, lighting, and other environmental conditions can result in robots colliding with obstacles, getting stuck in rubble, and falling over (Casper & Murphy, 2003). To better understand how operators remotely perceive and navigate unmanned ground vehicles, the present work investigated operators' abilities to negotiate corners of varying widths. In Experiment 1, we evaluated how instruction method impacts cornering time and collisions, looking specifically at the speed-accuracy tradeoff for negotiating corners. Participants navigated a virtual vehicle around corners under the instruction to focus on accuracy (i.e., avoiding collisions) or speed (i.e., negotiating the corners as quickly as possible). We found that as the task became more difficult, subjects' cornering times increased, and their probability of successful cornering decreased. We also demonstrated that the Fitts' law speed-accuracy tradeoff could be extended to a cornering task. In Experiment 2, we challenged two of the assumptions of Pastel et al.'s (2007) cornering law and assessed how corner angle and differences in path widths impacted cornering time. Participants navigated a virtual vehicle around corners of varying angles (45°, 90°, and 135°) and varying path widths. We found that increases in corner angle resulted in increased cornering times and a decreased probability of successful cornering. The findings from these experiments are applicable to contexts

where an individual is tasked with remotely navigating around corners (e.g., video gaming, USAR, surveillance, military operations, training).

ACKNOWLEDGEMENTS

This dissertation would not have been successful without the time, effort, and guidance of many individuals. I would like to extend my sincerest gratitude to my family, friends, and colleagues who have supported me these last five years.

I would like to thank my advisor, Dr. Chris Pagano. Thank you for creating a fun and supportive learning environment, for giving me the freedom to pursue what I wanted, and for sharing your expertise and guidance at every obstacle I encountered. I have learned so much from you and have truly enjoyed being in your lab. I would also like to express my gratitude to each of my committee members: Dr. Rick Tyrrell, Dr. Patrick Rosopa, and Dr. Sabarish Babu. Thank you for encouraging me to think critically and for providing your thoughtful feedback on this work.

I would like to thank Aaron Gluck, who developed the virtual environments for both experiments. Thank you for sharing your time and ideas and for producing high-quality work in a limited time frame. I am so grateful we could work together on this project. I would also like to acknowledge Soline McGee, Connor Margraf, Alyxandria Cicchinelli, and Hannah Levin for their assistance with piloting and data collection.

Lastly, I would like to thank my past and present lab members who have helped me grow as a researcher and as a person. To Leah Hartman and Bala Raveendranath: thank you for always listening to me and supporting me in all my research endeavors. To Katie Lucaites, my good friend and colleague: thank you for always making me feel welcome and for guiding me through the difficult times. My graduate school experience would not have been the same without you.

Table of Contents

Page

Title Page i

Abstract ii

Acknowledgements iv

List of Tables viii

List of Figures x

List of Equations xiii

CHAPTER

I. Introduction **1**
- Direct Perception 2
- Remote Perception 3
  - Affordance Perception 5
  - Adaptation and Learning 7
- Navigating Around Corners 8
  - Cornering Law Assumptions 13
- Purpose 15

II. Experiment I **17**
- Hypotheses 17
- Method 18
  - Experimental Design 18
  - Participants 21
  - Apparatus 22
  - Procedure 25
- Results 26
  - Cornering Time 27
    - Analysis Preparation 27
    - Mixed Effects Modeling 27

Turn Type....30
Block Order....31
Calibration....33
Number of Collisions....36
Collision Count....36
Distribution....36
Logistic Regression....36
Success Rate....38
Video Gaming Experience....39
Collision Information....41
Workload....42
Effective Index of Difficulty....45
Calculations....45
Analysis....46
Cornering Law....48
Discussion....49

III. Experiment II....58
Hypotheses....58
Method....59
Experimental Design....59
Participants....61
Apparatus....62
Procedure....63
Results....64
Cornering Time....64
Analysis Preparation....64
Mixed Effects Modeling....65
Turn Type....74
Block Order....75
Number of Collisions....77
Collision Count....77
Distribution....78
Logistic Regression....78
Success Rate....83
Video Gaming Experience....85
Collision Information....87
Workload....88
Cornering Law....91
Adapted Index of Difficulty....93
Discussion....97

IV. General Discussion 105
Contributions 106
Teleoperation Design Recommendations 108
Future Research 109
Conclusion 111

Appendices 113
A. Rating Scale Definitions for NASA-TLX 113
B. NASA-TLX Scale 114
C. Post-Experiment Questions 115
D. Virtual Driving Courses 116

References 117

LIST OF TABLES

Table Page

1. ID_C Values for Experiment 1 20

2. ID_C Values in Previous Cornering Studies 20

3. Mixed Effects Linear Regression Output Predicting Log-transformed Cornering Times 28

4. Cornering Time by Block Order and Instruction Method 32

5. Logistic Regression Output Predicting Cornering Success in Experiment 1 38

6. Video Gaming Experience for Experiment 1 Subjects 40

7. Descriptive Statistics for Collision Durations by Turn Type and Instruction Method 41

8. Number of Collisions on the Vehicle and the Corner in Experiment 1 42

9. Post-hoc Significance Tests for NASA-TLX Scales in Experiment 1 44

10. Vehicle Widths, Oncoming Oath Widths, and Current Path Widths for each ID_C Value 60

11. Omnibus F Test Results for the Model Predicting Log-transformed Cornering Times in Experiment 2 66

12. Descriptive Statistics for Cornering Times by Path Ratio and Corner Angle 66

13. Average Cornering Times by Block Order for Experiment 2 75

14. Logistic Regression Output Predicting Cornering Success in Experiment 2 79

15. Odds Ratios for each Path Ratio by Corner Angle 82

16. Odds Ratios for each Corner Angle by Path Ratio 83

17. Video Gaming Experience for Experiment 2 Subjects 86

18. Descriptive Statistics for Collision Durations by Turn Type and Corner Angle 88

19. Number of Collisions on the Vehicle and the Corner in Experiment 2 88

20. Post-hoc Significance Tests for NASA-TLX Scales in Experiment 2 91

21. Teleoperation Design Recommendations 109

LIST OF FIGURES

Figure Page

1. Corner Amplitude Depiction 11

2. Path Ratio Depictions 16

3. Wall Collision Locations 21

4. Practice Area for Experiment 1 23

5. Side Profile of the Virtual Vehicle (left), and the User's Perspective (right) 23

6. Example Driving Course Map 24

7. The Xbox One Controller 25

8. Estimated Cornering Time by Corner Amplitude 29

9. Estimated Cornering Time by ID_C Value and Instruction Method 30

10. Average Cornering Time by ID_C Value, Turn Type, and Instruction Method 31

11. Estimated Cornering Time by ID_C Value, Instruction Method, and Block Order 33

12. Median Cornering Time (top) and Median Collision Count (bottom) for the Accuracy Condition 34

13. Median Cornering Time (top) and Median Collision Count (bottom) for the Speed Condition 35

14. Insignificant Interaction Between ID_C Value and Instruction Method 38

15. Percentage of Successful Trials for Experiment 1 39

16. Average NASA-TLX Values by ID_C Value 44

17. Corner Definitions 46

18. Average Movement Times by Instruction Method and ID_e Value 47

19. Average Movement Times by ID_e fit to a First Order Regression Model (left) and a Second Order Regression Model (right) 47

20. Average Throughput by ID_e Value 48

21. Average Cornering Time by ID_C fit to a First Order Regression Model (left) and a Second Order Regression Model (right) in Experiment 1 49

22. Cornering Time and Collision Count by ID_C Value and Instruction Method 52

23. Corner Angles used in Experiment 2 60

24. Practice Area (left) and Virtual Vehicle Used (right) in Experiment 2 63

25. Camera Perspectives by Corner Angle 63

26. Cornering Time by ID_C Value in Experiment 2 67

27. Average Cornering Times by Corner Angle and Path Ratio 68

28. Estimated Cornering Time by ID_C Value and Corner Angle 70

29. Estimated Cornering Time by ID_C Value and Path Ratio 70

30. Estimated Cornering Time for each Corner Angle by ID_C Value and Path Ratio 72

31. Estimated Cornering Time for each Path Ratio by ID_C Value and Corner Angle 73

32. Average Cornering Times by ID_C Value, Corner Angle, and Turn Type 74

33. Average Cornering Times by Corner Angle and Block Order 76

32. Estimated Cornering Times by Block Order 77

35. Predicted Probability of Cornering Success by Corner Angle 80

36. Predicted Probability of Cornering Success by Path Ratio 81

37. Percentage of Successful Trials in Experiment 2 84

38. Average Collision Count by ID_C Value and Corner Angle 84

39. Estimated Cornering Time by ID_C Value and Gaming Experience in Experiment 2 86

40. Predicted Probability of Successful Cornering by Video Gaming Experience 87

41. Average NAS-TLX Values by Corner Angle 90

42. Average Cornering Time by ID_C fit to a First Order Regression Model (left) and a Second Order Regression Model (right) in Experiment 2 92

43. Average Cornering Time by ID_C and Corner Angle fit to a First Order Regression Model (left) and a Second Order Regression Model (right) 93

44. Average Cornering Time by Adapted ID_C Value 96

45. Average Cornering Time by Adapted ID_C Value fit to a Second Order Regression Model 96

46. Cornering Time and Collision Count by ID_C Value and Corner Angle 101

LIST OF EQUATIONS

Equation Page

1. Cornering Law 9

2. Index of Difficulty Based on the Limiting Case 9

3. Index of Difficulty Based on Information Theory 10

4. Index of Difficulty Incorporating Amplitude 11

5. Effective Index of Difficulty 11

6. Throughput 12

7. Path Ratio 15

8. Logistic Regression 37

9. Adapted Index of Difficulty 94

10. Effective Amplitude 94

11. Weighted Track Clearance 94

13. Adapted Index of Difficulty Based on Information Theory 95

CHAPTER I

INTRODUCTION

The use of teleoperated and autonomous robots has seen an increase in recent years. This is largely because the application of these vehicles spans across a variety of domains, such as surveillance (Di Paola et al., 2010; Milella et al., 2008; Rahmaniar & Wicaksono, 2020), inspection (Bengel et al., 2009; Katrasnik et al., 2010), space exploration (Ambrose et al., 2000; Bouloubasis et al., 2007; Gao & Chien, 2017), site maintenance (Luk et al., 2005; Sabater et al., 2006), and urban search and rescue (USAR; Casper et al., 2000; Casper & Murphy, 2003; Murphy, 2004; Shah & Choset, 2004). There are two primary purposes for these professional service robots. The first of which is to remove a human from harm's way. Rescue workers are subject to the emotional demands of working in life and death situations (Murphy, 2004; Shah & Choset, 2004). They are also likely to sustain cuts, burns, broken bones, and respiratory illnesses (Shah & Choset, 2004). The second purpose of a professional service robot is to navigate tight spaces that are impossible for humans and dogs. Teleoperated robots can more readily access voids in remaining building structures, making them suitable to search for remaining survivors, survey collapsed or structurally unsound buildings, map out safe routes for rescue workers, and monitor rescue environments.

Despite that teleoperated robots are relatively easy to replace and inexpensive compared to their human counterparts, remote perception (i.e., perceiving an environment indirectly) comes at a cost. For example, at the World Trade Center, camera angles, uneven terrain, lighting, and other environmental conditions made it difficult for

operators to perceive robot affordances. These issues ultimately resulted in robots colliding with obstacles, getting stuck in rubble, and falling over (Casper & Murphy, 2003). The present work aims to further explore how remote perception impacts operators' abilities to navigate unmanned ground vehicles (UGV) around corners of varying widths. In the following sections, we review in greater detail some of the factors that influence the successful teleoperation of UGVs, with a specific focus on navigating around corners.

Direct Perception

Before understanding how an operator remotely navigates a robot, it is first essential to understand navigation under normal circumstances (e.g., a human walking through a stable environment). This will allow us to highlight where remote perception can fail the operator.

James J. Gibson, an influential perception researcher, is often regarded as the father of the ecological approach to perception. The ecological approach considers the animal and environment as a mutual system where units of measurement and action are scaled intrinsically, according to the dimensions of the animal (Gibson, 1979). Under the ecological approach to perception, "…the animal has direct knowledge of, and a relationship to, its environment through ecological laws" (Duchon & Warren, 1994, p. 2272). In other words, no mental representation of the world is needed for control of movement and regulation of behavior; animals are capable of leveraging the information available in the global optic array to regulate their actions online (Blau & Wagman, 2022; Gibson, 1958; Warren, 1988). In a stationary environment, transformations in optic flow

patterns are revealed when an animal engages in self-produced motions (e.g., head bobbing, locomoting). This not only allows the animal to obtain information about the mapping of their environment but also to obtain information about their rate of self-motion and heading direction within that environment (Gibson, 1958).

That animals utilize direct perception for navigation and obstacle avoidance has been well-documented in the literature (Blau & Wagman, in press). For example, Lee and Reddish (1981) found that gannets' streamlining behavior was based on the optical parameter tau (see Lee et al., 2009) instead of strategies based on constant velocity, time-from-start, or height-from-start. There is also some research to suggest that humans utilize tau as opposed to first-order information like velocity and distance to engage in behaviors that require temporal prediction (e.g., Lee, 1976; but see, Tresilian, 1999). In addition, Srinivasan et al. (1991) showed that bees are sensitive to angular velocity and apparent motion, which allows them to fly through gaps and navigate around obstacles. This finding has also been documented in humans, who engage in optic flow equalization behavior (e.g., walking through the center of tunnels; Duchon & Warren, 2002; Lucaites, 2021). An individual's ability to perceive transformations in the global optic array, therefore, is crucial to navigation and collision avoidance in their environments (see Fajen & Warren, 2003).

Remote Perception

As previously mentioned, the ecological approach to perception maintains that humans are able to directly perceive transformations in the global optic array. How, then, is the human-environment interaction affected by the introduction of a robot?

Robots, in general, exhibit varying levels of autonomy (see e.g., Beer et al., 2014). Teleoperated robots, however, are classified as the lowest level of human-robot interaction because the robot is fully dependent on the operator for its movements (Bruemmer et al., 2005; Marble et al., 2003). This type of operation has historically been classified as a master-slave system (Milgram et al., 1995; Sanders, 2009; Thrun, 2004), but we refer to it here as a leader-follower system. In this type of system, the follower (e.g., the robot) mimics the movements of the leader (e.g., the human). In the case of teleoperation, the leader might be a joystick or controller that is then operated by a human (Dede & Tosunoglu, 2006; Moore et al., 2009). This leader-follower system is also commonly seen in the medical field for performing surgeries (e.g., Low & Phee, 2006; Shin et al., 2017). The design of a leader-follower system requires an "indirect interaction" (Thrun, 2004) with the environment, and this interaction necessitates that, "…the human perceptual processor is decoupled from the environment being explored" (Tittle et al., 2002, p. 261). Thus, the agent-environment system becomes an agent-console-robot-environment system (ACRE; Mantel et al., 2012). Therefore, in a teleoperation context, an operator's interaction with the environment depends on characteristics of the robot (e.g., mobility, camera angle, camera height), characteristics of the interface (e.g., screen resolution, screen size) through which the interaction occurs, and characteristics of the input device (e.g., joystick, pointer, controller). All these characteristics contribute to an operator's ability to perceive the remote environment veridically and navigate successfully.

Currently, there exists an overwhelming amount of research documenting poor performance when estimating distances, sizes, speeds, and impending collisions via virtual environments such as large screen displays, monitors, and head mounted displays (e.g., Banton et al., 2005; Geuss et al., 2012; Loomis & Knapp, 2003; Sahm et al., 2005; Solini & Andre, 2020; Thompson et al., 2004; Witmer & Kline, 1998; Witmer & Sadowski, 1998). The exact cause of this discrepancy between real and virtual environments is unclear; however, researchers contend that inaccurate performance in this context is likely due to a combination of factors including a lack of realism (Interrante et al., 2006), limited lamellar flow (Banton et al., 2005), and restricted field of view (Witmer & Sadowski, 1998). Ultimately, viewing a remote environment via video feed requires that the individual rely on monocular information (e.g., relative size, linear perspective) to scale the environment (Milgram et al., 1995). This lack of binocular information combined with poor image quality and poor camera angles can make it difficult for operators to perceive transformations in the global optic array, and thus, can result in deleterious effects on teleoperation performance.

Affordance Perception

One way in which teleoperation performance is impacted by the limitations of viewing environments remotely is an increased difficulty in perception of robot affordances. Several researchers have shown that in teleoperation conditions, operators were unable to accurately judge whether robots could pass through apertures (Casper & Murphy, 2003; Moore et al., 2009). For example, Moore et al. (2009) investigated how camera height and distance from an aperture influenced judgments of aperture passability

for robots in both teleoperation and direct line of sight conditions. They found that subjects made less accurate judgments in the teleoperation condition, such that they often judged apertures as passable, when they were too small for the robot to pass. Furthermore, they found that judgments of aperture passability were influenced by camera location and viewing distance. Specifically, they showed that judgments were less accurate when viewing the aperture from farther away and when the camera was located closest to the ground. That judgments of aperture passability improved when the camera was located higher off the ground is consistent with the ecological approach's view that organisms rely on eye-height information to appropriately scale environments.

In a similar experiment, Jones et al. (2011) found that subjects struggled to navigate robots through passable apertures without colliding with those apertures. That is, although it was possible for the robot to fit through the aperture, subjects did not always have to skills to navigate through the aperture without colliding with it. Thus, the passability of apertures not only depends on the dimensions of the robot passing through the aperture, but also the capabilities of the operator to navigate the robot. Additionally, research suggests that poor teleoperation performance can be exacerbated by the operator's workload and spatial relations ability (Chen et al., 2007; Long et al., 2011). In USAR, for example, operators are frequently tasked with both navigating the robot and identifying survivors, which is cognitively demanding (Murphy, 2004). Over time, the operator can exhibit cognitive fatigue and cognitive tunneling, which are worsened by technological limitations (e.g., inadequate video feed, time delays) and high stress environments (Chen et al., 2007; Murphy, 2004; Thomas & Wickens, 2001).

Environmental factors play an important role as well, as camera views can be obstructed by objects in the environment and precipitation (Tittle et al., 2002), making the operator's task increasingly difficult.

Adaptation & Learning

Because teleoperation extends the physical and perceptual capabilities of the operator, it can be considered tool use (Shaw et al., 1995). Consistent with the previous literature on tool use (e.g., Day et al., 2017), this means that despite technological limitations and environmental conditions, operators' performance can improve. For example, in a reanalysis of Jones et al.'s (2011) data, Schmidlin and Jones (2016) showed that operators exhibit learning over time. That is, subjects' judgments of robot passability improved throughout the experiment. Similarly, Helton et al. (2014) found that over the course of the experiment, subjects' cornering times and number of collisions decreased. These findings suggest that providing the opportunity for exploration and interaction with the robot can result in an improvement in performance over time (Armstrong et al., 2014, 2015). Again, this is consistent with the ecological approach's view that, through exploration, observers can learn to attune to the information that best specifies an object's property (Fajen, 2007; Gibson, 1969; Gibson & Gibson, 1995; Withagen & Michaels, 2005), allowing the observer to scale their actions appropriately to realize affordances. Other research on improving distance perception in virtual environments and calibration to sensory perturbations also support this concept (Kelly et al., 2013, 2014; Solini et al., 2021).

In addition to exploration, depth perception can be improved by providing radial outflow information. As mentioned, an issue with teleoperation is that information is degraded and/or lost when viewing the environment remotely, making it difficult to perceive transformations in optic flow patterns. Consequently, operators often struggle with perceiving depth information. When perceiving the environment directly, an animal can engage in head bobbing motions to obtain information about depth (e.g., Bingham & Pagano, 1998). However, head bobbing motions will not help an operator who is viewing the environment through video feed. Instead, Gomer et al. (2009) showed that providing radial outflow information by moving the robot's camera back and forth, thus mimicking head bobbing, can result in an improvement in depth perception.

Navigating Around Corners

Navigating unknown or unsafe environments is one of the main uses of teleoperated robots. In many instances, these environments require that the operator navigate around different corners. Navigating a robot around physical corners (e.g., hallways inside a building) and artificial corners (e.g., obstacles) can be challenging because the dimensions of the corner may be unknown. Further, because colliding with a corner can damage the robot, cause the robot to fall over, damage the environment, create dust and debris, etc., it is important to understand how operators navigate around corners as well as the factors that play an important role in successful cornering. Some common metrics for quantifying performance when navigating an environment with corners include completion time, number of collisions, and cornering time. Here, completion time refers to the total time taken to navigate a course or driving circuit, whereas cornering

time refers to the time taken to round a given corner. Recently, researchers have shown that cornering time in teleoperation can be modeled using a cornering law (Cross et al., 2018; Helton et al., 2014; Pastel et al., 2007).

The cornering law is based on Fitts' law for predicting movement time, where the time to move a cursor to a designated target depends on an index of difficultly (ID). Under Fitts' law, the ID is based on two criteria: the distance to the target and the size of the target. Similarly, the cornering law utilizes an index of difficulty (ID_C) to predict cornering time (CT) such that,

$$CT = a + b * ID_C \quad (1)$$

where *a* and *b* are derived from the regression analysis and correspond to the intercept and slope, respectively. There are, however, different ways in which the ID_C can be quantified. For example, Pastel et al. (2007) derived the following equation for calculating the ID_C,

$$ID_{C1} = \frac{p}{(w-p)} \quad (2)$$

where *p* corresponds to the width of the robot and *w* corresponds to the width of the corner width. The corner width is defined as the width of the oncoming path. These two phrases will be used synonymously for the remainder of this manuscript. Equation 2 is based on the limiting case, meaning that the ID_C approaches infinity as the corner width and vehicle width become equal (i.e., as the track clearance, *w*-*p*, becomes zero). Thus, corners comprised of the same corner width of the vehicle will be impossible to corner. It should be noted that the length of the vehicle is not considered but is assumed to be short enough to negotiate the corner successfully. In addition to the limiting case

equation, Pastel et al. (2007) also derived the mathematically similar equation for the ID_C based on information theory. This is calculated as,

$$ID_{C2} = log_2\left(\frac{w}{w-p}\right) \quad (3)$$

where *p* and *w* are defined as before. Equations 2 and 3 both produce a dimensionless ID_C that is intrinsically scaled; a corner that is 1.5 times the width of the vehicle will produce the same ID_C value regardless of the physical dimensions of the corner. To assess how well cornering time could be modeled by each ID_C proposed, Pastel et al. (2007) asked subjects to navigate a virtual hovercraft around 90° corners. When they modeled CT using both measures of ID_C, the results were nearly identical. Further, both models had coefficients of determination (R^2 values) that were greater than 0.85. Given its similarity to other indexes of difficulty, ID_C is frequently quantified using Equation 3.

It should be noted, however, that the cornering law necessitates that cornering times be averaged across each ID_C. That is, a single, average cornering time is computed for each ID_C value. Aggregating the data in this way allows for a better model fit but results in a loss of information about subject-to-subject variability as well as trial-by-trial variability. Furthermore, a limitation of the above measures of ID_C, as noted by Chan et al. (2019), is that they do not account for the amplitude of the corner. In a traditional Fitt's Law task, the amplitude is defined as the distance to the target; that is, how far away the target is located from the starting point. With respect to a cornering task, the amplitude would be measured as the distance from the start of the corner to the end of the corner, through the center of the current and oncoming paths (see Figure 1). A way of incorporating the amplitude of the corner is to define the ID_C as,

$$ID_{C3} = \frac{A}{(w-p)} \quad (4)$$

where *A* is the amplitude of the corner, and where *w* and *p* are defined as before.

Figure 1

Corner Amplitude Depiction

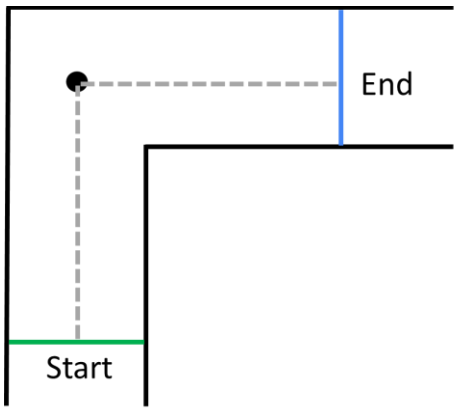

Note: The amplitude is the distance from the start point through the center of the corner to the end point, which is denoted by the gray dotted line. The start and end points are equidistant from the center of the corner, which is denoted by the black circle.

Lastly, a measure of task difficulty that incorporates subjects' movements is the effective index of difficulty (ID_e), calculated as,

$$ID_e = log_2\left(\frac{A_e}{4.133 * SD_x} + 1\right) \quad (5)$$

The A_e term corresponds to the average amplitude of movements over a sequence of trials; this is also referred to as the effective distance travelled. The SD_x term corresponds to the standard deviation of the subject's position relative to the target. In the context of a cornering task, we define the target as the center of the corner, as depicted in Figure 1. The benefit of utilizing the ID_e is that it quantifies the task each subject performed,

instead of the presented task (Brickler et al., 2020). Along with the index of difficulty measures, throughput is often quantified as a measure of task performance. Throughput (TP) is calculated as follows,

$$TP = \frac{ID_e}{MT} \tag{6}$$

where ID_e is the effective index of difficulty and MT is the average movement time over a sequence of trials.

Ultimately, the ID_C for negotiating corners is a measure of the cornering affordance, or corner-ability; it quantifies whether a corner is passable and how challenging that task is. In other passability domains, such as aperture passability, the affordance is quantified by body-scaled information such as the ratio of the aperture width relative to the human's shoulder width (e.g., Bhargava et al., 2020; Lucaites et al., 2020; Warren & Whang, 1987). Therefore, the ID_C might also be expressed as the ratio of the path width relative to the vehicle width, or, in more general terms, the ratio of the path width relative to the organism's width.

Since Pastel et al.'s (2007) original paper on the cornering law, there has been further research investigating the factors that influence cornering time. For example, Helton et al. (2014) investigated how camera view (bird's eye view vs. first-person view) impacted cornering time. They found that cornering time and the number of collisions was not significantly impacted by camera view. In addition, they showed that Pastel et al.'s (2007) cornering law sufficiently modeled cornering time for both camera views. In a related study, Cross et al. (2018) assessed the effects of lighting conditions and time delays on teleoperation in indoor and outdoor settings. In the outdoor driving circuit,

subjects completed time trials for either a simple or complex circuit. They found that driving speed was reduced when there was a time delay and when the lighting conditions were harsh (i.e., at nautical dusk with a single spotlight). It was also clear from their results that the cornering tasks (i.e., driving around obstacles) were the most challenging for subjects. In their second experiment, Cross et al. (2018) investigated cornering time. They found that mean cornering time increased as the ID_C increased and as the time delay increased. Anecdotally, they noted that under ambient and dark lighting conditions, subjects were more likely to collide with the inside of the corners, but in the spotlight condition, subjects were more likely to collide with the outside of the corner.

To further test the cornering law, Chan et al. (2019) explored how the geometry of the corner impacted cornering time. Across three different corner geometries they found that performance was similar. Track clearance (i.e., the difference between the corner width and the robot width) appeared to be the most important factor predicting cornering time. Importantly, Chan et al. (2019) highlighted that the number of collisions was positively correlated with movement time. However, they could not conclude whether increases in movement time were related to the track clearance or the control method used by the operator. Interestingly, Helton et al. (2014) found that there was not a strong correlation between the number of collisions and movement time. Disambiguating this relationship requires a look at different instruction methods (e.g., emphasizing speed vs. accuracy). Thus, the aim of Experiment 1 was to assess the speed-accuracy tradeoff in the context of navigating around corners.

Cornering Law Assumptions

In its current state, Pastel et al.'s (2007) index of difficulty holds several assumptions. A few of these assumptions are that (1) the negotiating corner is 90°, that (2) the current and oncoming path widths are equivalent, and that (3) the amplitude of the corner is irrelevant. Though these assumptions are not explicitly stated, the law itself was developed under these conditions, and additional research has failed to investigate how these factors might play a role in cornering time. In a user-interface study, however, Pastel (2006) showed that movement time depends on corner angle. In their experiment subjects negotiated corners of varying widths and angles using a cursor. It was found that movement time was greatest for 90° corners and smallest for sharp corners. Pastel (2006) suggested that the reason for the decrease in movement time for the sharp corners was because the subject could use their limb as a cantilever to engage in the cursor motion. Thus, the subject could engage in loaded and unloaded movements as they approached and exited the corners. The findings from Pastel's (2006) study imply that cornering time in a teleoperation context may not only be impacted by the vehicle width and corner width, but the corner angle as well. Notably, negotiating corners in a teleoperation context does not often depend on hand and arm motions. Rather, operators utilize a controller, keyboard, smartphone, or other input device to control the robot. As such, the differences in movement time for different corner angles in a teleoperation context will likely differ from those found by Pastel (2006).

Another assumption of the cornering law is that the path widths of the current path and the oncoming path are equivalent. In Pastel et al.'s (2007) original cornering law, corner width was defined as the width of the oncoming path. It is possible, however,

that in many real-world settings (e.g., driving, USAR) the path widths will not be equivalent. That is, the current path may be smaller or larger in width, relative to the oncoming path (see Figure 2). We denote this relationship as the path ratio, which is computed as follows

$$Path\ Ratio = \frac{w_1}{w_2} \tag{7}$$

where w_1 denotes the current path width and w_2 denotes the oncoming path width. Therefore, a path ratio less than 1.0 would indicate that the current path is narrower than the oncoming path; a path ratio greater than 1.0 would indicate that the current path is wider than the oncoming path; and a path ratio equal to 1.0 would indicate that the current and oncoming path widths are equivalent. Given the limited research on how corner geometry plays a role in negotiating corners, the aim of Experiment 2 was to test how cornering time is impacted by corner angle and the widths of the current and oncoming paths (i.e., the path ratio).

Purpose

The purpose of the present work was twofold. First, Experiment 1, will empirically evaluate how instruction method impacts cornering time and number of collisions, looking specifically at the speed-accuracy tradeoff for negotiating corners. Second, a thorough test of the cornering law will be conducted. Much of the previous literature has focused on how cornering time is impacted by a number of environmental conditions and technological limitations. However, researchers have yet to examine how well the cornering law holds for corners that are not 90° or for corners that have varying path widths. Experiment 2, therefore, examined corning time and number of collisions for

a variety of corner angles and path widths. Ultimately, the goal of the present work was to further understand how operators negotiate corners as a function of instruction method and corner angle.

Figure 2

Path Ratio Depictions

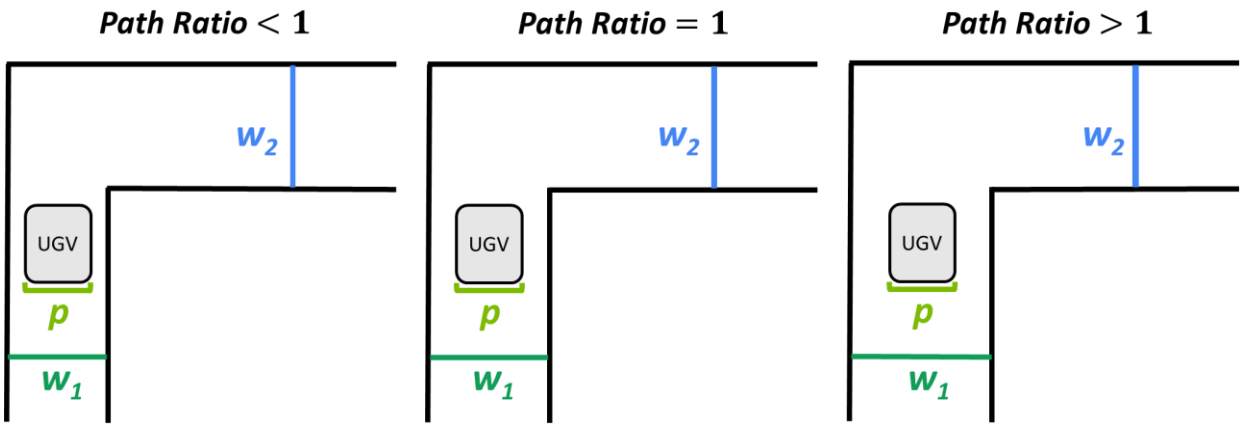

Note: This figure illustrates how the current path width (w_1) might be smaller than (left), equal to (middle), or larger than (right) the oncoming path width (w_2). UGV refers to the vehicle, with p defined as the vehicle's width. The path ratio is calculated from Equation 7.

CHAPTER II

METHOD

Experiment 1

The aim of Experiment 1 was to understand how performance on cornering tasks differed depending on instruction method. That is, we investigated the speed-accuracy tradeoff in the context of navigating around corners. In this experiment, subjects navigated a virtual vehicle through driving courses under two different instruction methods. In the accuracy condition, subjects were asked to navigate around the corners in the driving course as accurately as possible – being careful not to collide with any walls. In the speed condition, subjects were asked to navigate around the corners in the driving course as quickly as possible. In addition to navigating around corners under different instruction methods, we manipulated the ID_C of the corners. This allowed us to assess the speed-accuracy tradeoff as a function of ID_C value.

Hypotheses

Consistent with previous cornering research (e.g., Cross et al., 2018; Pastel et al., 2007), we hypothesized that cornering time and the number of collisions would increase as the ID_C value increased. That is, we expected subjects to have longer cornering times and more collisions as the cornering task became more difficult. We also expected there to be an effect of instruction method on cornering time and collision count. Consistent with prior findings on the speed-accuracy tradeoff (e.g., MacKenzie & Isokoski, 2008), we hypothesized that cornering time would increase when subjects focused on accuracy instead of speed. We also expected that the number of collisions would be greater when

subjects focused on speed instead of accuracy. While this may seem counterintuitive, we expected that collisions in the speed condition would not be detrimental to their cornering times. Thus, these subjects would have more collisions, but shorter cornering times compared to those subjects in the accuracy condition.

Method

Experimental Design

This experiment used a 2 (instruction method) by 3 (ID_C value) by 3 (amplitude) mixed model design. Instruction method was a between-subjects variable, such that half of the subjects completed trials where accuracy was emphasized, and half of the subjects completed trials where speed was emphasized. The ID_C was a repeated-measures variable. Subjects navigated through driving courses with corners of each ID_C value, with path widths that were 1.4, 1.8, and 2.2 times the width of the virtual vehicle. Thus, the ID_C values utilized for this experiment equated to 1.807, 1.17, and 0.874, respectively (see Table 1). These ID_C values were similar to those used in previous cornering studies (see Table 2). We also manipulated the amplitude of the corner, which has no effect on the ID_C value. The amplitude was defined as the distance of the straight-line path from the start of the corner to the end of the corner (see Figure 1). To manipulate the amplitude, we extended the start and end points, such that the amplitude of the corner was equivalent to 9, 12, and 15 times the width of the vehicle.

The main dependent variables in this experiment were cornering time and the number of collisions. Cornering time was calculated as the time in seconds taken to round each corner from when the nose of the vehicle entered the start of the corner until the

nose of the vehicle exited the corner. The number of collisions was calculated as the total number of times the vehicle collided with the walls as it was navigated around each corner. The vehicle had collider indicators, which were distributed across the front, sides, and back of the vehicle. Furthermore, the walls that comprised the corners had collider indicators that logged whether the collision occurred on the outside of the corner or the inside of the corner. Therefore, a collision was counted when any part of the vehicle collided with any wall. Additionally, collisions were logged into two groups: collisions before the turn and collisions after the turn. A collision was denoted as occurring before the turn when the vehicle collided with any wall on the current path, and a collision was denoted as occurring after the turn when the vehicle collided with any wall on the oncoming path (see Figure 3). We also collected data on the duration of each collision, which was defined as the time in seconds from when the vehicle initially made contact with a wall to when it seceded making contact with a wall. Lastly, each participant session was screen recorded.

To compute the effective index of difficulty, we collected data on the distance travelled between the straight-line paths and the deviations from the center targets. The center target was defined as the center of each of the corners. For each driving course, we obtained the distance travelled between the corner centers for the 13 straight-line paths that comprised the 14 corners. Additional detail on how these data were collected and calculated can be found in the Results section.

Table 1

IDc Values for Experiment 1

Vehicle Width (p)	Path Width (w)	$ID_C = \log_2(w/(w-p))$	Corner Amplitude
2.44 m	3.42 m	1.807	21.96 m 29.28 m 36.6 m
2.44 m	4.39 m	1.17	21.96 m 29.28 m 36.6 m
2.44 m	5.37 m	0.874	21.96 m 29.28 m 36.6 m

Table 2

ID_C Values in Previous Cornering Studies

Study	Vehicle Width (p)	Path Width (w)	$ID_C = \log_2(w/(w-p))$
Pastel et al. (2007)	192 uu	512 uu	0.68
		556 uu	0.61
		680 uu	0.48
		1,024 uu	0.3
		1,536 uu	0.19
		3,072 uu	0.09
Helton et al. (2014)	21 cm	31.5 cm	1.58
		35 cm	1.32
		38.5 cm	1.14
Cross et al. (2018)	67 cm	85 cm	2.24
		95 cm	1.76
		105 cm	1.47
		115 cm	1.26
Chan et al. (2019)	174 mm	280 mm	1.4
		300 mm	1.25
		320 mm	1.13
	194 mm	290 mm	1.6
		310 mm	1.42
		330 mm	1.28
	214 mm	300 mm	1.8
		320 mm	1.6
		340 mm	1.43

Note: “uu” denotes unreal units

Figure 3

Wall Collision Locations.

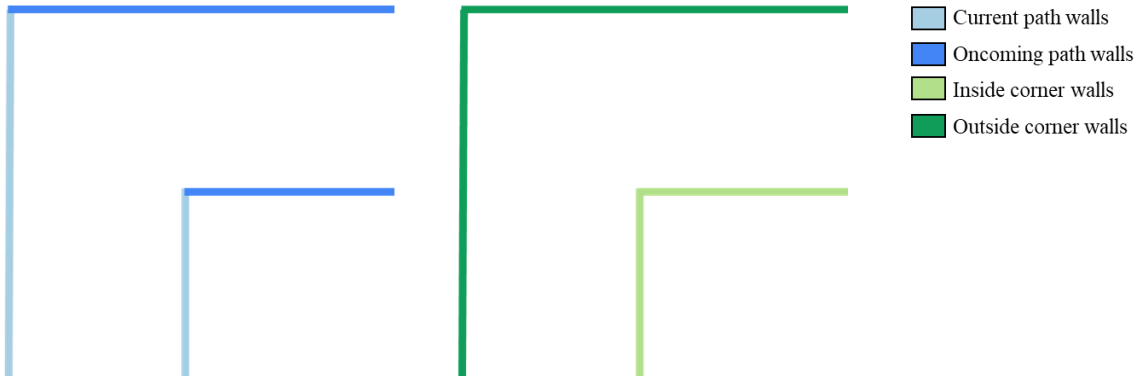

Participants

To determine the number of participants needed for this study, we utilized the "simr" package in R (Green & MacLeod, 2016). This involves using pilot data or generated data to estimate the approximate number of subjects and trials needed to obtain sufficient power. Because we did not have pilot data, we instead used the fitted model from Pastel et al.'s (2007) second experiment to generate approximate cornering times for the three values of ID_C we intended to utilize. These cornering times corresponded to the accuracy condition. To obtain approximate cornering times for the speed condition, we again used Pastel et al.'s (2007) fitted model to generate data, but reduced cornering times by 10%. In the simulation, we compared the full mixed effects model to a reduced model (i.e., a model without the interaction between ID_C and instruction method). Ultimately, we found that we needed 10 participants to complete at least 24 trials (i.e., round 24 corners) for each instruction method and index of difficulty to obtain power above .80. Thus, 20 participants total were needed: 10 for the accuracy condition, and 10

for the speed condition. The R code for the analysis process described above can be found here: https://osf.io/87krn/.

We recruited 22 Clemson University students (M_{age} = 20.91 years, SD_{age} = 2.11) with visual acuity of 20/25 or better. Subjects were recruited through Clemson University's Psychology SONA pool and through word of mouth, and they were compensated with partial course credit or with a $10 gift card.

Apparatus

The virtual environment was developed using Unity and consisted of a practice area and nine different driving courses (3 ID_C values x 3 amplitudes). The virtual environment was viewed on a 19-inch Dell monitor with a 1440x900 pixel display. The refresh rate was 60 Hz. The practice area was a 40 by 40-meter room with five pillars (see Figure 4). The pillars were included to encourage the participant to practice corner negotiation. The virtual vehicle used front wheel steering and was based on Unity's standard asset vehicle. It was 2.44 meters wide and 2.5 meters long, with a maximum speed of 10 miles per hour and a maximum steering angle of 40°. The camera was fixed just above virtual vehicle at 1.64 meters above the roadway. The camera was placed 1.38 meters from the front axle and 0.02 meters from the rear axle, which allowed the hood of the vehicle to be in view (see Figure 5). The camera had a field of view of 60° and was rotated downward 20°; the camera's viewpoint was not adjustable.

Figure 4

Practice Area for Experiment 1.

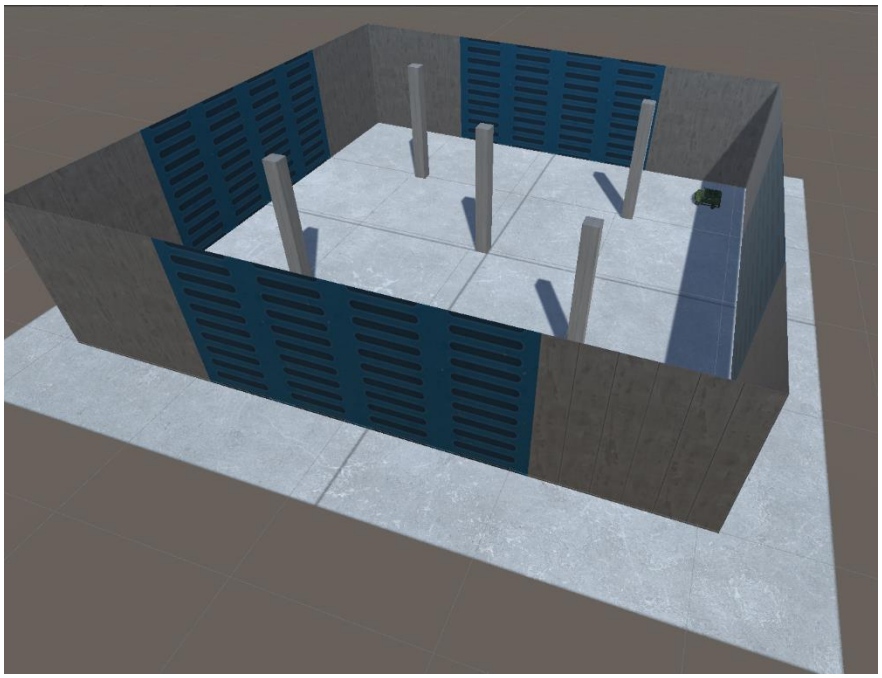

Figure 5

Side Profile of the Virtual Vehicle (left), and the User's Perspective (right).

Each virtual driving course consisted of a hallway with 14 corners of the same width. An example driving course map can be seen in Figure 6; the remaining driving

course maps used in the Experiment can be found in Appendix D. We chose to use 14 corners so that we could quantify the ID_e of the 13 straight line paths between the center of each corner and so that the number of left and right turns would be the same. The utilization of at least 12 trials in a sequence for calculating the ID_e is standard (Babu et al., 2020). The ID_C and the amplitude of the corners remained the same within each driving course but varied across driving courses. Subjects used a wired Xbox Controller to navigate the virtual vehicle within the virtual environment (see Figure 7). The left joystick was used for forward and backward movements (i.e., acceleration and deceleration), and the right joystick was used for leftward and rightward movements of the virtual vehicle. Therefore, simultaneously pressing the left joystick forward and the right joystick leftward would move the virtual vehicle forward and to the left (i.e., it would produce a left turn).

Figure 6

Example Driving Course Map

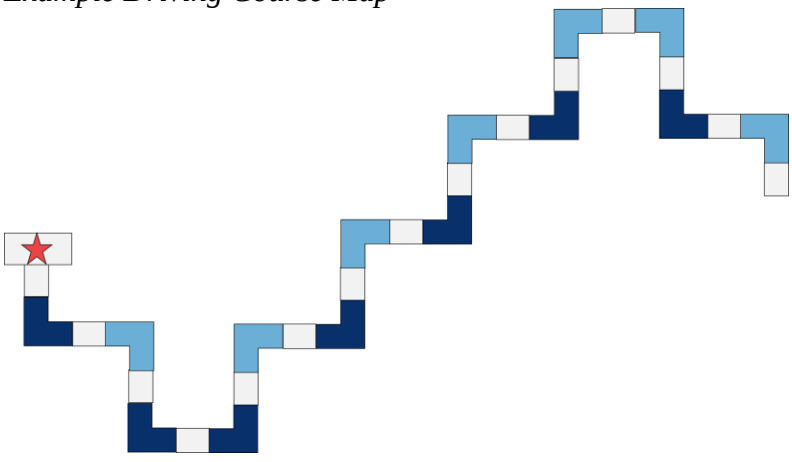

Note: Light blue corners correspond to left turns, and dark blue corners correspond to right turns. The star represents where the virtual alarm system was located.

Figure 7

The Xbox One Controller

Procedure

After signing the informed consent, participants completed a visual acuity test. The visual acuity test was conducted using a Snellen Eye Chart placed 10 feet away. Subjects completed the test with both eyes open. Following this, the experimental procedure began. The experiment consisted of a practice phase and three blocks of driving courses. To start, subjects completed the practice phase, where they were told to take some time to familiarize themselves with the controls of the virtual vehicle. Participants were then randomly assigned to either the accuracy condition or speed condition. In the accuracy condition, subjects received the following instructions, which were adapted from Helton et al. (2014):

> *You are working at a nuclear power plant. Your task is to navigate the vehicle through the building to get to the alarm system. Any collision, even a small one, can be serious and should be avoided. Generally, operations conducted with*

unmanned ground vehicles take place in unstable environments. Collisions can further destabilize the environment, which could damage the vehicle, injure a civilian, or prevent the recovery of both the vehicle and civilian. As such, even small collisions, can be dangerous and should be avoided at all costs.

In the speed condition, participants received the following instructions:

You are working at a nuclear power plant. The alarm system needs to be disabled immediately to avoid the power plant from shutting down. Your task is to navigate the vehicle through the building to get to the alarm system. Your only concern is to get to the alarm system as fast as possible.

In each condition, subjects navigated through a driving course with corners in a series of three blocks – one for each ID_C value. The vehicle was located at the center of the path at the start of each driving course. Within each block, subjects navigated around 42 corners (14 corners x 3 amplitudes). After each block, subjects completed the NASA-TLX (Hart & Staveland, 1988; see Appendices A-B). The presentation of blocks was randomized across participants using a Latin square design, and the three driving courses within each block were presented in a randomized order. Once the subject completed all three blocks, they answered questions about their age, gender, and experience playing video games (see Appendix C). They were debriefed and provided with contact information prior to leaving. Each session took approximately 45 minutes. In total, each subject navigated around 126 corners, which yielded a total of 2,772 observations across the 22 subjects.

Results

Cornering Time

Analysis Preparation. Prior to conducting any analysis, we visualized the distribution of the cornering time variable. Using the "moments" package in R (Komsta & Novomestky, 2015), we found that the cornering time variable had a skewness value of 4.53 and kurtosis value of 38, which indicated that the distribution was positively skewed and leptokurtic. We also extracted the residuals from a linear mixed effects model predicting cornering time to evaluate the errors. A Quantile-Quantile (QQ) plot revealed that the normality assumption was violated. To address this issue, we performed a logarithmic transformation of the cornering time variable. We then refit the linear mixed effects model and removed standardized residuals with values greater than +/- 3. Less than 2% of the data were removed as a result of this outlier analysis. After performing the log-transformation and outlier analysis, the residuals were more normally distributed.

Mixed Effects Modeling. We submitted ID_C, instruction method, and amplitude to a linear mixed effects model predicting the log-transformed cornering times. The amplitude and ID_C variables were mean-centered, and the accuracy condition was the reference category for the instruction method variable. A random effect of participant number was included in the model to account for nesting within participants. Results from the regression output can be found in Table 3. Because we performed a logarithmic transformation on the cornering time variable, the coefficients represent the change in log-transformed cornering times. For continuous variables, the coefficient has an additive effect on the log-transformed cornering times, where a one-unit increase in the predictor variable elicits a β value increase in log-transformed cornering times. For categorical

variables, the coefficient represents the difference in average log-transformed cornering times from the reference group. Exponentiating the coefficients provides the change in terms of the original cornering scale.

There is not currently an agreed upon best method for computing and reporting individual effect sizes for mixed effects and multilevel models, as there are multiple sources of variance (see Hofmann, 1997). Instead, we used the "MuMIn" package in R (Barton, 2009) to compute the marginal and conditional R^2 values, which represent the amount of variance explained by the fixed effects alone and the amount of variance explained by both the fixed effects and the random effect(s) in the model. We found that 57.4% of the variance in log-transformed cornering times could be accounted for by the fixed effects alone, and 68.3% of the variance could be accounted for by both the fixed effects and the random effect of participant number.

Table 3

Mixed Effects Linear Regression Output Predicting Log-transformed Cornering Times

Predictor	β (*SE*)	Exp(β)	*t*
ID_C	0.53 (0.01)	1.69	37.77***
Instruction Method	-0.15 (0.05)	0.86	-2.9**
Amplitude	0.03 (< 0.001)	1.03	49.65***
ID_C * Instruction Method	-0.17 (0.02)	0.85	-8.38***

Note: * denotes $p < .05$, ** denotes $p < .01$, *** denotes $p < .001$

As expected, ID_C was a significant predictor of log-transformed cornering time, such that cornering time increased as the ID_C increased. We also found that instruction method was a significant predictor of transformed cornering time; on average, cornering times were 18% greater in the accuracy condition (*M* = 8.52 seconds, *SD* = 3.7) compared to the speed condition (*M* = 7.22 seconds, *SD* = 2.65). There was also an effect of amplitude on transformed cornering time, with cornering time increasing as the amplitude increased (see Figure 8).

Figure 8

Estimated Cornering Time by Corner Amplitude. Gray shading around the lines indicates +/- 1 standard error

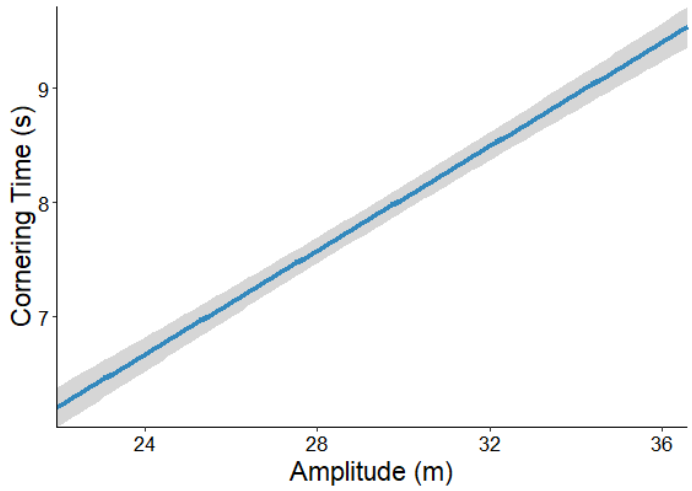

Lastly, there was a significant interaction between the ID_C and instruction method. The slope for the accuracy condition was significantly steeper than the slope for the speed condition, indicating that cornering times increased at a faster rate as the ID_C increased when subjects were told to focus on accuracy as compared to speed (see Figure

9). A simple slopes analysis revealed that the slopes for both lines were significantly different from zero (*p*s < .001).

Figure 9

Estimated Cornering Time by ID_C Value and Instruction Method. Gray shading around the lines indicates +/- 1 standard error

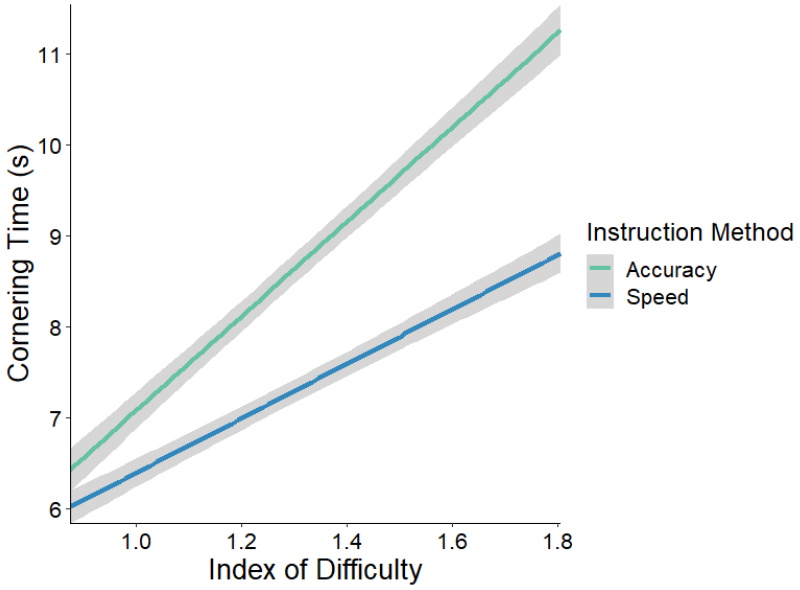

Turn Type. We also investigated whether there were differences in cornering time based on the turning direction (left vs. right). We split the data by instruction method and conducted two independent samples t-tests using the log-transformed cornering times. Results indicated that there was not a statistically significant difference in transformed cornering times depending on turn type for the accuracy condition, $t(1,362) = 1.83$, $p = .067$, nor for the speed condition, $t(1,360) = 1.83$, $p = .907$ (see Figure 10).

Figure 10

Average Cornering Times by ID_C Value, Turn Type, and Instruction Method. Error bars represent +/-1 standard error

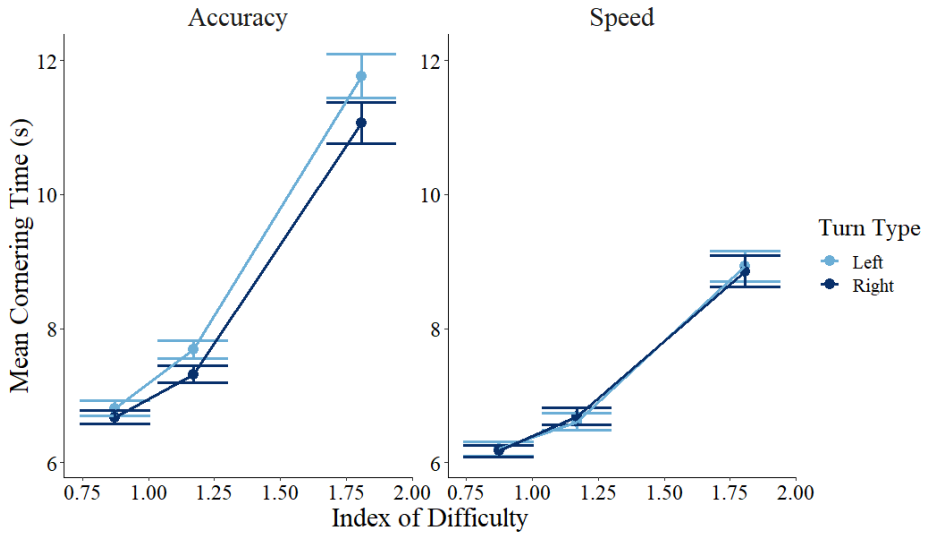

Block Order. We also assessed the extent to which the order of the blocks impacted performance. The order of presented ID_C values for each block number can be found in Table 4. We fit a mixed effects model predicted the log-transformed cornering times with block order, instruction method, and ID_C as independent variables. A random effect of participant number was included in the model.

There was an overall effect of order on the log-transformed cornering times, $F(2, 16) = 4.26$, $p = 0.033$. Post-hoc comparisons revealed that, on average, log-transformed cornering times were greater in block order three compared to block order one, $t(16) = 2.91$, $p = 0.26$. There was also a significant interaction between block order and ID_C, $F(2, 2{,}704) = 50.63$, $p < .001$. While the log-transformed cornering times increased as the ID_C value increased, we found that the slope for block order three ($\beta = 0.64$, $SE = 0.02$) was

significantly steeper than the slope for block order two (β = 0.42, *SE* = 0.02, *t*(2,704) = 6.44, *p* < .001) and for block order one (β = 0.32, *SE* = 0.02, *t*(2,704) = 9.97, *p* < .001). The slope for block order two was also significantly steeper than the slope for block order one, *t*(2,704) = 3.29, *p* = .003. A simple slopes analysis revealed that the slopes for each block order were all significantly different from zero, *p*s < .001.

Table 4

Cornering Time by Block Order and Instruction Method.

Instruction Method	Block Order	Order of ID_C values	*M* (*SD*)	Median	Maximum
Accuracy	1	0.874, 1.17, 1.807	7.62 (2.37)	7.5	21.32
	2	1.17, 1.807, 0.874	8.09 (3.16)	7.74	21.94
	3	1.807, 0.874, 1.17	10.4 (5.02)	8.26	26.66
Speed	1	0.874, 1.17, 1.807	7.01 (2.39)	6.3	20.5
	2	1.17, 1.807, 0.874	7.6 (2.85)	7.61	19.86
	3	1.807, 0.874, 1.17	7.15 (2.71)	6.34	23.66

There was also an interaction between block order and instruction method. Post-hoc comparisons revealed that for the accuracy condition, log-transformed cornering times were significantly greater in block order three compared to block order two, *t*(16) = 3.2, *p* = 0.15, and compared to block order one, *t*(16) = 3.74, *p* = .005. There were no other statistically significant differences.

Lastly, there was a statistically significant three-way interaction between block order, instruction method, and ID_C, *F*(2, 2,704) = 26.76, *p* < .001. For the accuracy condition, we found that the slope for block order three (β = 0.87, *SE* = 0.04) was

significantly steeper than the slope for block two (β = 0.51, *SE* = 0.03, *t*(2,704) = 7.39, *p* < .001) and the slope for block one (β = 0.3, *SE* = 0.03, *t*(2,704) = 11.74, *p* < .001). The slope for block two was also significantly steeper than the slope for block, *t*(2,704) = 4.77, *p* < .001. There were no significant differences among the slopes for the speed condition. A simple slopes analysis revealed that the slopes for both accuracy and speed conditions all significantly differed from zero, *p*s < .001 (see Figure 11).

Figure 11

Estimated Cornering Times by ID_C Value, Instruction Method, and Block Order. Gray shading around the lines indicates +/- 1 standard error

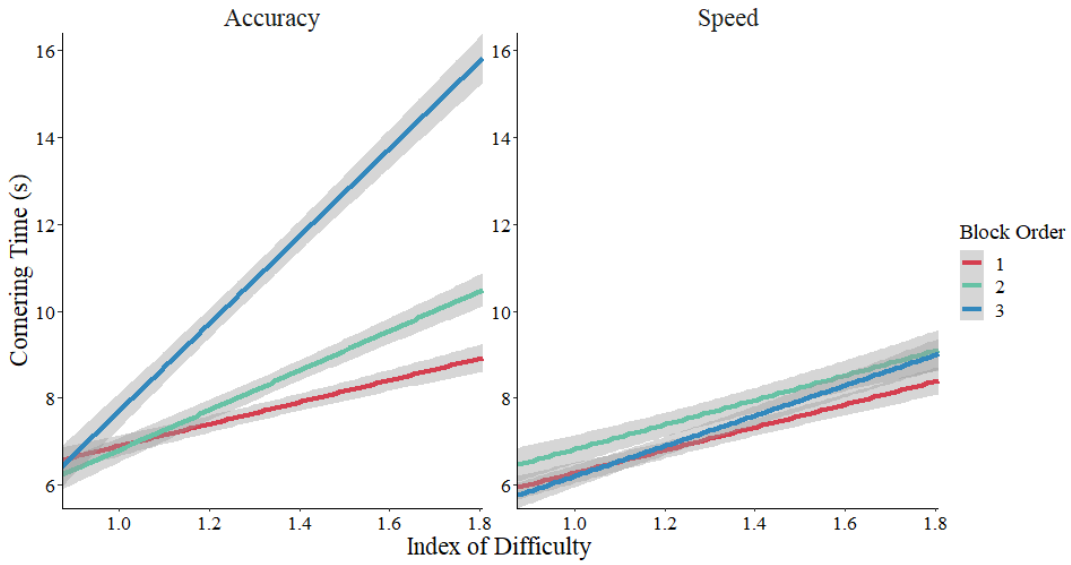

Calibration. To determine whether subjects calibrated to the virtual environment, we looked at the median cornering times and the median number of collisions for each corner and for each driving course (i.e., across amplitude and ID_C values) and instruction condition. We chose to use the median values as both cornering time and collision count

were positively skewed variables. The corner number refers to the negotiated corner within the driving course; corner one refers to the first corner in the course, and corner 14 refers to the last corner in the course. For the accuracy condition, we saw that cornering times generally decreased as the corner number increased (i.e., as they progressed through the driving course). Further, median collision count was always fewer than one (see Figure 12).

Figure 12

Median Cornering Time (top) and Median Collision Count (bottom) for the Accuracy Condition

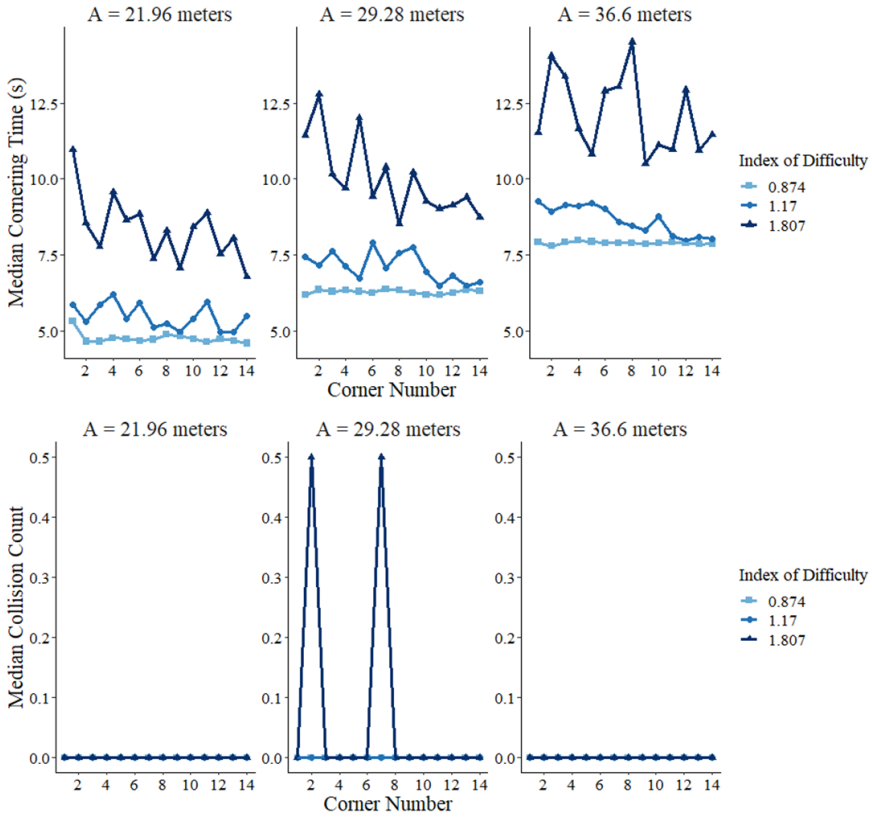

For the speed condition, the median number of collisions was zero when the ID_C value was 0.874 and 1.17. similarly, the median cornering time was consistent as corner number increased. For the most difficulty driving courses (i.e., when the ID_C value was 1.807), the median number of collisions was consistently greater than zero, but the median cornering time showed a general decrease as corner number increased (see Figure 13).

Figure 13

Median Cornering Time (top) and Median Collision Count (bottom) for the Speed Condition

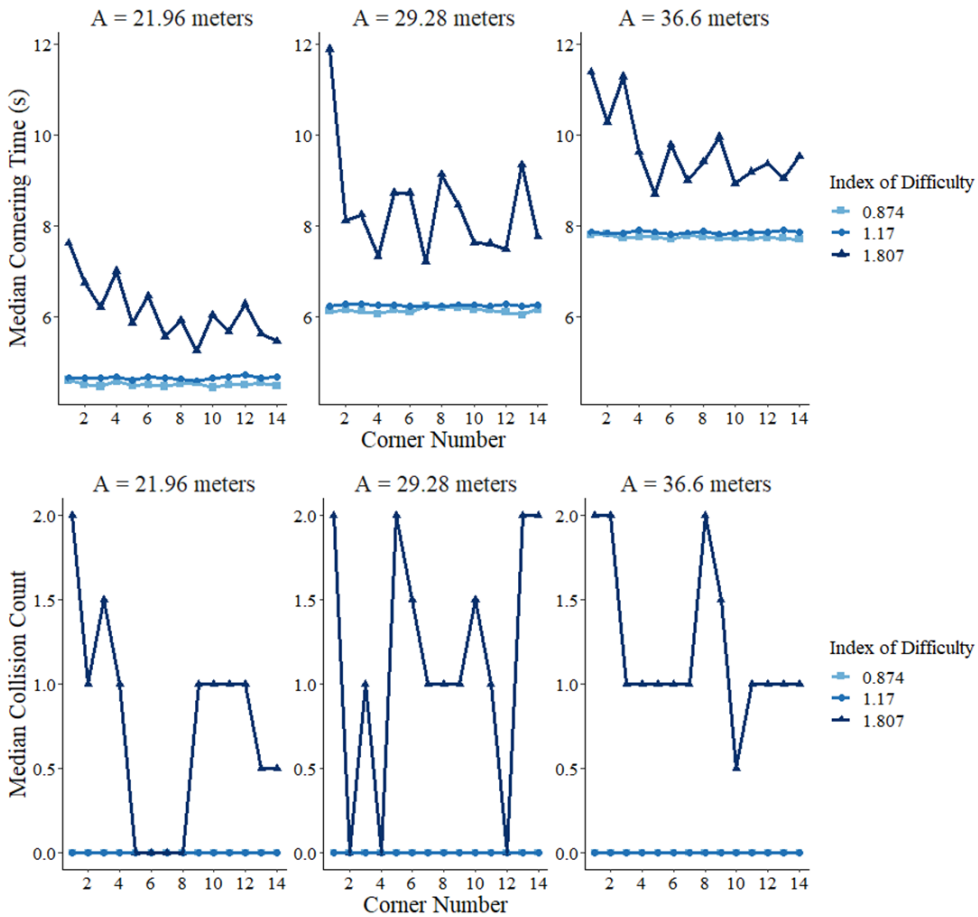

Number of Collisions

Collision Count As a reminder, a collision was logged when any part of the vehicle collided with any wall. Therefore, when multiple parts of the vehicle hit a wall at the same time, multiple collisions were logged. To avoid inflating the total number of collisions, we rounded the collision start time to the nearest second and removed duplicate values. Therefore, when multiple parts of the vehicle collided with a wall at approximately the same time, only one collision was logged. In total, there were 2,625 collisions, and 1,685 of those were considered unique collisions, according to how we defined them above. We utilized only the unique collisions to assess collision count.

Distribution. We found the distribution of unique collision to be positively skewed and leptokurtic, with a skewness value of 8.06 and a kurtosis value of 104.79. This was expected, as the number of collisions was a count variable. However, further inspection revealed that the majority of observations (80.5%) had a count value of zero. As such, we decided to convert the collision count variable into a binary success variable; trials with a collision count of zero were considered successful trials, and trials with a collision count greater than zero were considered unsuccessful.

Logistic Regression. We conducted a mixed effects logistic regression to determine the impact of ID_C value, instruction method, and amplitude on cornering success (see Table 5). The ID_C and amplitude variables were both mean centered. A random effect of participant number was included in the model to account for nesting within participants.

In a logistic regression, the response variable represents the probability of success, π, at a given predictor variable, x; this probability is denoted, $\pi(x)$. The logit, or logarithm of the odds, of this probability takes a linear form (Agresti, 2018), such that

$$\text{logit}[\pi(x)] = \alpha + \beta x \tag{8}$$

The coefficients in a logistic regression have an additive effect on the logit; they represent the rate of change in the S-shaped curve for the probability of success (Agresti, 2018). By exponentiating the coefficients, we obtain the odds ratio, which has a multiplicative effect on the dependent variable. Therefore, the odds of success increase when the odds ratio has a value greater than one, and they decrease when the odds ratio has a value less than one.

Our results indicated that the ID_C was a significant predictor of cornering success. For every one-unit increase in ID_C value, the odds of successful cornering decreased by nearly 100%. This was somewhat expected, given that the difficulty of negotiating a corner approaches infinity as the ID_C value increases. We also found that instruction method was a significant predictor of cornering success. The odds of cornering success decreased by 89.3% when participants were instructed to focus on speed instead of accuracy. In fact, we found that 73.6% of the unique collisions occurred in the speed condition.

Although the odds of cornering success decreased as the corner amplitude increased, this relationship was not statistically significant. The interaction between instruction method and ID_C value was also not a statistically significant predictor of cornering success (see Figure 14).

Table 5

Logistic Regression Output Predicting Cornering Success in Experiment 1

Predictor	β (*SE*)	Odds Ratio	95% CI for Odds Ratio		*z*
			Lower limit	Upper limit	
ID_C	-4.99 (0.41)	0.007	0.003	0.015	-12.14***
Instruction Method	-2.24 (0.7)	0.107	0.02	0.43	-3.22**
Amplitude	-0.02 (0.01)	0.98	0.96	1	-1.67
ID_C * Instruction Method	0.58 (0.48)	1.78	0.72	4.73	1.21

Figure 14

Predicted Probability of Cornering Success by ID_C Value and Instruction Method

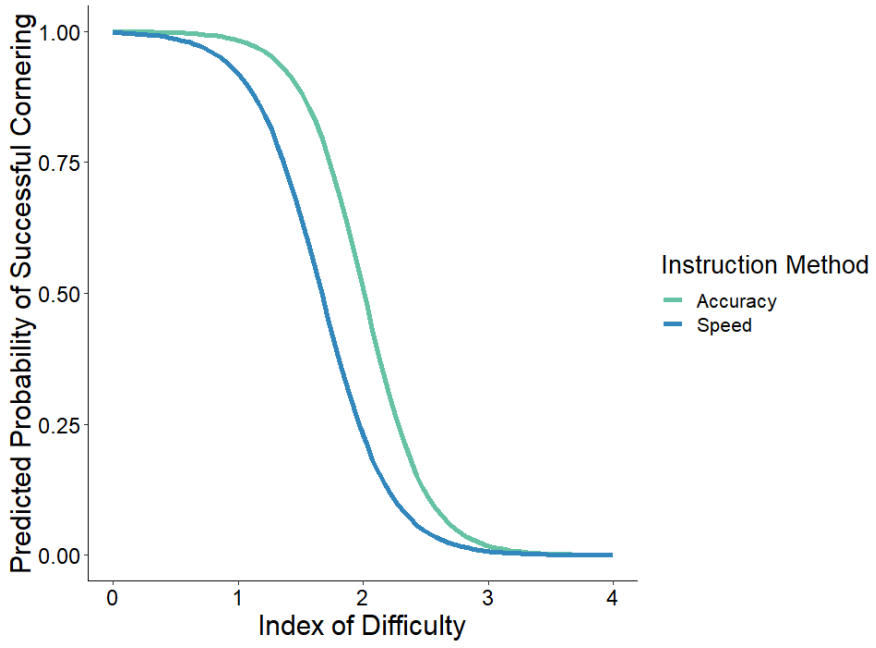

Success Rate. We defined success rate as the overall percentage of successful trials by within each driving course for each instruction method. To reiterate, a trial was

considered successful if the corner was negotiated without collision. In general, the success rate decreased as the ID_C value increased, which was expected. Further, success rate was, on average, greater in the accuracy condition compared to the speed condition (see Figure 15).

Figure 15

Percentage of Successful Trials for Experiment 1

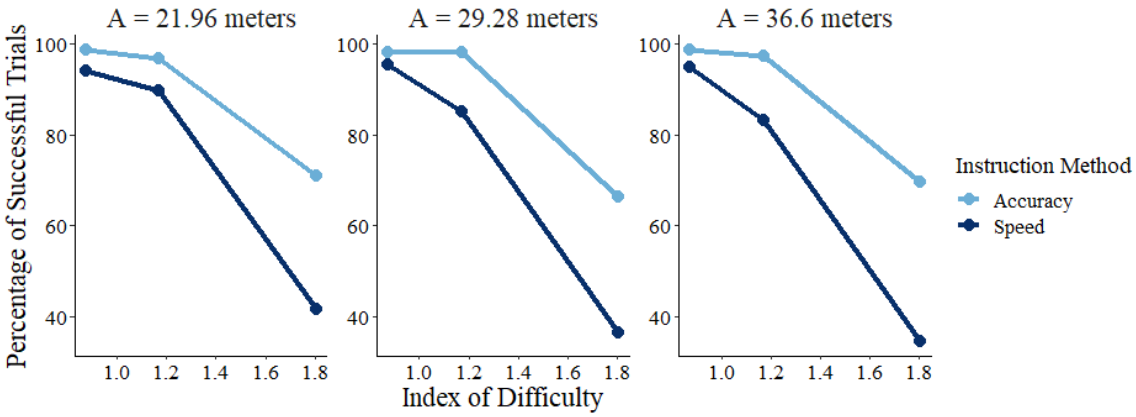

Video Gaming Experience

At the end of each session, subjects rated the frequency at which they play video games on six-point scale from "Never" to "Very often". Due to the little variability in videogaming experience, we created a binomial gaming variable to assess the effect. Subjects who responded that they play "Never", "Almost Never", or "Not very often" were denoted as having limited gaming experience. Subjects who responded that they play at least "Often" were considered to have moderate gaming experience. Participants' gaming experience ratings can be found in Table 6.

Table 6

Video Gaming Experience for Experiment 1 Subjects

Instruction Method	Video Gaming Frequency	*N*	Gaming Experience
Accuracy	Never	3	Limited
	Almost Never (Less than 1 time a month)	2	
	Not Very Often (1-2 times a month)	1	
	Often (1-2 times a week)	2	Moderate
	Fairly Often (3-4 times a week)	2	
	Very Often (5-7 times a week)	1	
Speed	Never	8	Limited
	Almost Never (Less than 1 time a month)	1	
	Not Very Often (1-2 times a month)	0	
	Often (1-2 times a week)	1	Moderate
	Fairly Often (3-4 times a week)	0	
	Very Often (5-7 times a week)	1	

We conducted a mixed effects linear model predicting the log-transformed cornering times with ID_C, instruction method, and the binary gaming experience variable as predictors. Results indicated that the effect of gaming experience and the interactions involving gaming experience were not statistically significant, *p*s > .05. That is, gaming experience did not have a significant effect on cornering time.

We also conducted a mixed effects logistic regression to determine whether gaming experience was a significant predictor of cornering success. We found that gaming experience was a significant predictor of cornering success (β= 2.52, *SE* = 0.98, *z* = 2.47, *p* = .013). The odds of cornering success increased by more than a thousand percent when gaming experience was moderate compared to limited. None of the interactions involving the gaming experience variable were statistically significant.

Collision Information

Using the unique collision count, we found that collision durations were similar between right and left turns (see Table 7). Collision durations were similar between the two instruction methods, but they were slightly longer in the accuracy condition, with a maximum collision duration that was more than 1.5 times the maximum collision duration for the speed condition. For both instruction methods, we found that more than 80% of collision durations were less than one second.

Table 7

Descriptive Statistics for Collision Durations (s) by Turn Type and Instruction Method

Variable	Levels	*M* (*SD*)	Median	Maximum
Turn Type	Right	0.64 (0.9)	0.38	10.6
	Left	0.61 (0.87)	0.36	11.64
Instruction Method	Accuracy	0.68 (1.18)	0.38	11.65
	Speed	0.61 (0.76)	0.36	6.86

To better understand vehicle collisions, we also looked at the total number of collisions, as opposed to the unique collision count. This allowed us to identify where on the corner and where on the vehicle any collision occurred. We found that 58% of collisions occurred on the inside of the corner, and 42% of collisions occurred on the outside of the corner. As previously mentioned, collisions were logged into two groups: collisions before the turn and collisions after the turn. For both before and after the turn, most collisions on the inside of the corner occurred on the side of the vehicle compared to

the front or back of the vehicle. Similarly, for both before and after the turn collisions on the outside of the mostly occurred at the back or sides of the vehicle compared to the front of the vehicle (see Table 8).

Table 8

Number of Collisions on the Vehicle and the Corner in Experiment 1

Instruction Method	Corner Location	Front	Back	Left Side	Right Side
Accuracy	Inside	107 (29.2%)	0 (0%)	151 (41.1%)	109 (29.7%)
	Outside	77 (24.7 %)	6 (2%)	111 (35.5%)	118 (37.8%)
Speed	Inside	435 (37.7%)	6 (.5%)	439 (38%)	275 (23.8%)
	Outside	181 (22.9%)	32 (4%)	360 (45.5%)	218 (27.6%)

Workload

Perceived workload was assessed using the NASA-TLX and was recorded after each block. This allowed us to determine the extent to which perceived workload was influenced by ID_C value. As expected, we found that all facets of perceived workload increased as ID_C value increased (see Figure 16). For performance, a higher NASA-TLX value is associated with poorer perceived performance.

To determine whether there was an effect of ID_C on each of the NASA-TLX scales, we conducted repeated measures analyses of variance. We treated ID_C as a categorical variable so that we could assess whether there were significant differences in perceived workload at each value of ID_C. There was an effect of ID_C on mental demand scores, $F(2, 62) = 10.91$, $p < .001$. Post-hoc comparisons revealed that scores were

significantly higher when the ID_C value was 1.807 compared to 1.17, $t(62) = 3.8$, $p < .001$ and compared to 0.874, $t(62) = 4.23$, $p < .001$.

There was an effect of ID_C on physical demand scores, $F(2, 62) = 4.54$, $p = .014$. Post-hoc comparisons revealed that scores were significantly higher when the ID_C value was 1.807 compared to 0.874, $t(62) = 2.85$, $p = .016$. There was also an effect of ID_C value on temporal demand scores, $F(2, 62) = 8.16$, $p < .001$. Post-hoc comparisons revealed that scores were significantly higher when the ID_C value was 1.807 compared to 1.17, $t(62) = 3.2$, $p = .006$ and compared to 0.874, $t(62) = 3.74$, $p = .001$.

There was an effect of ID_C on effort score, $F(2, 62) = 11.96$, $p < .001$. Post-hoc comparisons revealed that scores were significantly higher when the ID_C value was 1.807 compared to 1.17, $t(62) = 3.57$, $p = .002$ and compared to 0.874, $t(62) = 4.68$, $p < .001$. Further, there was an effect of ID_C on performance scores, $F(2, 62) = 20.76$, $p < .001$. Post-hoc comparisons revealed that scores were significantly higher when the ID_C value was 1.807 compared to 1.17, $t(62) = 5.58$, $p < .001$ and compared to 0.874, $t(62) = 5.58$, $p < .001$.

Lastly, there was an effect of ID_C on frustration scores, $F(2, 62) = 9.93$, $p < .001$. Post-hoc comparisons revealed that scores were significantly higher when the ID_C value was 1.807 compared to 1.17, $t(62) = 3.41$, $p = .003$ and compared to 0.874, $t(62) = 4.19$, $p < .001$. Table 9 provides an overview of which post-hoc comparisons were statistically significant.

Table 9

Post-hoc Significance Tests for NASA-TLX Scales in Experiment 1

NASA-TLX Scale	0.874 vs. 1.17	1.17 vs 1.807	0.874 vs. 1.807
Mental Demand	-	*	*
Physical Demand	-	-	*
Temporal Demand	-	*	*
Effort	-	*	*
Performance	-	*	*
Frustration	-	*	*

Note: * denotes $p < .05$, - denotes $p > .05$

Figure 16

Average NASA-TLX Values by Corner Angle

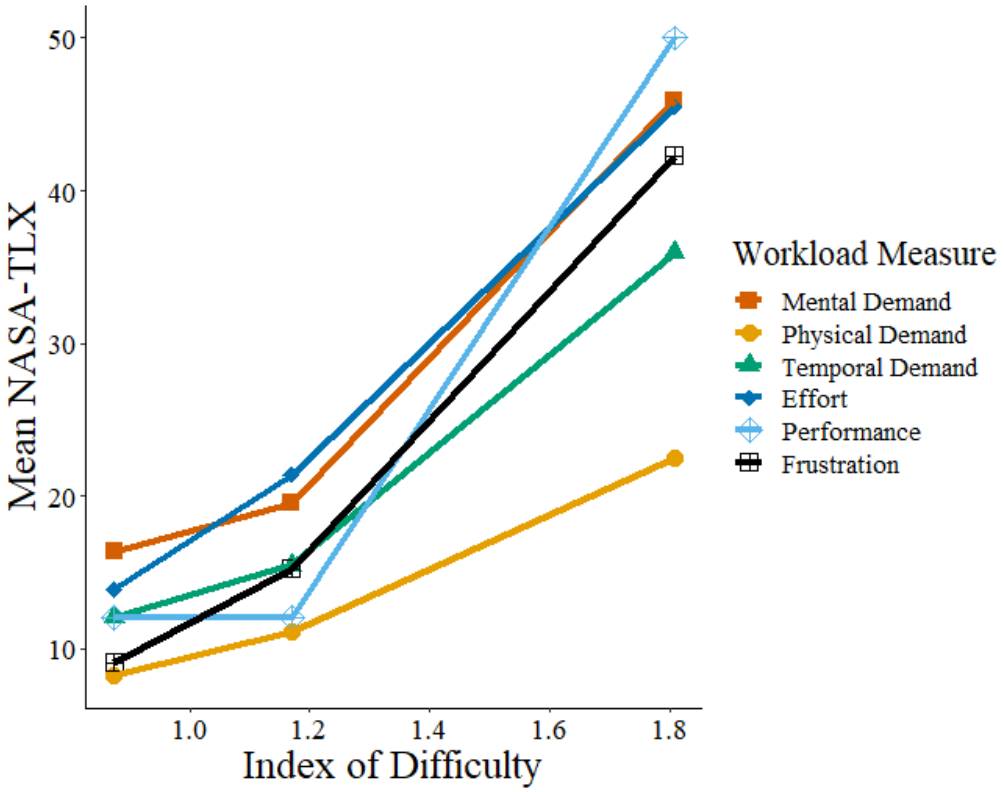

Effective Index of Difficulty

Calculations. To calculate the effective index of difficulty, we obtained the average movement times to navigate the straight-line paths within the driving course, the standard deviation of the vehicle's position relative to the center of the corners, and the average amplitude of movements (i.e., average distance travelled) between each of the straight-line paths. These data were collected for each driving course and for each instruction method, which yielded nine effective index of difficulty values for each instruction method

The average movement time to navigate the straight-line paths within each driving course was computed by dividing the total time to navigate each course (in seconds) by the number of corners within each driving course, which was 14. To get the standard deviation of the error, we first logged the location of the center of the vehicle as it crossed the center of the corner (i.e., the target). The target width was defined as the width of the corner, as seen in Figure 17. We computed the distance between where the vehicle hit the target and the center of the target to obtain the error. We then computed the standard deviation of those error values. Lastly, the amplitude of movements, which represents the effective distance of the target, was calculated by taking the distance travelled between the corner centers. These data were obtained for each driving course and for each instruction method, which yielded nine effective index of difficulty values for each instruction method. The ID_e was computed using Equation 5.

Figure 17

Corner Definitions

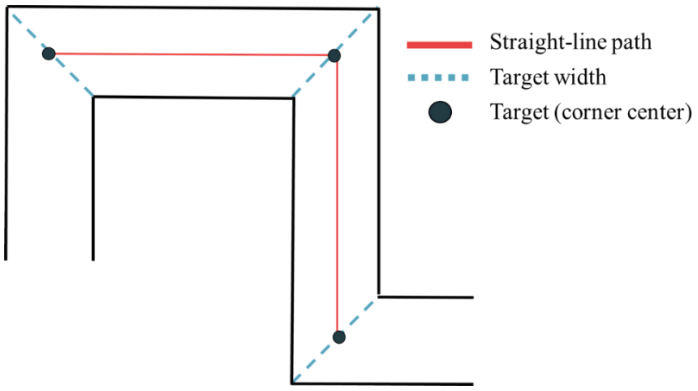

Analysis. As expected, we found that movement time increased as the ID_e value increased (see Figure 18). For the accuracy condition, we found that MT = -15.64 + 5.45*ID_e, with an adjusted R^2 value of .84. Similarly, for the speed condition, we found that MT = -10.72 + 4.39*ID_e, with an adjusted R^2 value of .89. In both instances, the regression was statistically significant, ps < .001. However, there was not a statistically significant difference in movement times between the two instruction methods. When collapsed across instruction method, we found that both the first order only and second order regression equations fit the data well (see Figure 19).

In addition to movement time, we also evaluated the effect of ID_e and instruction method on throughput (see Figure 20). Throughput was calculated according to Equation 6. As expected, we found that ID_e was a significant predictor of throughput, $t(15) = -5.76$, $p < .001$. Overall, estimated throughput decreasing by -0.11 bits/s as ID_e value increased by one. Instruction method was not a significant predictor of throughput.

Figure 18

Average Movement Times by Instruction Method and ID_e Value

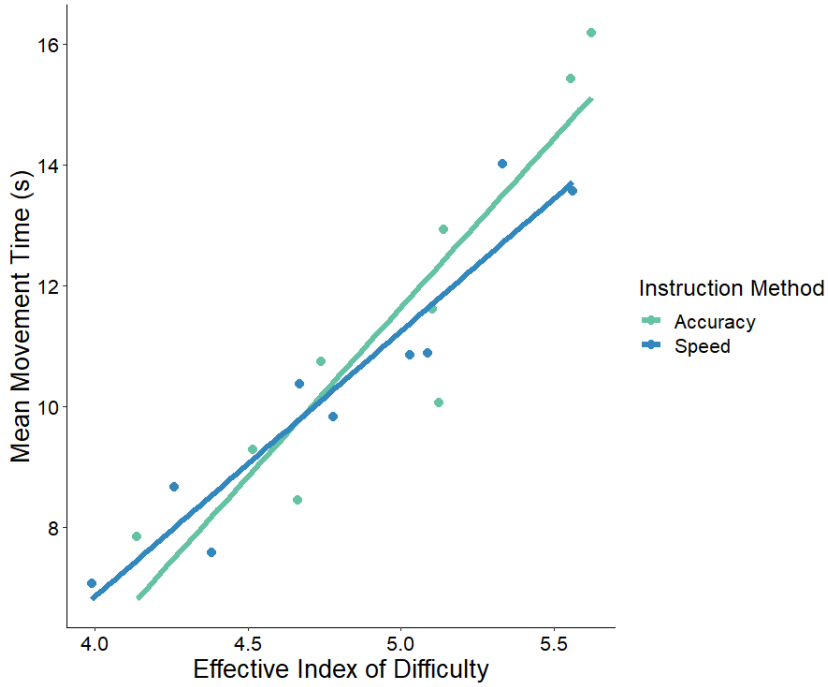

Figure 19

Average Movement Time by ID_e Value fit to a First Order Regression Model (left) and a Second Order Regression Model (right)

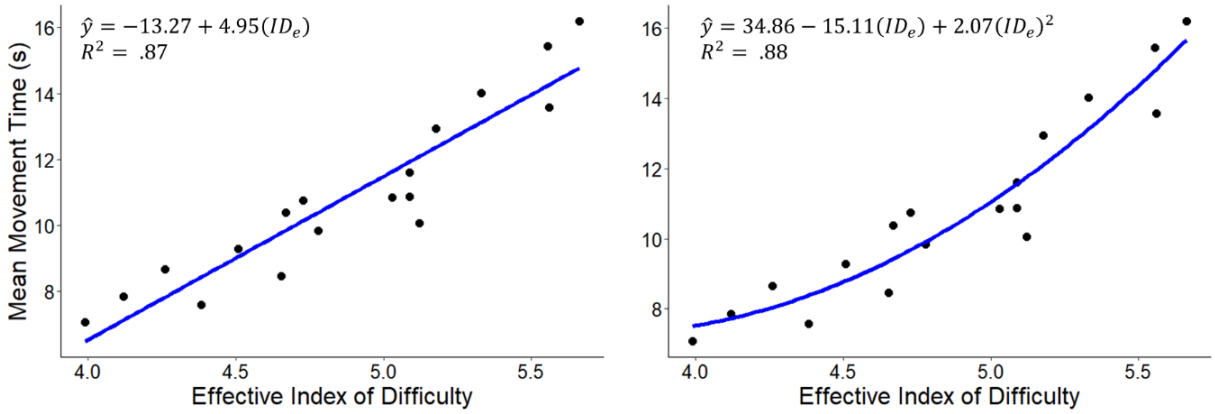

Figure 20

Average Throughput by ID_e Value

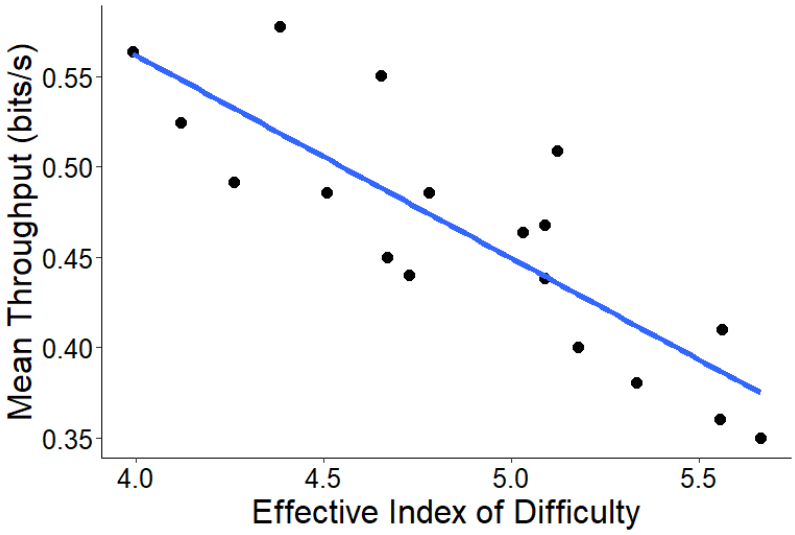

Cornering Law

Typically, analysis of Fitts' law and cornering law experiments require the data be aggregated by the index of difficulty values (e.g., Cross et al., 2018; Pastel et al., 2007). Therefore, to assess Pastel et al.'s (2007) cornering law, we aggregated the data by ID_C value and fit a linear model with the ID_C as a predictor of cornering time (see Eq. 1). The IDc was calculated using Equation 3. Even though the data were aggregated across the different instruction conditions, we found that the model fit the data well, with an R^2 value of .94. Interestingly, we found that including the second order term of IDc produced a better model fit (see Figure 21). We should note that aggregating the data in this way not only inflates the R^2 value, but also results in a loss of information about subject-to-subject variability and trial-by-trial variability.

Figure 21

Average Movement Time by ID_C Value fit to a First Order Regression Model (left) and a Second Order Regression Model (right) in Experiment 1.

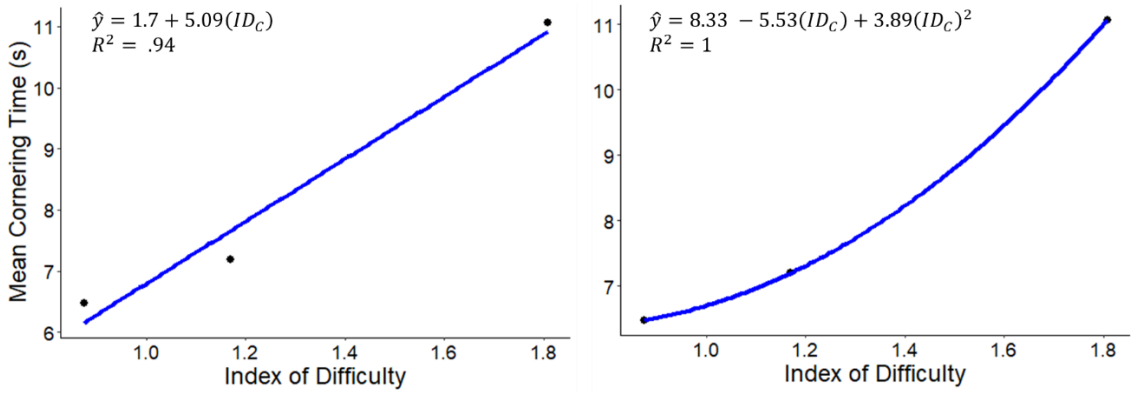

Discussion

In Experiment 1, we evaluated teleoperation performance on a virtual navigation task in terms of both cornering time and the number of collisions. By having subjects focus on either speed or accuracy, we were able to evaluate the speed-accuracy tradeoff.

With respect to cornering time, we hypothesized that increases in the ID_C value and having subjects focus on accuracy would both yield greater cornering times. Our results supported these hypotheses. Cornering times increased as the task became more difficult, and this effect was more pronounced for subjects in the accuracy condition. These findings are consistent with the previous cornering literature (Chan et al., 2019; Cross et al., 2018; Helton et al., 2014; Pastel et al., 2007) as well as previous literature on the speed accuracy tradeoff (Brickler et al., 2021; MacKenzie & Isokoski, 2008). As expected, we found that cornering time increased as the amplitude increased. This was not surprising because increasing the amplitude of the corner necessitates that the subject

navigates the vehicle a longer distance. In general, we found that cornering times for a given ID_C value varied drastically, even within the same instruction method. The considerable variability in cornering times may be explained by differences in operator skill and spatial abilities (see Lathan & Tracey, 2002; Long et al., 2011), but we did not explicitly investigate these differences. Furthermore, we failed to find a significant effect of videogaming experience on cornering time, which is inconsistent with prior findings that gaming experience can impact reaction times and task performance (Dye et al., 2009; Nenna & Gamberini, 2022).

In addition to cornering time, we also hypothesized that the number of collisions would be impacted by the ID_C value and instruction method. Instead of analyzing the number of collisions, we decided to analyze cornering success; that is, whether the subject could negotiate the corner without collision. We found that the probability of successfully negotiating a corner increased as the task became easier. This was consistent with the previous cornering literature (Chan et al., 2019; Pastel et al., 2007). Results also indicated that the probability of successful cornering was greater when subjects were told to focus on accuracy. In fact, one subject in the accuracy condition negotiated every single corner without collision. In addition, we found that subjects with moderate gaming experience, compared to limited gaming experience, were much more likely to negotiate corners without collision. This further suggests that operator skill has an impact on teleoperation performance.

An important distinction between a point and click Fitts' law task and a cornering task is the opportunity for collision. For instance, an error in a Fitts' law task is usually

denoted when the subject misses the target (e.g., they click outside the target box). In a cornering task, an error occurs when the subject collides the vehicle into a wall. The main difference between these two tasks is that an error in a cornering task can have a detrimental impact on subjects' cornering times. Therefore, the relationship between cornering time and collision count is critical. If cornering time and collision count are positively correlated, then subjects told to focus on speed would likely have more collisions and longer cornering times than subjects told to focus on accuracy. We found, however, that subjects in the speed condition had more collisions but maintained faster cornering times than subjects in the accuracy condition. To better illustrate this, we plotted the relationship between cornering time and the number of collisions (see Figure 22). While there is a positive relationship between cornering time and number of collisions, this relationship is much more evident for the difficult corners (i.e., when the ID_C value was 1.807). In other words, when the task was easy, there were fewer collisions, making it more difficult to establish a relationship between cornering time and collision count. In fact, for the accuracy condition, there was substantial variability in cornering time when the collision count was zero. This may explain why Helton et al. (2014) failed to find a strong association between cornering errors and cornering time, as they instructed participants to focus on accuracy.

A possible explanation for our somewhat counterintuitive finding regarding cornering time and collision count for subjects in the speed condition could be the duration of the collisions. Our results indicated that subjects in the speed condition had somewhat shorter collision durations than subjects in the accuracy condition, which

suggests that they made more frequent, but shorter collisions. We reason that subjects in the accuracy condition travelled at slower speeds, which made them more likely to get stuck and unable to maneuver out of a tight corner.

Figure 22

Cornering Time and Collision Count by ID_C Value and Instruction Method.

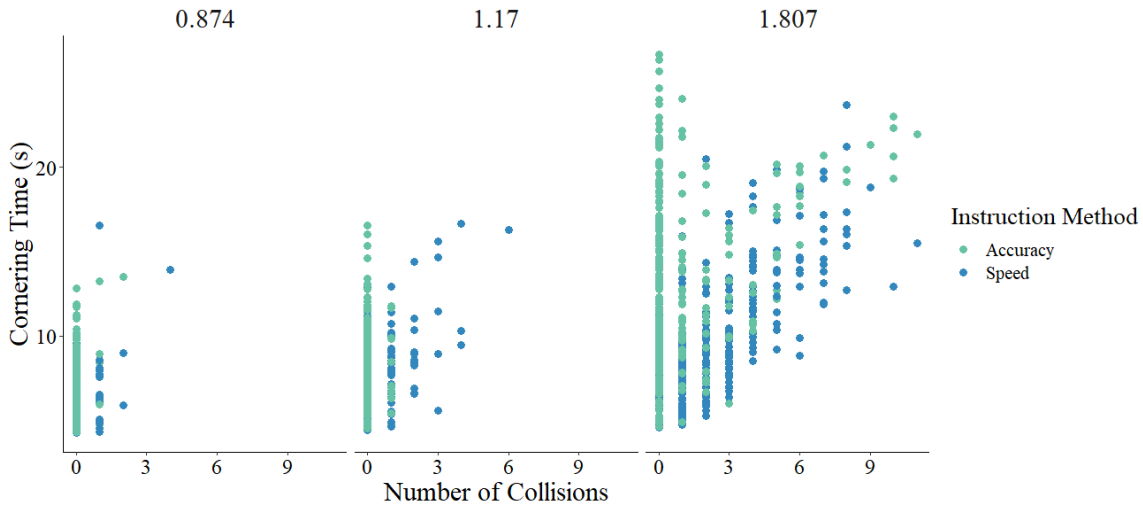

An important extension we made to the previous cornering literature was the empirical evaluation of collision locations. Cross et al. (2018) noted that collision locations differed depending on lighting conditions, but this observation was purely anecdotal. In the present experiment, we recorded each collision instance and logged where those collisions occurred with respect to the path walls and the vehicle. For both instruction conditions, the data indicated that collisions occurred slightly more frequently on the inside of the corner compared to the outside of the corner. This implies that subjects attempted to cut the corners. On the inside corner, there were over three times

the number of total collisions in the speed condition compared to the accuracy condition, which may indicate that those subjects were more likely to attempt cutting the corner.

There are various explanations for the frequent collisions on the inside of the corner. For those subjects focusing on accuracy, cutting off the corner could imply a lack of appropriate scaling of the environment; they may not have accurately perceived the space and dimensions of the virtual environment. While this is commonplace for perception of virtual environments (e.g., Guess et al., 2012), improvement in teleoperation performance over time would suggest that subjects eventually calibrated to the environment. Specifically for the speed condition, it is possible that subjects learned that they could collide with the inside of the corner without serious consequences to their cornering times. This is consistent with our finding that collision durations were, on average, shorter in the speed condition. For both the inside and outside of the corner, collisions most frequently occurred on the front and sides of the vehicle, with hardly any collisions occurring on the back of the vehicle. We believe that the minimal number of collisions on the back of the vehicle may indicate that there were few instances of reversing the vehicle to make corrective movements. It could also indicate that if the subject reversed the vehicle, they were able to correct their path without backing into the wall behind the vehicle.

In this experiment, subjects negotiated 126 corners. As such, it was expected that there would be some evidence of a calibration effect. That is, we expected subjects to adapt to the dimensions of the vehicle and the controller inputs and exhibit improvements in teleoperation performance. We evaluated whether calibration was present in two ways:

by looking at the influence of block order on performance and by looking at teleoperation performance over time. We found that cornering times were, on average, shorter when subjects completed the most difficult driving courses in the last block; this effect was more evident for the accuracy condition. To investigate further, we looked at changes in the number of collisions and cornering time over the 14 corners within each driving course to see if performance improved as individuals progressed though the experiment. Looking at median cornering times, there was a general downward trend as subjects progressed through each driving course. At the same time, median collision counts consistently remained below a value of one. Taken together, these findings suggest that, over time, subjects were able to negotiate corners faster without sacrificing accuracy. For the speed condition, subjects' cornering times and collisions were consistent for the two easier ID_C values (0.874 and 1.17). For the more difficult corners, cornering times showed a decreasing trend, again suggesting an improvement in performance over time. Although all subjects were required to complete a practice phase, our findings indicate that there was an additional calibration effect, which is consistent with the previous teleoperation literature spanning a variety of tasks (Armstrong et al., 2014, 2015; Helton et al., 2014; Schmidlin & Jones, 2016).

In addition to evaluating the impact of task difficulty on teleoperation performance, we also evaluated the ID_e on teleoperation performance. To our knowledge, the present study is the only one to investigate whether the ID_e could be applied to a cornering task. As previously discussed, the ID_e quantifies the task completed, as opposed to the task presented. To apply this measure to a cornering task, we evaluated

performance along the straight-line paths that comprised the corners in the driving courses. This allowed us to calculate and evaluate the ID_e and compare our findings to other Fitts' law tasks that involve moving a cursor between two points. Our results were consistent with previous findings (e.g., Brickler et al., 2020) wherein movement time increased as the ID_e increased, and throughput decreased as the ID_e increased. Furthermore, the lack of difference in movement time between the instruction methods was consistent with previous findings (MacKenzie & Isokoski, 2008) and is in accordance with the ID_e's ability to account for differences in speed and accuracy.

However, there were several limitations to quantifying the ID_e for a cornering task. Because the user was constrained by the corner walls, it was unlikely for them to navigate the vehicle toward the outside of the corner center. That is, they were more likely to cut the corner than overshoot the corner. This type of constraint is not typical of a Fitts' law task and inherently limits the amount of deviation that can be made from the corner center. As such, there can be greater deviation as the corner width increases. The corner walls also meant that subjects could make collisions, which is also atypical for a Fitts' law task. Subjects could also reverse directions to correct for collisions, which increases the effective distance travelled for a given straight-line path. Lastly, looking at the straight-line paths between corner centers means that the performance on the current path of a corner was coupled with performance on the oncoming path of the previous corner. So, while our results are consistent with previous findings, it is not entirely clear whether the ID_e, as quantified in the present work, truly represented the task completed. Another important finding regarding the ID_e is that, like the aggregating cornering

analysis, the data were modelled equally well with inclusion of the quadratic term of the ID_e. Again, these findings question whether the relationship between movement time and task difficulty is truly linear.

Our results further indicated that perceived workload increased as the task difficulty increased. In fact, scores on all six of the workload scales were significantly greater for the driving courses with an ID_C of 1.807 (i.e., the hardest driving courses) compared to the driving courses with an ID_C of 0.874 (i.e., the easiest driving courses). These results are consistent with previous findings that perceived workload increases as task demands increase (Shao et al., 2020). However, Helton et al. (2014) found that the dimensions of perceived workload were stable as time on task increased. Taken together, these results suggests that task difficulty may have a stronger impact on perceived workload than time spent completing the task.

With respect to Pastel et al.'s (2007) cornering law, we found that our model fit the data well, despite being aggregated across the different instruction methods (accuracy vs. speed). We found that adding the quadratic term for the ID_C also fit the data well, which could suggest that the relationship is not entirely linear, but it might also be a case of overfitting the model. It is important to consider that for this analysis, the data were aggregated to obtain a single average cornering time for each index of difficulty value; thus, only three data points were used to fit the model. Although aggregating data in some manner is typical for analysis of the cornering law and Fitts' law tasks (e.g., Brickler et al., 2021; Pastel et al., 2007), the loss of variability as a result of data

aggregation effectively changes the dependent variable (Osborne, 2000) and can produce misrepresented relationships among the variables (Raudenbush & Bryk, 1992).

In sum, Experiment 1 replicated previous cornering law findings. We showed that cornering time and cornering success were associated with Pastel et al.'s (2007) index of difficulty for cornering. As the task became more difficult, subjects' cornering times increased, and their probability of successful cornering decreased. We also showed that teleoperation performance was moderated by instruction method. That is, we demonstrated that the Fitts' law speed-accuracy tradeoff could be extended to a cornering task.

CHAPTER III

Experiment 2

Previously, researchers have validated Pastel et al.'s (2007) cornering law, finding that cornering time can be modeled using an index of difficulty derived from information theory (Eq. 3). Despite finding that cornering time can be appropriately modeled under different lighting conditions (Cross et al., 2018), time delays (Cross et al., 2018), and camera perspectives (Helton et al., 2014), it remains unclear how corner angle and the path ratio impact cornering time and whether the index of difficulty can sufficiently capture these aspects of the task. Thus, in Experiment 2 we assessed the impacts of corner angle and the path ratio on cornering time and number of collisions. In this experiment, subjects navigated a virtual robot around 45°, 90°, and 135° corners. The current and oncoming path widths were manipulated for each corner angle to create three path ratio conditions: a path ratio that was less than one, a path ratio that was equal to one, and a path ratio that was greater than one.

Hypotheses

Like Experiment 1, we hypothesized that cornering time and the number of collisions would increase as the ID_C value increased. That is, we expected subjects to have longer cornering times and more collisions as the cornering task became more difficult. Given Pastel's (2006) earlier finding that corner angle impacts movement times when navigating interfaces, we hypothesized that there would be an effect of corner angle on teleoperation performance. Specifically, we expected that cornering time and the number of collisions would increase as the corner angle increased. Lastly, we

hypothesized that there would some effect of the path ratio on cornering time and the number of collisions.

Method

Experimental Design

This experiment used a 3 (corner angle) by 4 (ID_C value) by 3 (path ratio) repeated measures design. Corner angle was defined as the degree of deviation from the initial heading direction (see Figure 23). The corner angles used in this experiment were 45°, 90°, and 135°. ID_C values were based on the oncoming path width (as opposed to the current path width), and these oncoming path widths were 2.2, 2.6, 3.0, and 3.4 times the width of the virtual vehicle. Thus, the ID_C values utilized for this experiment were 0.874, 0.7, 0.585, and 0.503, respectively. Path ratio corresponded to the relationship between the current path width relative to the oncoming path width and was calculating using Equation 7. Here, the oncoming path width was less than, equal to, or greater than the current path width (see Table 10). Like Experiment 1, the main dependent variables in this experiment were cornering time and the number of collisions. We also collected data on the duration of each collision and the collision locations on the corner and vehicle. These variables were obtained and calculated in the same manner as in Experiment 1.

Table 10

Vehicle Widths, Oncoming Path Widths, and Current Path Widths for each ID_C Value

Vehicle Width (p)	Oncoming Path Width (w_2)	Current Path Width (w_1)	Path Ratio w_1/w_2	IDc = $\log_2(w_2/(w_2-p))$
2.44 m	5.37 m	4.29 m	0.8	0.874
		5.37 m	1.0	
		6.44 m	1.2	
	6.34 m	5.08 m	0.8	0.7
		6.34 m	1.0	
		7.61 m	1.2	
	7.32 m	5.86 m	0.8	0.585
		7.32 m	1.0	
		8.78 m	1.2	
	8.3 m	6.64 m	0.8	0.503
		8.3 m	1.0	
		9.96 m	1.2	

Figure 23

Corner Angles Used in Experiment 2

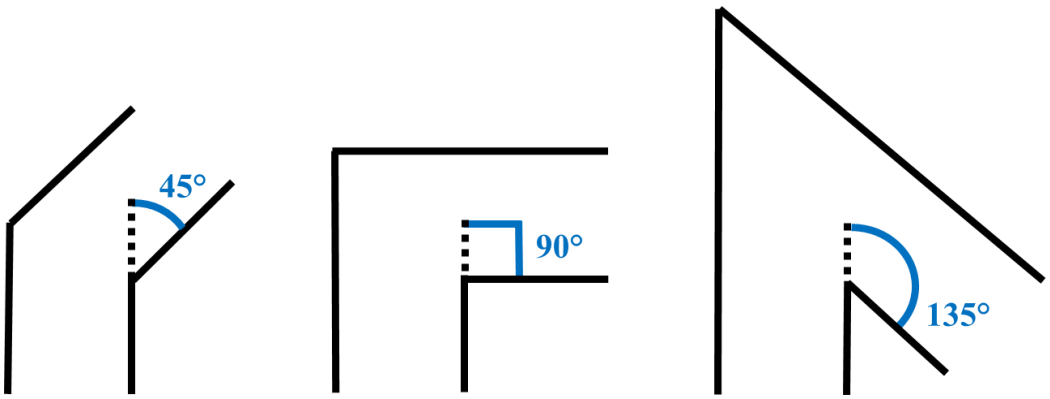

Participants

Like Experiment 1, we generated data using the "simr" package in R (Green & MacLeod, 2016) to determine the number of participants and trials needed. We, again, used the fitted model from Pastel et al.'s (2007) second experiment to generate approximate cornering times for the three values of ID_C we intend to utilize. These cornering times corresponded to the 90° corner angle condition. To obtain approximate cornering times for the 135° corner angle condition, we used Pastel et al.'s (2007) fitted model to generate data, but increased cornering times by 20%. Similarly, we decreased estimated cornering times by 20% for the 45° corner angle condition. Due to the lack of previous research on cornering times and path width, we did not have a hypothesized effect for how the path ratio would impact cornering time. As such, we were mainly interested in the interaction between ID_C and corner angle. In the simulation, we compared the full mixed effects model to a reduced model (i.e., a model without the interaction between ID_C and corner angle). Ultimately, we found that we needed 42 subjects to complete six trials (i.e., round six corners) for each corner angle and index of difficulty to obtain power above .80. This would produce 72 observations for each subject, for a total of 3,024 observations. The R code for the analysis process described above can be found here: https://osf.io/87krn/

We recruited 42 Clemson University students (M_{age} = 21.9 years, SD_{age} = 4.92) with visual acuity of 20/32 or better. Subjects were recruited through Clemson University's Psychology SONA pool and through word of mouth, and they were compensated with partial course credit or with a $10 gift card.

Apparatus

The virtual environment was developed using Unity and consisted of a practice area and 36 different corners (4 ID_C values x 3 corner angles x 3 path ratios). The virtual environment was viewed on a 19-inch Dell monitor with a 1440x900 pixel display. The refresh rate was 60 Hz. The practice area was a 40 by 40-meter room with five pillars (see Figure 24). The pillars were included to encourage the participant to practice corner negotiation. Like Experiment 1, the virtual vehicle used front wheel steering and was based on Unity's standard asset vehicle. The virtual vehicle was 2.44 meters wide and 6.33 meters long with a maximum speed of 10 miles per hour and a maximum steering angle of 40°. The camera was fixed just above the virtual vehicle at 4.04 meters above the roadway. The camera was located 3.11 meters from the front axle and 0.46 meters from the rear axle, which allowed the hood of the vehicle to be in view (see Figure 25). The camera had a field of view of 60° and was rotated downward 30°; the camera's viewpoint was not adjustable. Like Experiment 1, subjects used a wired Xbox Controller to navigate the virtual vehicle within the virtual environment. The controls were the same as in Experiment 1.

Figure 24

Practice Area (left) and Virtual Vehicle Used (right) in Experiment 2

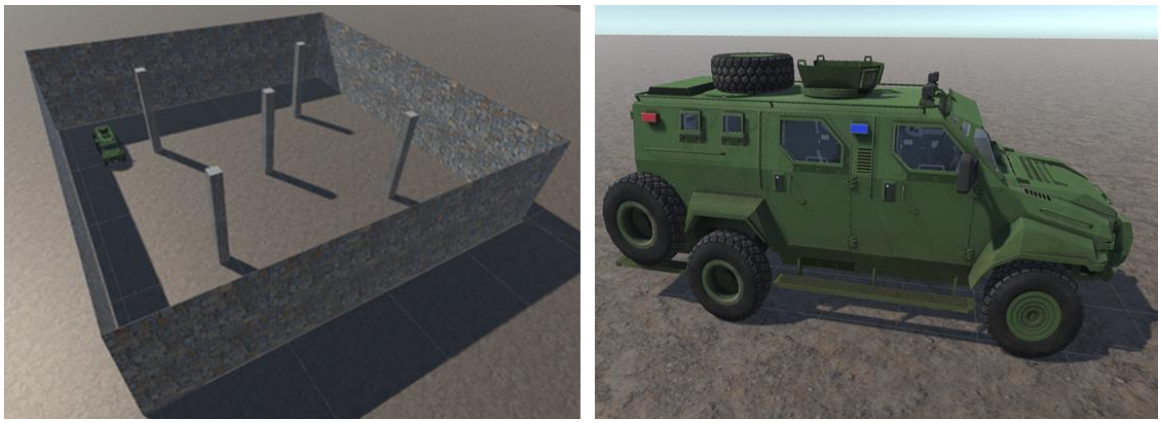

Figure 25

Camera Perspectives by Corner Angle.

Procedure

After signing the informed consent, participants completed a visual acuity test. The visual acuity test was conducted using a Snellen Eye Chart placed 10 feet away. Subjects completed the test with both eyes open. All participants had visual acuity of 20/32 or better. Following this, the experimental procedure began. The experiment consisted of a practice phase and three blocks of trials. To start, subjects completed the

practice phase, where they were told to take some time to familiarize themselves with the controls of the virtual vehicle. After spending time in the practice environment, subjects completed a block of 24 trials (2 trials x 4 ID_C values x 3 path ratios) for each corner angle. Each trial consisted of a single corner. To mitigate an effect of turn type, half of the trials were left turns, and the other half were right turns. At the start of each block of trials, subjects were instructed to navigate around each corner as quickly and accurately as possible. The virtual vehicle was located at the center of the path at the beginning of every trial. The presentation of blocks was randomized across subjects using a Latin square design, and trials within each block were presented in a randomized order. After each block of trials, subjects completed the NASA-TLX questionnaire. Once subjects completed all three blocks, they answered questions about their age, gender, and experience playing video games (see Appendix C). They were debriefed and provided with contact information prior to leaving. Each session took approximately 45 minutes.

Results

Cornering Time

Analysis Preparation. Prior to conducting any analysis, we visualized the distribution of the cornering time variable. We found that the cornering time variable had a skewness value of 10.06 and kurtosis value of 170.33, which indicated that the distribution was positively skewed and leptokurtic. We extracted the residuals from a linear mixed effects model predicting cornering time to evaluate the errors. A QQ plot revealed that the normality assumption was severely violated. In an effort to normalize the residuals without performing an elaborate and difficult-to-interpret transformation, we

decided to perform a log-transformation on the cornering time variable. We then refit the linear mixed effects model predicting log-transformed cornering time and removed standardized residuals with values greater than +/- 3. Less than 2% of the data were removed as a result of this outlier analysis. After performing the log-transformation and outlier analysis, the residuals were more normally distributed. While this did not completely resolve the lack of normality in the residuals, researchers have shown that minor violations in normality are well-tolerated (Knief & Forstmeier, 2021; Schmidt & Finan, 2018), especially with a larger sample size, like we have here.

Mixed Effects Modeling. We submitted corner angle, ID_C, and path congruency to a linear mixed effects model predicting the log-transformed cornering times. The ID_C variable was mean-centered, and a random effect of participant number was included in the model to account for nesting within participants. This model yielded a marginal R^2 value of .42, indicating that the fixed effects alone accounted for 42% of the variance in log-transformed cornering times. The amount of variance explained increased to 63% with both the fixed effects and the random effect of participant number. All post-hoc comparisons include p-values adjusted using the Tukey method. Results from the Omnibus F test can be found in Table 11.

As expected, ID_C value was a significant predictor of log-transformed cornering times ($\beta = 0.61$, $SE = 0.08$ $t(2,914) = 7.61$, $p < .001$), with time increasing as the ID_C value increased. This can be seen in Figure 26. There was also a significant effect of the path ratio. On average, log-transformed cornering times differed between the 1.2 path ratio and the 1.0 path ratio conditions, $t(2,914) = -6.77$, $p < .001$, between the 1.2 path

ratio and the 0.8 path ratio conditions, $t(2,914) = -18.01$, $p < .001$, and between the 1.0 path ratio and the 0.8 path ratio conditions, $t(2,914) = -11.26$, $p < .001$. In general, cornering times increased as the path ratio decreased (see Table 11).

Table 11

Omnibus F Test Results for the Model Predicting Log-transformed Cornering Times in Experiment 2

Predictor	df1	df2	*F*
ID_C	1	2,914	1,609.96***
Path Ratio	2	2,914	167.77***
Corner Angle	2	2,914	79.63***
ID_C * Path Ratio	2	2,914	33.33***
ID_C * Corner Angle	2	2,914	658.53***
Path Ratio * Corner Angle	4	2,914	60.81***
ID_C * Path Ratio * Corner Angle	4	2,914	4.24**

Note: * denotes $p < .05$, ** denotes $p < .01$, *** denotes $p < .001$

Table 12

Descriptive Statistics for Cornering Times by Path Ratio and Corner Angle

Variable	Levels	*M* (*SD*)	Median	Maximum
Path Ratio	0.8	10.9 (6.52)	8.64	66
	1.0	9.6 (4.52)	8.57	52.1
	1.2	8.91 (3.74)	8.37	49.6
Corner Angle	45°	8.85 (1.58)	8.64	34.9
	90°	9.31 (3.54)	8.24	46.7
	135°	11.3 (7.85)	7.72	66

Figure 26

Cornering Time by ID_C Value in Experiment 2

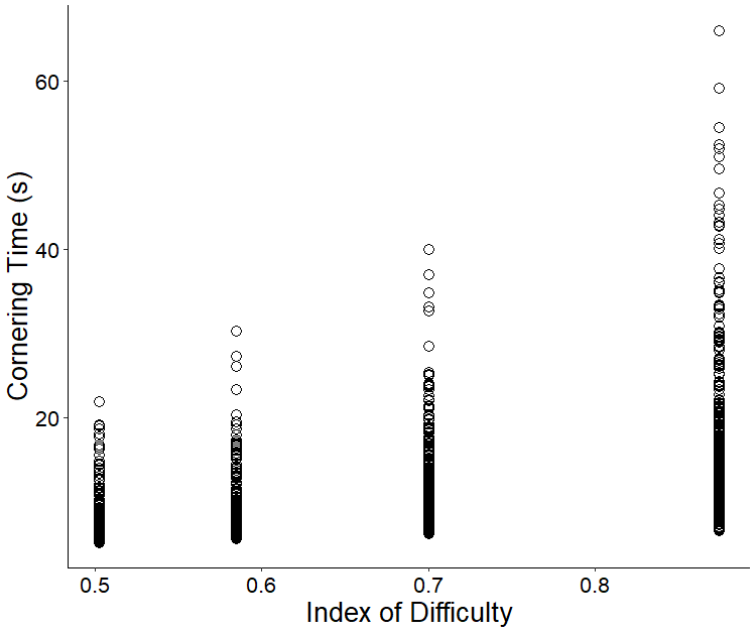

There was a significant effect of corner angle. Post-hoc comparisons indicated that log-transformed cornering times differed between 135° corners and 90° corners, $t(2,914) = 8.99$, $p < .001$, between 135° and 45° corners, $t(2,914) = 11.46$, $p < .001$, and between 90° and 45° corners, $t(2,914) = 2.46$, $p = .037$. Overall, cornering times increased as corner angle increased (see Table 12).

For the significant interaction between path ratio and corner angle, post-hoc comparisons revealed that, for 45° corners, there were no statistically significant differences in log-transformed cornering times among the three path ratios. For the 90° corners, log-transformed cornering times were significantly different between the 0.8 and 1.0 path ratio conditions, $t(2,914) = 5.2$, $p < .001$, and between the 0.8 and 1.2 path ratio

conditions, $t(2,914) = 7.56$, $p < .001$. There was not a statistically significant difference in log-transformed cornering times between the 1.0 and 1.2 path ratios. For 135° corners, log-transformed cornering times were different between the 0.8 and 1.0 path ratio conditions, $t(2,914) = 13.5$, $p < .001$, between the 0.8 and 1.2 path ratio conditions, $t(2,914) = 22.25$, $p < .001$, and between the 1.0 and 1.2 path ratio conditions, $t(2,914) = 8.77$, $p < .001$. In terms of the original scale, cornering times increased as the path ratio decreased; this effect was more pronounced as the corner angle increased (Figure 27).

Figure 27

Average Cornering Times by Corner Angle and Path Ratio. Error bars represent +/- 1 standard error.

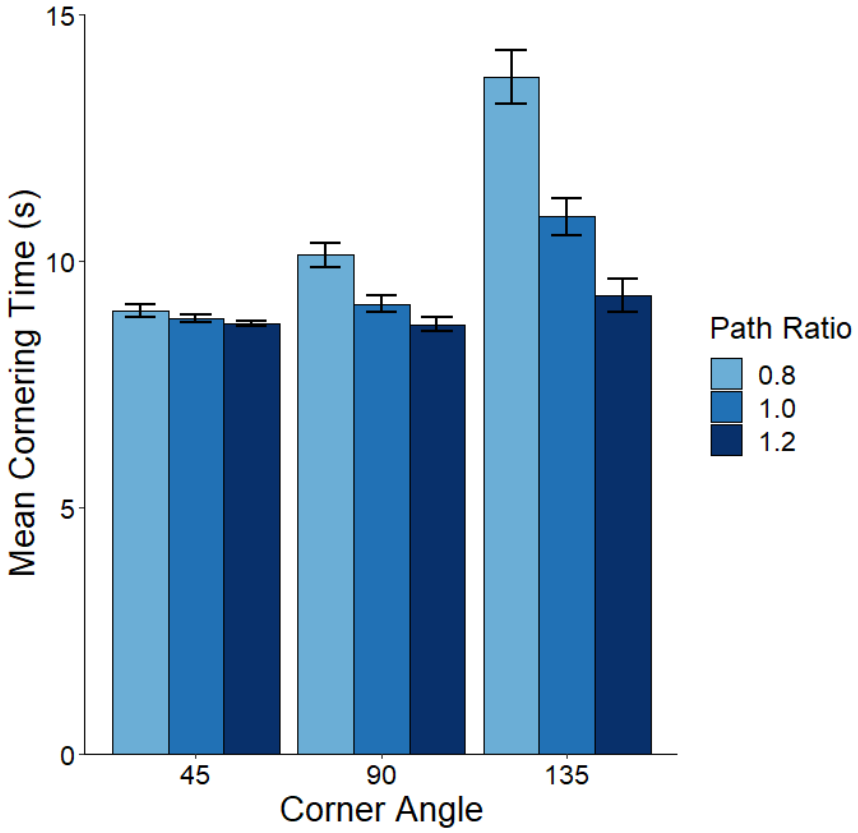

For the following interactions involving ID_C, we evaluated the slope of the line as the ID_C value increases for each condition of the specified categorical variable. For example, post-hoc comparisons for the interaction between corner angle and ID_C revealed that the slope for 45° corners ($\beta = 0.12$, $SE = 0.05$) was significantly shallower than the slope for 90° corners ($\beta = 0.69$, $SE = 0.05$, $t(2,914) = -8.67$, $p < .001$) and the slope for 135° corners ($\beta = 2.43$, SE = 0.05, $t(2,914) = -34.97$, $p < .001$). Additionally, the slope for 90° corners was significantly shallower than the slope for 135° corners, $t(2,914) = -26.3$, $p < .001$. We also conducted a simple slopes analysis to determine whether the slopes of the lines for each of the three corner angle conditions differed from zero. We found that the slopes for the 90° and 135° corners both significantly differed from zero, ps < .001. The slope for 45° corners was not significantly different from zero, which suggests that cornering times were essentially unaffected by changes in ID_C value. In terms of the original scale, cornering times increased as ID_C increased, but they increased at a more drastic rate as the corner angle increased (see Figure 28).

There was also a significant interaction between path ratio and ID_C value (see Figure 29). Post-hoc comparisons revealed that the slope for 0.8 path ratio ($\beta = 1.37$, $SE = 0.05$) was significantly steeper than the slope for 1.0 path ratio ($\beta = 1.02$, $SE = 0.05$, $t(2,914) = 5.4$, $p < .001$) and the slope for 1.2 path ratio ($\beta = 0.84$, $SE = 0.05$, $t(2,914) = 8.02$, $p < .001$). Additionally, the slope for 1.0 path ratio was significantly steeper than the slope for 1.2 path ratio, $t(2,914) = 2.66$, $p = .021$). A simple slopes analysis revealed that the slopes for all path ratio conditions significantly differed from zero, ps < .001.

Figure 28

Cornering Time by Corner Angle and ID_C Value. Gray shading around the lines indicates +/- 1 standard error.

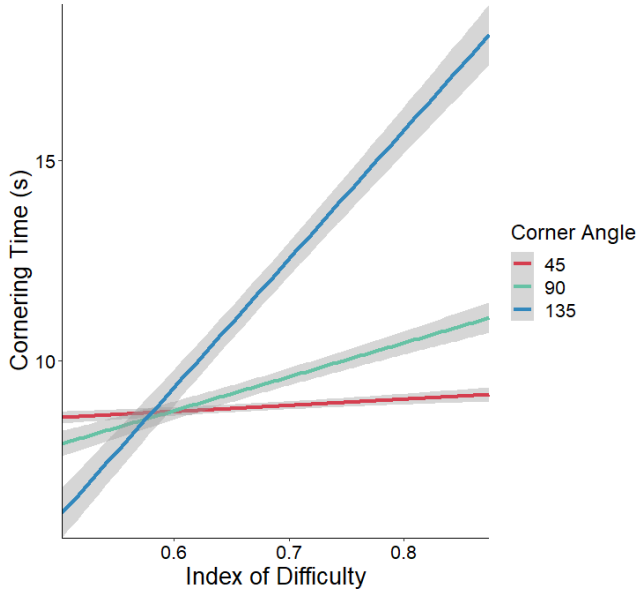

Figure 29

Estimated Cornering Time by ID_C Value and Path Ratio

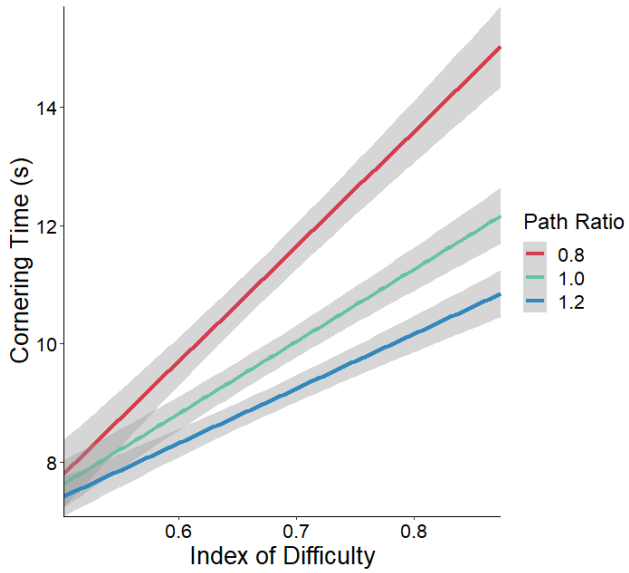

Lastly, there was a statistically three-way interaction among corner angle, path ratio, and ID_C. To evaluate this interaction, we first split the data by corner angle and evaluated differences among the path ratios as a function of ID_C. For 45° corners, there were no differences in the slopes among the different path ratio conditions. A simple slopes analysis revealed that the slope for the 0.8 path ratio was significantly different from zero, $t(2,914) = 2.56$, $p = .011$. The slopes for the 1.0 and 1.2 path ratio conditions were not significantly different from zero.

For 90° corners, the slope for the 1.2 path ratio ($\beta = 0.35$, $SE = 0.08$) was marginally different than the slope for the 1.0 path ratio ($\beta = 0.61$, $SE = 0.08$, $t(2,914) = -2.31$, $p = .055$) and significantly shallower than the slope for the 0.8 path ratio ($\beta = 1.1$, $SE = 0.08$, $t(2,914) = -6.63$, $p < .001$). In addition, the slope for the 1.0 path ratio was significantly shallower than the slope for the 0.8 path ratio, $t(2,914) = -4.33$, $p < .001$. A simple slopes analysis revealed that all slopes significantly differed from zero, ps < .001. Looking at the original scale, cornering times increased as the ID_C increased, but they increased at a more drastic rate as the path ratio decreased (see Figure 30).

For 135° corners, the slope for the 0.8 path ratio ($\beta = 2.81$, $SE = 0.08$) was significantly steeper than the slope for the 1.0 path ratio ($\beta = 2.33$, $SE = 0.08$, $t(2,914) = 4.2$, $p < .001$) and significantly steeper than the slope for the 1.2 path ratio ($\beta = 2.15$, $SE = 0.08$, $t(2,914) = -5.72$, $p < .001$). There was not a significant difference in the slopes between the 1.0 and 1.2 path ratio conditions. A simple slopes analysis revealed that all slopes significantly differed from zero, ps < .001. On the original scale, cornering times,

again, increased as the ID_C increased, and the rate of increase was the most drastic for the smallest path ratio.

Figure 30

Estimated Cornering Time for each Corner Angle by ID_C Value and Path Ratio

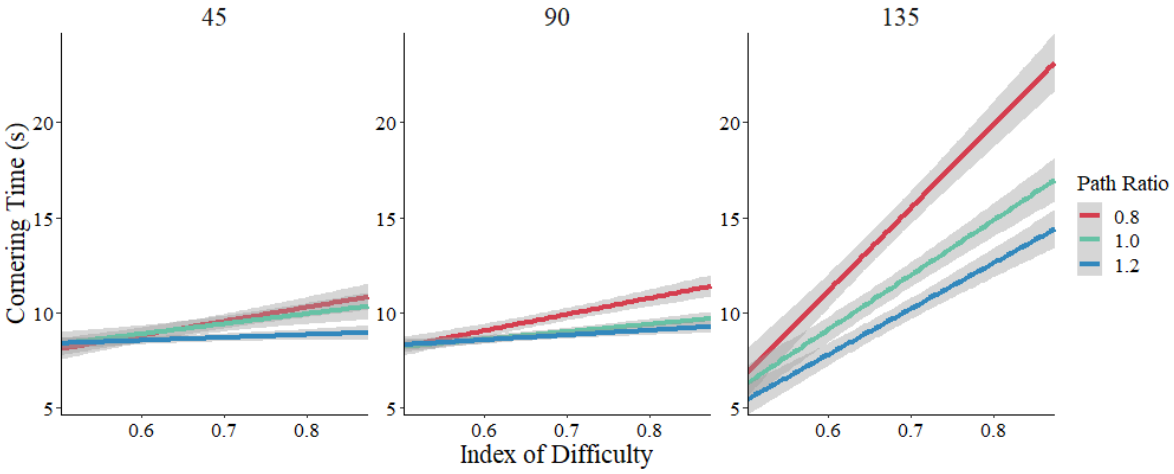

We also split the data by path congruency condition and evaluated differences among corner angles as a function of ID_C. For the 0.8 path ratio condition, the slope for 135° corners (β = 2.81, *SE* = 0.08) was significantly steeper than 90° corners (β = 1.1, *SE* = 0.08, $t(2,914) = 14.77$, $p < .001$) and 45° corners (β = 0.2, *SE* = 0.08, $t(2,914) = 22.68$, $p < .001$). The slope for 90° corners was significantly steeper than the slope for 45° corners, $t(2,914) = 7.9$, $p < .001$. The simple slopes analysis revealed that all slopes were significantly different from zero, *p*s < .05.

Similarly, for the 1.0 path ratio condition, the slope for 135° corners (β = 2.33, *SE* = 0.08) was significantly steeper than 90° corners (β = 0.61, *SE* = 0.08, $t(2,914) = 15.06$,

$p < .001$) and 45° corners (β = 0.12, *SE* = 0.08, $t(2,914) = 19.41$, $p < .001$). Further, the slope for 90° corners was significantly steeper than the slope for 45° corners, $t(2,914) = 4.33$, $p < .001$. The simple slopes analysis revealed that the slopes for 90° and 135° corners were significantly different from zero, *p*s < .001.

Lastly, for the 1.2 path ratio condition, the slope for 135° corners (β = 2.15, *SE* = 0.08) was significantly steeper than 90° corners (β = 0.35, *SE* = 0.08, $t(2,914) = 15.71$, $p < .001$) and 45° corners (β = 0.04, *SE* = 0.08, $t(2,914) = 18.46$, $p < .001$). The slope for 90° corners was significantly steeper than the slope for 45° corners, $t(2,914) = 2.76$, $p = .016$. The simple slopes analysis revealed that the slopes for 90° and 135° corners were significantly different from zero, *p*s < .001. Looking at the original scale, it is evident that cornering times increase at a more drastic rate for the 135° corners as the task became more difficult, and this was the case for all path ratio conditions (see Figure 31).

Figure 31

Estimated Cornering Time for each Path Ratio by ID_C Value and Corner Angle.

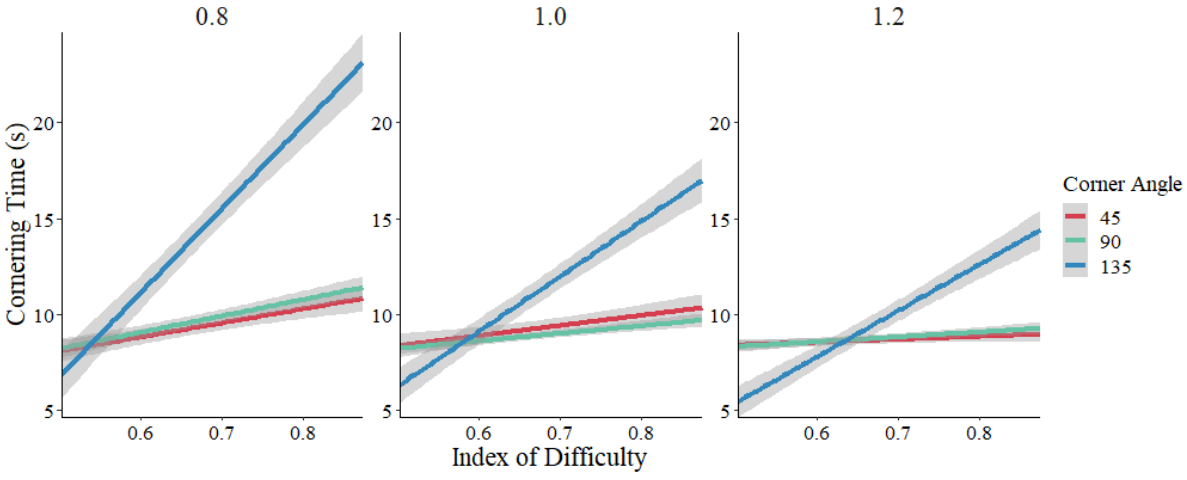

Turn Type. We also investigated whether there were differences in cornering time based on the turning direction (left vs. right). Using the log-transformed cornering times, we conducted an independent samples t-test between left turns and right turns. Results indicated that there was not a statistically significant difference in log-transformed cornering times depending on turn type, $t(2,944) = 1.67$, $p = .09$. Upon plotting the average cornering times by corner angle, ID_C, and turn type, it was clear that there were only minor differences in the cornering times between the left and right turns (see Figure 32). While overall average cornering times were greater for left turns (M = 9.97, SD = 5.48) compared to right turns (M = 9.62, SD = 4.72), this discrepancy was trivial.

Figure 32

Average Cornering Times by ID_C, Corner Angle, and Turn Type. Error bars represent +/-1 standard error.

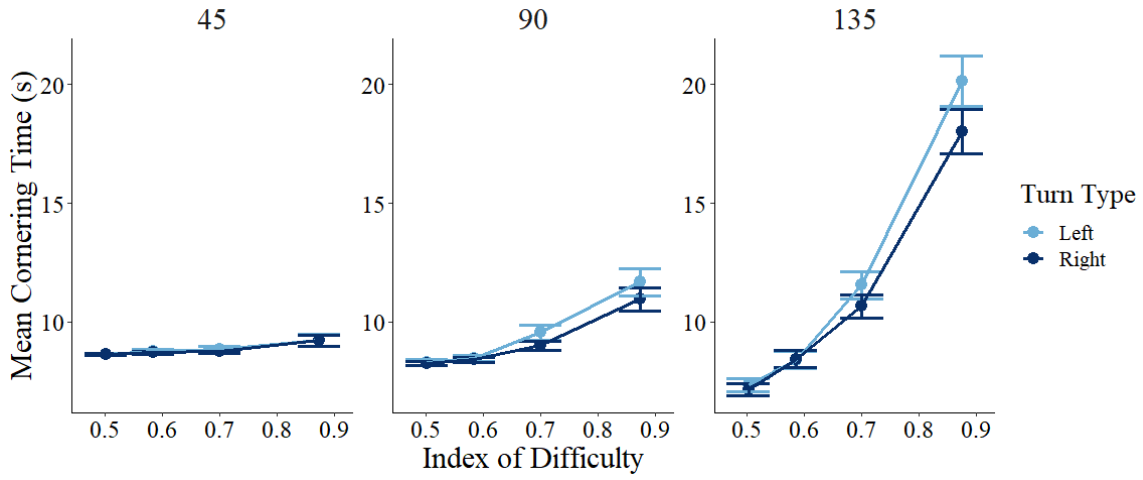

Block Order. Furthermore, we assessed the extent to which the order of the blocks impacted performance. The order of presented corner angles for each block number can be found in Table 13. We fit a mixed effects model predicted the log-transformed cornering times with block order, corner angle, and ID_C as independent variables. A random effect of participant number was included in the model. There was not a significant effect of block order on the log-transformed cornering times, but there was a significant interaction between block order and corner angle, $F(4, 2{,}922) = 4.31$, $p = .002$. However, after controlling for family-wise error rate, post-hoc comparisons did not yield any significant differences. In other words, cornering times were, on average, faster when the most difficult corners (i.e., 135° corners) were negotiated last, but this effect was not statistically significant (see Figure 33).

Table 13

Average Cornering Times by Block Order in Experiment 2

Block Order	Order of Corner Angles	*M* (*SD*)	Median	Maximum
1	135°, 90°, 45°	10.07 (5.39)	8.62	66
2	90°, 45°, 135°	9.1 (3.91)	8.52	44.83
3	45°, 135°, 90°	10.17 (5.82)	8.54	52.06

Figure 33

Average Cornering Times by Corner Angle and Block Order

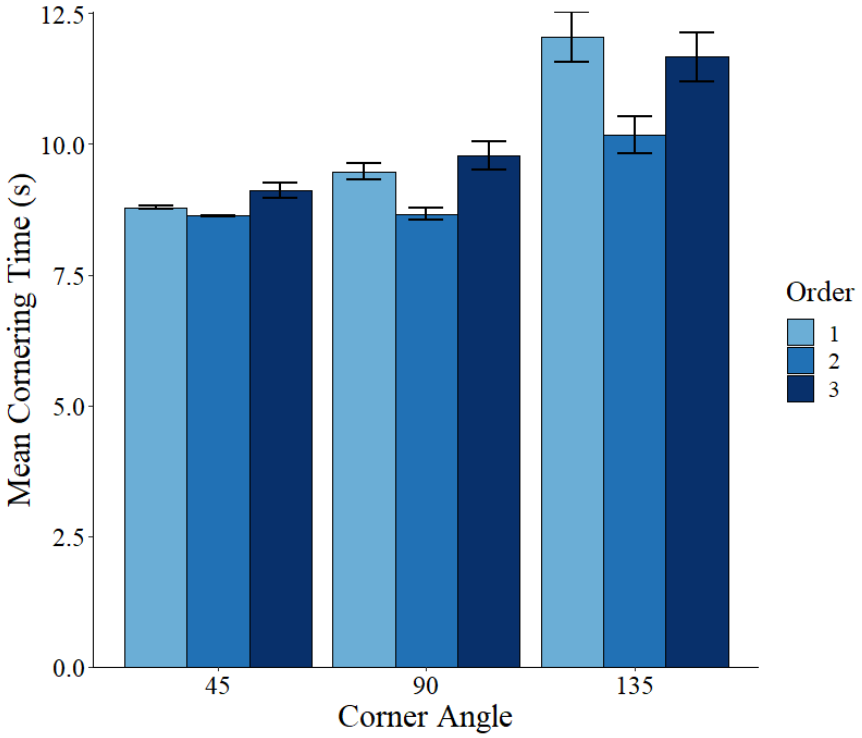

The interaction between ID_C and block order was also a significant predictor of log-transformed cornering times, $F(2, 2922) = 3.31$, $p = .037$. Post-hoc comparisons revealed that the slope for block one ($\beta = 1.12$, $SE = 0.06$) was significantly steeper than the slope for block two ($\beta = 0.92$, $SE = 0.06$ $t(2,922) = 2.37$, $p = .047$). There was not a significant difference between the slopes for block one and block three ($\beta = 1.1$, $SE = 0.06$) nor between block two and block three. A simple slopes analysis revealed that all three slopes for block order significantly differed from zero, $ps < .001$ (see Figure 34).

Figure 34

Estimated Cornering Times by Block Order. Gray shading around the lines indicates +/- 1 standard error.

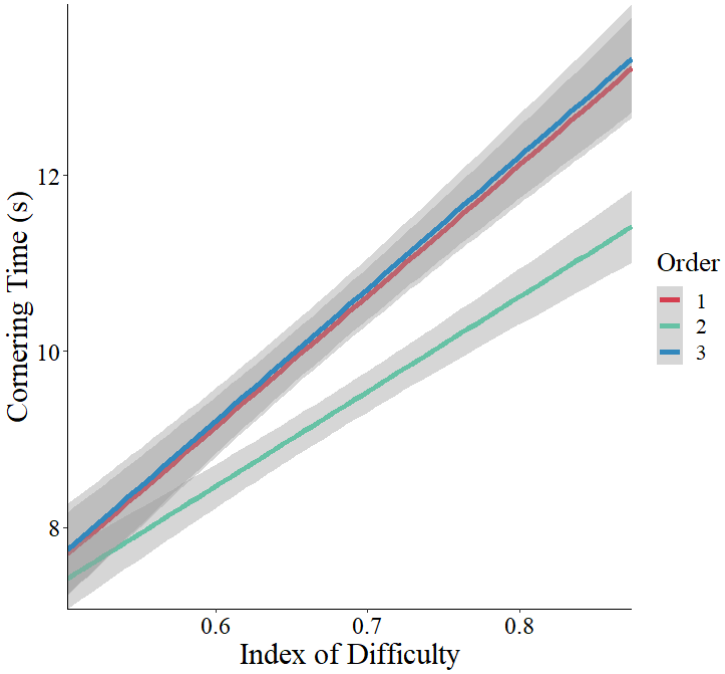

Number of Collisions

Collision Count. As a reminder, a collision was logged when any part of the vehicle collided with any wall. Like Experiment 1, we rounded the collision start time to the nearest second and removed duplicate values. This yielded a single collision count when multiple parts of the vehicle collided with a wall at approximately the same time. Due to a technical error, one participant's collision data was not collected. In total, there were 4,426 collisions, and 1,388 of those were considered unique collisions, according to how we defined them above.

Distribution. We found the distribution of the number of unique collisions variable to be positively skewed and leptokurtic, with a skewness value of 13.52 and a kurtosis value of 252.1. Further inspection revealed that the majority of observations (86.4%) had a count value of zero. Like Experiment 1, we decided to convert the collision count variable into a binary success variable; trials with a collision count of zero were considered successful trials, and trials with a collision count greater than zero were considered unsuccessful.

Logistic Regression. Using the unique collision data, we conducted a mixed effects logistic regression to determine the impact of ID_C value, corner angle, and path ratio on cornering success. A random effect of participant number was included in the model. The ID_C variable was mean-centered, and the 90° corner angle condition and 1.0 path ratio condition were set as the reference categories for the corner angle and path ratio variables, respectively. Therefore, changes in the odds ratios for these variables reflect changes from their respective reference group. To compare across all three levels of corner angle and path ratio, we changed the reference categories and refit the model.

Our results indicated that ID_C was a significant predictor of cornering success (see Table 14). As the ID_C value increased by one, the odds of successful cornering decreased by nearly 100%. This was somewhat expected, given that the difficulty of negotiating a corner approaches infinity as the ID_C value increases.

Table 14

Logistic Regression Output Predicting Cornering Success in Experiment 2.

Predictor	β (*SE*)	Odds Ratio	95% CI for Odds Ratio		*z*
			Lower limit	Upper limit	
ID_C	-10.38 (1.85)	< 0.001	< 0.001	0.001	-5.62***
Corner Angle					
45°	0.85 (0.62)	2.33	0.69	7.86	1.37
135°	-2.14 (0.4)	0.12	0.05	0.26	-5.29***
Path Ratio					
0.8	0.01 (0.48)	1.01	0.4	2.55	0.01
1.2	0.69 (0.52)	1.99	0.72	5.48	1.33
ID_C * Corner Angle					
ID_C * 45°	9.32 (2.81)	11,187	45.25	2,765,873	3.32***
ID_C * 135°	-6.65 (1.98)	0.001	< 0.001	0.06	-3.36***
ID_C * Path Ratio					
ID_C * 0.8	-7.32 (2.14)	< 0.001	< 0.001	0.04	-3.41***
ID_C * 1.2	0.77 (2.06)	2.17	0.04	123.73	0.37
Corner Angle * Path Ratio					
45° * 0.8	0.04 (0.79)	1.04	0.22	4.86	0.05
135° * 0.8	-1.23 (0.53)	0.29	0.1	0.83	-2.31*
45° * 1.2	0.7 (1.22)	2.01	0.18	22.17	0.57
135° * 1.2	0.48 (0.51)	1.61	0.59	4.39	0.93

With respect to corner angle, we found that the odds of successful cornering decreased by 82% when the corner angle was 135° compared to 90°. Although not statistically significant, results indicated that the odds of successful cornering increased by 133% when the corner angle was 45° compared to 90°. Overall, the odds of successful

cornering increased as the corner angle decreased. Results indicated that there were no significant differences in the odds of cornering success depending on path ratio.

We found that the effect of ID_C was moderated by corner angle. Results indicated that all slopes were significantly different from each other, *p*s < .001. As seen in Figure 35, the probability of successful cornering decreased at a more rapid rate as the corner angle increased. The ID_C also moderated by path ratio. Results indicated that the slope for the 0.8 path ratio was significantly different from the slope for the 1.0 and 1.2 path ratios, *p*s < .001. There was not a significant difference in the slopes between the 1.0 and 1.2 path ratios (Figure 36).

Figure 35

Predicted Probability of Cornering Success by Corner Angle

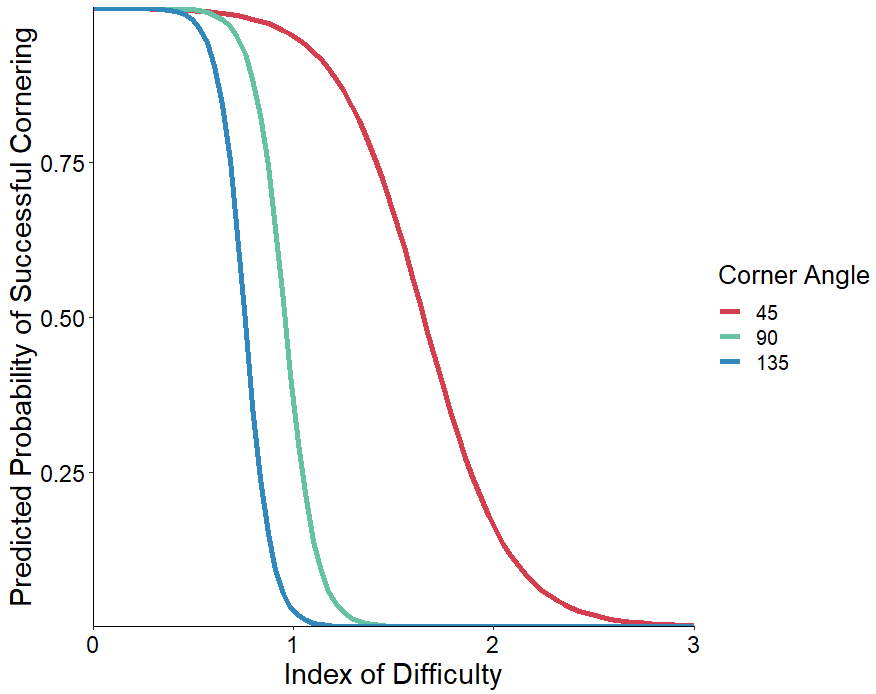

Figure 36

Predicted Probability of Cornering Success by Path Ratio

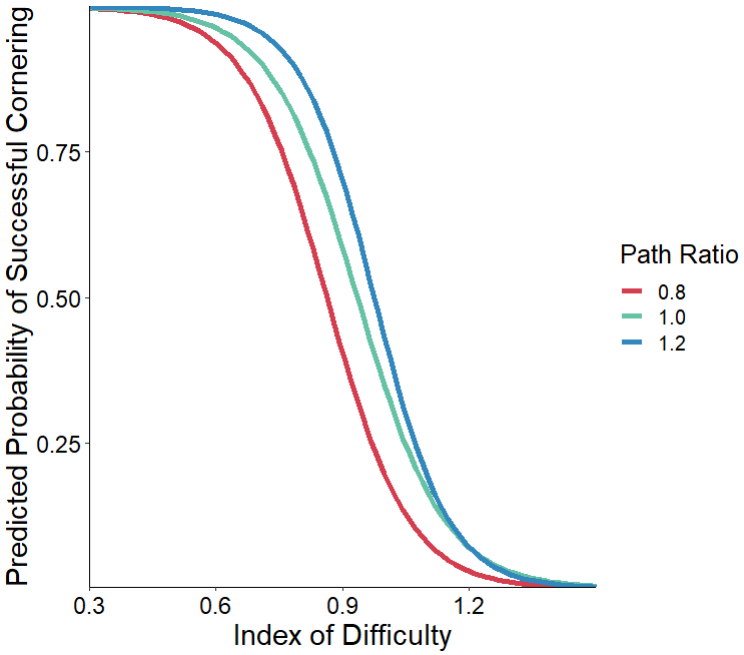

To evaluate the interaction between path ratio and corner angle on cornering success, we first split the data by corner angle to assess the change in odds ratios among the different path ratios. For 45° corners, there was not a significant difference between the path ratios on cornering success (see Table 16). That is, the odds of successful cornering were similar regardless of path ratio.

For both 90° and 135° corners, the odds of successful cornering decreased significantly when the path ratio was 0.8 compared to 1.0 and when the path ratio was 1.0 compared to 1.2. Additionally, the odds of successful cornering increased when the path ratio was 1.2 compared to 0.8. In other words, the odds of successful cornering increased as the path ratio also increased.

We also split the data by path ratio condition to evaluate changes in the odds ratios among the different corner angles. Across all path ratios, we found that the odds of cornering success increased by more than 100% when the corner angle was 45° compared to 90° and when the corner angle was 90° compared to 135° (see Table 16). Furthermore, across all path ratios, the odds of cornering success decreased by nearly 100% when the corner angle was 135° compared to 45°. In other words, the odds of cornering success increased as the angle decreased across all path ratio conditions.

Table 15

Odds Ratios for each Path Ratio by Corner Angle

Corner Angle	Path Ratio	Odds Ratio	95% CI for Odds Ratio		*z*
			Lower Limit	Upper Limit	
45°	0.8 (ref. = 1.0)	0.56	0.14	1.88	-0.92
	1.0 (ref. = 1.2)	0.24	0.01	1.68	-1.25
	1.2 (ref. = 0.8)	7.33	1.28	138	1.85
90°	0.8 (ref. = 1.0)	0.32	0.17	0.6	-3.52***
	1.0 (ref. = 1.2)	0.44	0.19	0.97	-1.98*
	1.2 (ref. = 0.8)	7.11	3.4	16.24	4.96***
135°	0.8 (ref. = 1.0)	0.25	-.14	0.43	-4.92***
	1.0 (ref. = 1.2)	0.24	0.13	0.43	-4.67***
	1.2 (ref. = 0.8)	17.26	9.06	34.65	8.35***

Note: * denotes $p < .05$, ** denotes $p < .01$, *** denotes $p < .001$

Table 16

Odds Ratios for each Corner Angle by Path Ratio

			95% CI for Odds Ratio		
Path Ratio	Corner Angle	Odds Ratio	Lower Limit	Upper Limit	*z*
0.8	45° (ref. = 90°)	11.82	5.18	30.72	5.51***
	90° (ref. = 135°)	37.71	17.24	91.19	8.57***
	135° (ref. = 45°)	0.002	0.001	0.006	-10.93***
1.0	45° (ref. = 90°)	6.36	2.26	22.63	3.23***
	90° (ref. = 135°)	18.23	9.36	38.17	8.14***
	135° (ref. = 45°)	0.009	0.002	0.02	-8.18***
1.2	45° (ref. = 90°)	11.94	2.17	223.3	2.31*
	90° (ref. = 135°)	18.61	8.14	48.26	6.48***
	135° (ref. = 45°)	0.005	< 0.001	0.023	-5.1***

Note: * denotes $p < .05$, ** denotes $p < .01$, *** denotes $p < .001$

Success Rate. Like Experiment 1 success rate was defined as the overall percentage of successful trials by corner angle, path congruency, and ID_C. To reiterate, a trial was considered successful if the corner was negotiated without collision. As expected, subjects negotiated 45° corners quite successfully, with a success rate consistently greater than 90%, regardless of path congruency and ID_C value (see Figure 37). For 90° corners, success rate exceeded 93% across all ID_C values except the most difficult one: 0.874. On those more difficult trials, the success rate fell, and even hit below 50% for the narrow path congruency. Lastly, for 135° corners, success rate decreased as ID_C value increased (i.e., as the task became more difficult). These results are further supported by looking at the average collision count by corner angle (see Figure 38).

Figure 37

Percentage of Successful Trials in Experiment 2

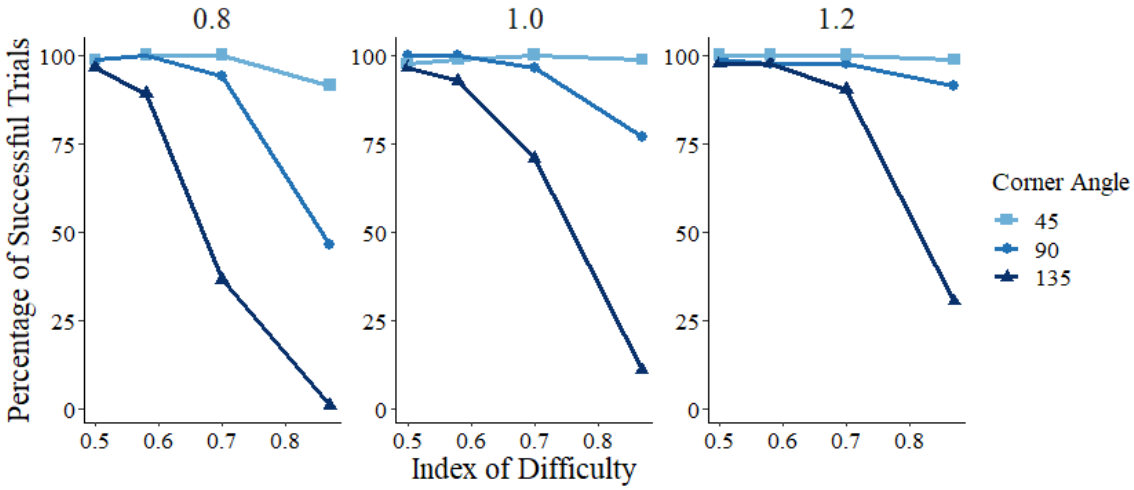

Figure 38

Average Collision Counts by ID_C and Corner Angle in Experiment 2

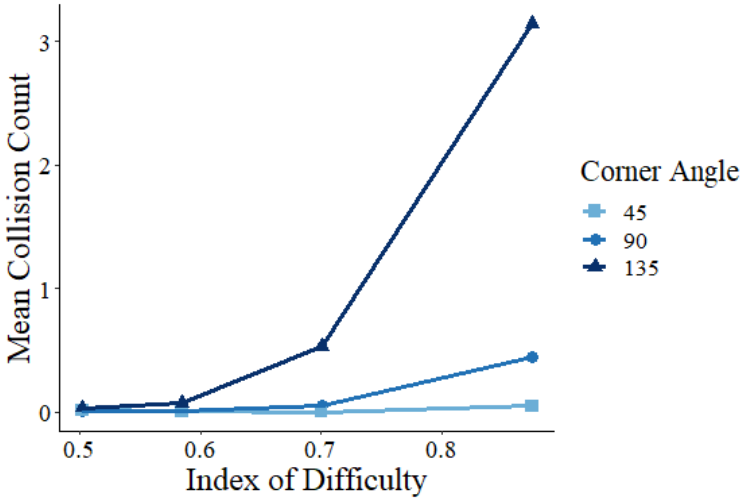

Video Gaming Experience

Like Experiment 1, we asked subjects to rate the frequency at which they play video games. We again converted this into a binary gaming experience variable, where those individuals who responded on the lower end of the scale (options 1-3) were denoted as having limited gaming experience, and those individuals who responded on the higher end of the scale (options 4-6) were denoted as having moderate gaming experience. Participants' gaming experience ratings can be found in Table 17.

We fit a linear mixed model predicting log-transformed cornering time with ID_C, corner angle, and gaming experience as predictor variables. The ID_C variable was mean-centered, and a random effect of participant number was included in the model. Here, we only focus on the results involving the gaming variable. Results indicated that there was not a main effect of gaming experience on log-transformed cornering times, but there was a significant interaction between gaming experience and corner angle, $F(2, 2935) = 15.52$, $p < .001$. However, post-hoc comparisons revealed that there were no significant differences between limited and moderate gaming experience for each corner angle. There was also a significant interaction between gaming experience and ID_C value, $F(2, 2{,}925) = 5.35$, $p = .02$, such that the slope for individuals with limited gaming experience was significantly steeper than the slope for individuals with moderate gaming experience (see Figure 39). We also conducted a mixed effects binomial logistic regression to determine whether gaming experience was a significant predictor of cornering success. There was, however, no significant difference in cornering success depending on gaming experience. This can easily be seen in Figure 40.

Table 17

Video Gaming Experience for Experiment 2 Subjects.

Video Gaming Frequency	*N*	Gaming Experience
Never	10	
Almost Never (Less than 1 time a month)	13	Limited
Not Very Often (1-2 times a month)	7	
Often (1-2 times a week)	6	
Fairly Often (3-4 times a week)	2	Moderate
Very Often (5-7 times a week)	4	

Figure 39

Estimated Cornering Time by ID_C and Gaming Experience in Experiment 2

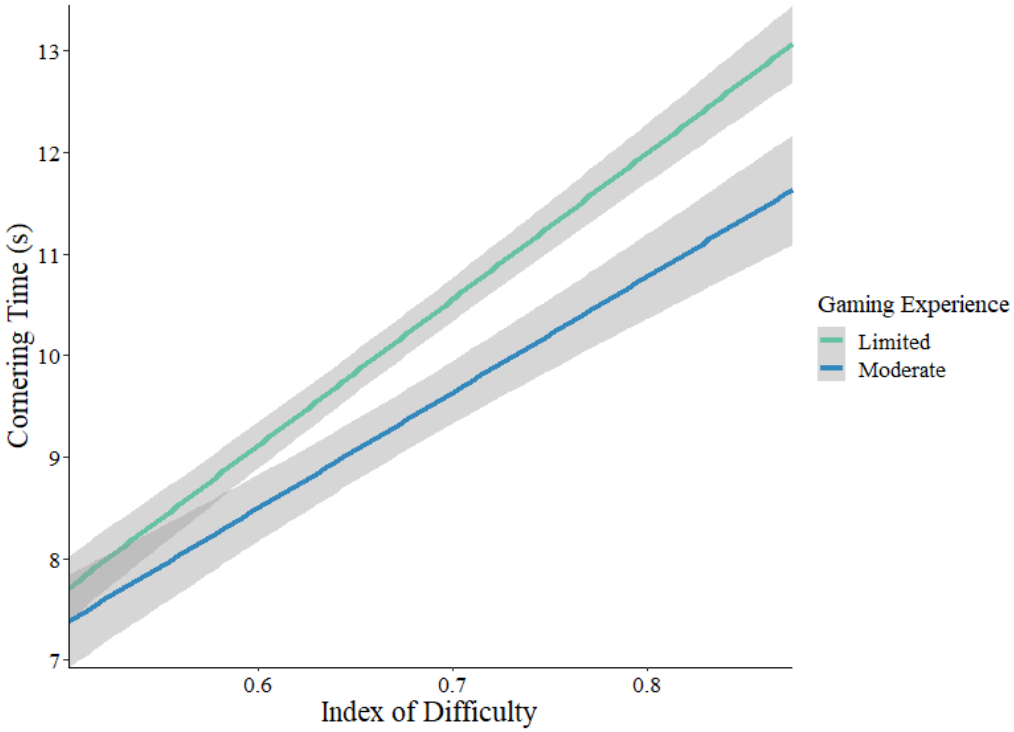

Figure 40

Predicted Probability of Successful Cornering by Video Gaming Experience

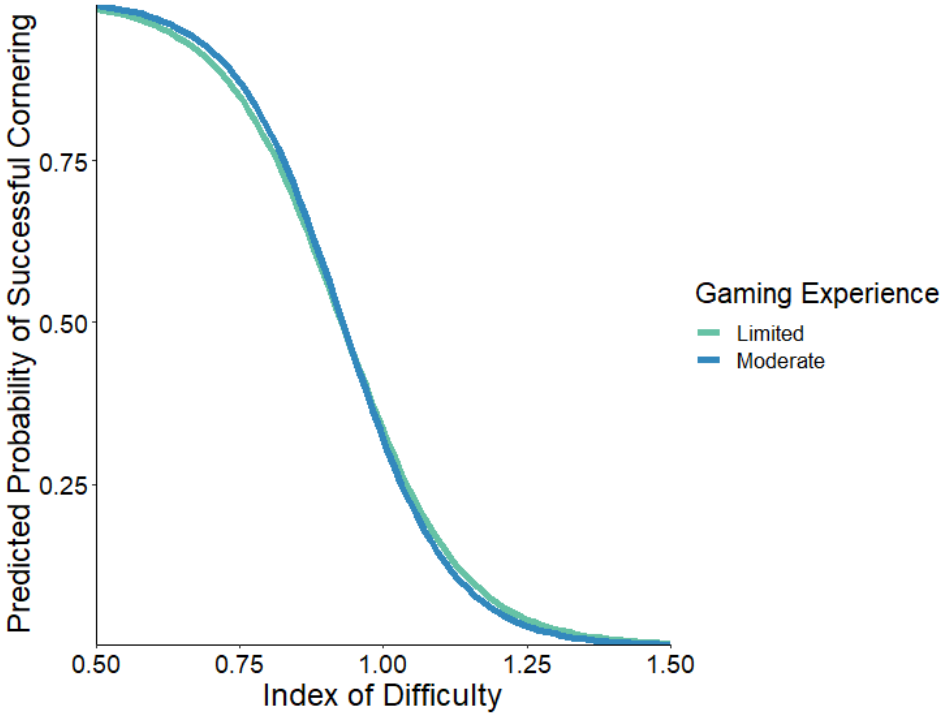

Collision Information

Using the unique collision count, we found that collision durations increased as corner angle increased and that collision durations were, on average, slightly greater for right turns compared to left turns (see Table 18). We found that 68.5% of collisions were less than one second.

As previously mentioned, collisions were logged into two groups: collisions before the turn and collisions after the turn. For both before and after the turn, most collisions on the inside of the corner occurred on the side of the vehicle compared to the front or back of the vehicle (see Table 19). This was not the case for collisions on the

outside of the corner. When collisions on the outside of the corner occurred before the turn, they mostly occurred at the back (40.4%) or sides (55.1%) of the vehicle compared to the front of the vehicle (4.5%). Collisions after the turn most frequently occurred at the front of the vehicle (86.5%) compared to the back (0.5%) or sides (13%) of the vehicle.

Table 18

Descriptive Statistics for Collision Durations (s) by Turn Type and Corner Angle

Variable	Levels	M (SD)	Median	Maximum
Turn Type	Right	1.66 (3.77)	0.58	40.2
	Left	1.25 (1.9)	0.64	15.74
Corner Angle	45°	1.11 (1.62)	0.55	13.5
	90°	1.38 (2.78)	0.62	27.5
	135°	1.69 (3.54)	0.64	40.2

Table 19

Number of Collisions on the Vehicle and the Corner in Experiment 2.

Corner Location	Front	Back	Left Side	Right Side
Inside	140 (2.5%)	81 (4.3%)	1,677 (51.7%)	1,345 (41.5%)
Outside	239 (20.2%)	544 (46%)	185 (15.6%)	215 (18.2%)

Workload

Perceived workload was assessed using the NASA-TLX and was recorded after each block of trials. This allowed us to determine the extent to which perceived workload was influenced by corner angle. As expected, we found that all facets of perceived

workload increased as the corner angle increased (see Figure 41). For performance, a higher NASA-TLX value is associated with poorer perceived performance.

We conducted repeated measures analyses of variance to determine whether NASA-TLX scores for each scale varied significantly by corner angle. There was an effect of corner angle on mental demand scores, $F(2, 122) = 63.11$, $p < .001$. Post-hoc comparisons revealed that mental demand scores were significantly different between 135° corners and 90° corners, $t(122) = 8.37$, $p < .001$ and between 135° and 45° corners, $t(122) = 10.68$, $p < .001$. There was a marginally significant difference in mental demand scores between 90° and 45° corners, $t(122)= 2.31$, $p = .058$.

There was also an effect of corner angle on physical demand scores, $F(2, 122) = 5.43$, $p = .005$. Post-hoc comparisons revealed that there was a significant difference between 135° and 45° corners, $t(122) = 3.25$, $p = .004$. Similarly, there was an effect of temporal demand scores, $F(2, 122) = 6.25$, $p = .003$, with a significant difference in scores between 135° and 45° corners, $t(122) = 3.49$, $p = .002$.

There was an effect of corner angle on effort scores, $F(2, 122) = 33.48$, $p < .001$. Post-hoc comparisons revealed that all corner angles were significantly different from each other ps $< .01$. There was also an effect of corner angle on performance scores, $F(2, 122) = 61.67$, $p < .001$. Post-hoc comparisons revealed that performance scores were significantly different between 135° corners and 90° corners, $t(122) = 8.24$, $p < .001$ and between 135° and 45° corners, $t(122) = 10.57$, $p < .001$. There was a marginally significant difference in mental demand scores between 90° and 45° corners, $t(122) = 2.34$, $p = .055$.

Lastly, there was a significant effect of corner angle on frustration scores, $F(2, 122) = 26.53$, $p < .001$. Post-hoc comparisons revealed that mental demand scores were significantly different between 135° corners and 90° corners, $t(122) = 8.24$, $p < .001$ and between 135° and 45° corners, $t(122) = 10.57$, $p < .001$. There was a marginally significant difference in mental demand scores between 90° and 45° corners, $t(122) = 2.34$, $p = .055$. Table 20 provides an overview of which post-hoc comparisons were statistically significant.

Figure 41

Average NASA-TLX Values by Corner Angle

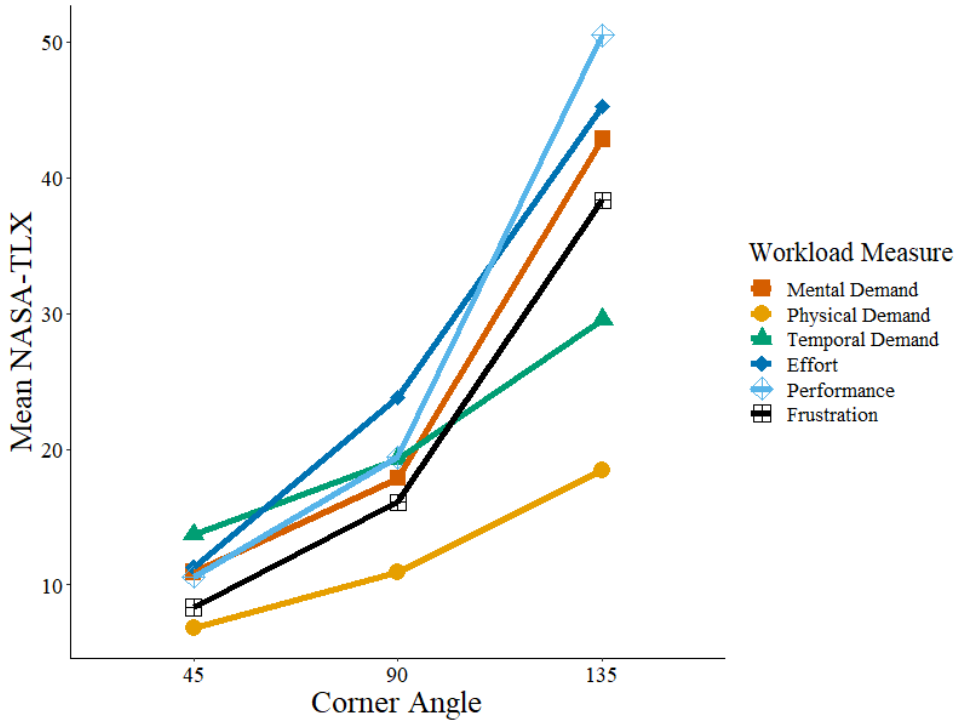

Table 20

Post-hoc Significance Tests for NASA-TLX Scales in Experiment 2

NASA-TLX Scale	45° vs. 90°	90° vs. 135°	45° vs. 135°
Mental Demand	-	*	*
Physical Demand	-	-	*
Temporal Demand	-	-	*
Effort	*	*	*
Performance	-	*	*
Frustration	-	*	*

Note: * denotes $p < .05$, - denotes $p > .05$

Cornering Law

Like Experiment 1, we assessed Pastel et al.'s (2007) cornering law by aggregating the data by ID_C value and fitting a linear model with the ID_C as a predictor of cornering time (see Eq. 1). The IDc was calculated using Equation 3. Even though the data were aggregated across the different cornering angles and path ratios, we found that the model fit the data well, with an R^2 value of .93. Like Experiment 1, we again found that including the second order term of IDc produced a better model fit (see Figure 42). Looking at average cornering times by corner angle yielded similar findings (see Figure 43). That is, simply using the ID_C to predict cornering time for each corner angle was sufficient but incorporating the second order term of ID_C fit the data better.

Figure 42

Average Cornering Time by ID_C fit to a First Order Regression Model (left) and a Second Order Regression Model (right) in Experiment 2.

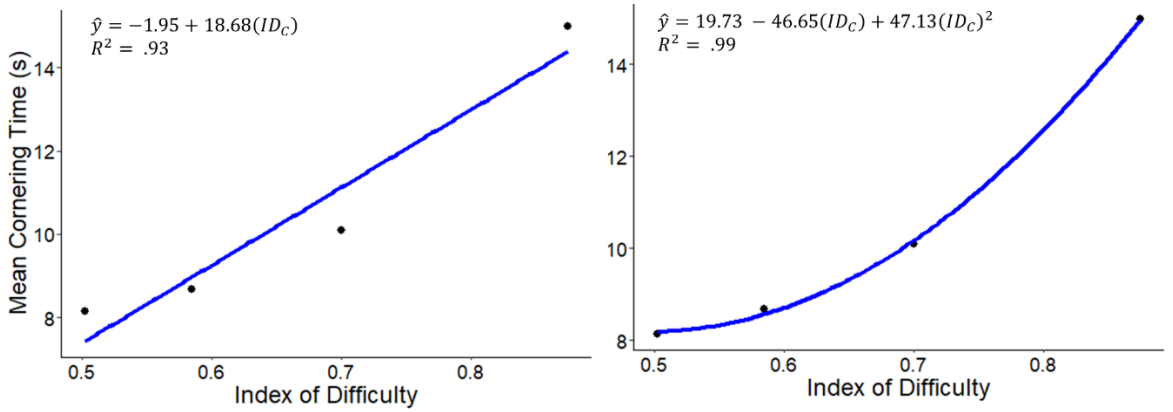

We also conducted a series of Pearson product moment correlations to examine the relationship between log-transformed cornering time and the oncoming path width, the current path width, and the ID_C value. For 45° corners, there was a statistically significant correlation between log-transformed cornering time and oncoming path width, $r(1,005) = -.15$, $p < .001$, between log-transformed cornering time and current path width $r(1,005) = -.15$, $p < .001$, and between the ID_C and log-transformed cornering time, $r(1,005) = .16$, $p < .001$. For 90° corners, there was a statistically significant correlation between log-transformed cornering time and oncoming path width, $r(995) = -.37$, $p < .001$, between log-transformed cornering time and current path width $r(995) = -.38$, $p < .001$, and between the ID_C and log-transformed cornering time, $r(995) = .39$, $p < .001$. Similarly, for 135° corners, there was a statistically significant correlation between log-transformed cornering time and oncoming path width, $r(967) = -.62$, $p < .001$, between

log-transformed cornering time and current path width $r(967) = -.61$, $p < .001$, and between the ID_C and log-transformed cornering time, $r(967) = .64$, $p < .001$. In sum, the oncoming path width, current path width, and ID_C were all similarly related to log-transformed cornering times. Additionally, the correlations were stronger as the corner angle increased.

Figure 43

Average Cornering Time by ID_C and Corner Angle fit to a First Order Regression Model (left) and a Second Order Regression Model (right)

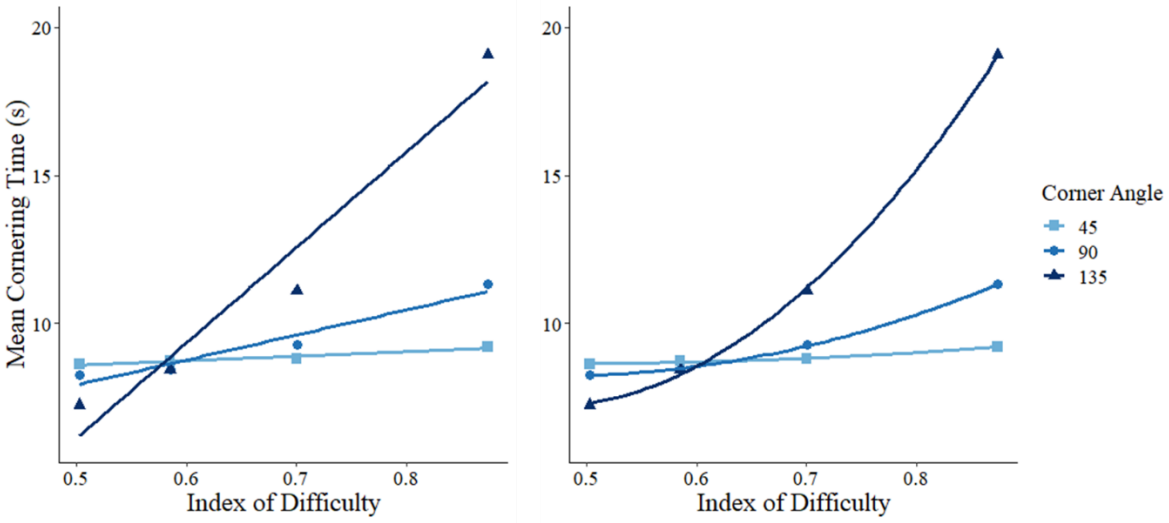

Adapted Index of Difficulty. Given the large discrepancies in cornering time across the various corner angles and path ratios, we investigated how to adapt the ID_C equation to incorporate the influence of these variables. As shown above, cornering times varied drastically for 135° corners. While these corners required more turning of the

vehicle, there was also the opportunity to cut off the corner, decreasing the distance travelled and the cornering time. Thus, for corners greater than 90°, we believed incorporating an estimated distance travelled into the task difficulty was appropriate. We adapted the ID_C equation as follows:

$$ID_{C4} = \begin{cases} \frac{A}{C_w}(0.003(x-90)+1), & x \leq 90° \\ \frac{A_e}{C_w}(0.003(x-90)+1), & x > 90° \end{cases} \quad (9)$$

where A is the amplitude of the corner, A_e is the effective amplitude of the corner, C_w is the weighted track clearance of the corner, and x is the corner angle. Because we did not capture the vehicle's distance travelled from start to finish for each corner in this experiment, we calculated the effective corner amplitude as,

$$A_e = CT * v_{max} \quad (10)$$

where CT is the cornering time and v_{max} is the maximum speed of the vehicle. Finally, the weighted track clearance was computed as,

$$C_w = c_1(w_1 - p) + c_2(w_2 - p) \quad (11)$$

where w_1 is the current path width, w_2 is the oncoming path width, p is the vehicle widths, and c_1 and c_2 are weights whose values sum to one. We found that using weight values of 0.5 worked best. In other words, the C_w was simply the average track clearance. Here, we should note that Equation 11 assumes that the vehicle width is smaller than both path widths. The last part of the adapted ID_C equation incorporates an adjustment for the corner angle. This adjustment term takes on a value of one when the corner angle is 90°, and it deviates by a value of 0.003 for every degree of deviation from 90°. Therefore, the ratio, A_e/C_w, is multiplied by a value greater than one when the corner angle exceeds 90°,

resulting in a larger ID_C value, and the ratio term is multiplied by a value less than one when the corner angle is less than 90°, resulting in a smaller ID_C value.

This adapted ID_C is based on Equation 4. In fact, when the path widths are equal and the corner angle is 90°, Equations 4 and 9 become identical. To maintain similarity with information theory, we can adapt the ID_C further to,

$$ID_{C5} = \begin{cases} log_2\left(\frac{A}{C_w}(0.003(x-90)+1)\right), & x \leq 90° \\ log_2\left(\frac{A_e}{C_w}(0.003(x-90)+1)\right), & x > 90° \end{cases} \quad (12)$$

The adapted ID_C equations should yield an ID_C value for each corner angle, amplitude, oncoming path width, and current path width combination. For the data from Experiment 2, we obtained 36 adapted ID_C values. To evaluate how well our adapted ID_C equations performed, we first fit linear regression predicting cornering time with the adapted ID_C from Equation 9 as the predictor variable. We found that the data fit the model well, with an R^2 value of .96 (see Figure 44). Using Equation 12, we fit a second order regression model and found that the data fit the model equally well, with an R^2 value of .97 (see Figure 45).

Figure 44

Average Cornering Time by Adjusted ID_C Value

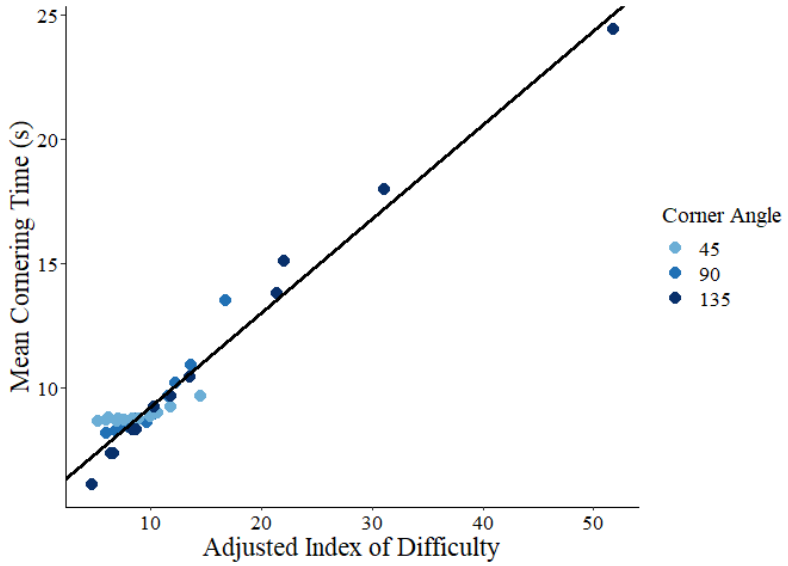

Note: The adjusted ID_C value was computed using Equation 9.

Figure 45

Average Cornering Time by Adjusted ID_C Value fit to a Second Order Regression Model

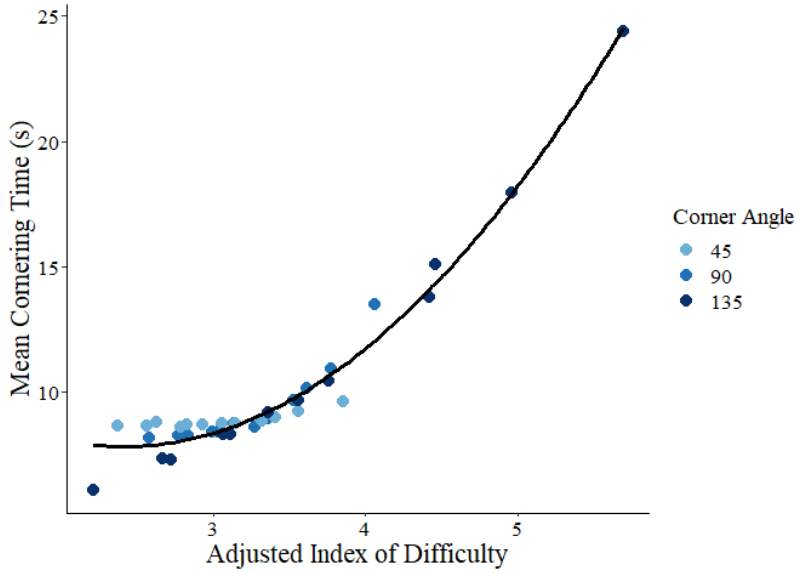

Note: The adjusted ID_C value was computed using Equation 12.

Discussion

In Experiment 2, we tested how teleoperation performance varied as the corner angle, ID_C value, and path ratio were manipulated. With respect to cornering time, we hypothesized that time would increase as the ID_C increased and as the corner angle increased. We also anticipated that there would be some effect of path ratio on cornering time. Consistent with the prior cornering law studies (Chan et al., 2019; Cross et al., 2018; Helton et al., 2014; Pastel et al., 2007), we found that cornering time did increase as the ID_C increased; subjects took longer to negotiate corners that had a higher task difficulty. We extended previous cornering research by showing that corner angle is an important aspect of the cornering task difficulty. In general, we found that cornering times increased as the corner angle increased, but the increase in cornering times between 45° and 90° corners was not nearly as drastic as the increase in cornering times between 90° and 135° corners. An important exception to this finding was when the ID_C value was lowest ($ID_C = 0.5$). In this instance, cornering times were shortest for 135° corners. Upon reviewing the video recordings, we found this was because subjects were consistently cutting the corners. They travelled a shorter distance, and therefore, negotiated the corner in a shorter period of time.

That cornering time increased as the corner angle increased is somewhat inconsistent with Pastel's (2006) findings. In their study, subjects negotiated corners of varying angles using a cursor. They found that movement time was shortest for the sharp corners and longest for 90° corners. This difference in findings is likely due to the difference in nature between the two tasks. When negotiating corners with an optical

mouse, the cursor mimics the movements of one's hand/arm, but when negotiating corners with a controller, the virtual vehicle mimics the movements of the controller input. As Pastel (2006) noted, when specifically negotiating the sharp corner, subjects' arms could engage in a loaded and unloaded movement, which could explain the shorter movement time. The ability to negotiate the corner is inherently dependent on numerous factors of the vehicle, such as its weight, speed, dimensions, and turning radius, to name a few. For example, Wynn et al. (2015) found that quolls (a small marsupial similar to the opossum) reduced their turning speed when negotiating corners with greater angles, which allowed for an increase in turning rate and a decrease in turning radius. For consistency across different path widths, we kept various aspects of the vehicle the same (e.g., maximum speed, weight), but future research is needed to understand better how these factors influence teleoperation performance.

Another important distinction between our task and Pastel's (2006) task is the point of view. Pastel's (2006) subjects viewed the entirety of the corner from a top-down perspective, while subjects in our experiment viewed the corner from a first-person perspective. For our subjects, this made it more difficult to determine the length of the vehicle, which may provide some explanation for the frequent collisions on the inside of the corner. There is some research to suggest that perspective does have an impact of driving performance and corner negotiation. For example, Helton et al. (2014) noted that cornering times were somewhat faster when viewing in a top-down perspective compared to a first-person perspective. However, Bateman et al. (2001) found that virtual driving

performance was worse when viewing from an overhead perspective compared to a first-person or third-person point of view.

Similar to Experiment 1, we found that cornering times for a given ID_C value varied drastically. Again, we contend that the considerable variability in cornering times is likely due to differences in operator skill and spatial abilities. Unlike Experiment 1, we found that subjects with moderate gaming experience negotiated corners faster than subjects with limited gaming experience, which is consistent with previous findings (Dye et al., 2009; Nenna & Gamberini, 2022).

Regarding the path ratio, we found that overall cornering times increased as the path ratio decreased. That is, subjects took longer to negotiate corners when the current path was narrower than the oncoming path. A possible explanation for this finding is that subjects had more space to reorient the vehicle prior to the turn when the current path was wider than the oncoming path. When starting out on a narrower path, relative to the oncoming path, there is less room to reposition the vehicle as it approaches the apex of the corner. Looking at the collision data, we found that there were more collisions when the current path was narrower than the oncoming path (i.e., when the path ratio was 0.8), which could explain the increased cornering time and decreased probability of cornering success.

We also hypothesized that the number of collisions would increase as the ID_C increased and as the corner angle increased. Like Experiment 1, we analyzed cornering success; that is, whether the subject could negotiate the corner without collision. As expected, we found that the probability of successful cornering decreased as ID_C value

increased, and this effect was more pronounced as the corner angle increased and as the path ratio decreased. In other words, subjects were more likely to negotiate the corner without collision when the corner angle was 45° and when the path ratio was 1.2 (i.e., when the current path was wider than the oncoming path). The increased probability of collision at larger corner angles is consistent with Wynn et al.'s (2015) findings for quolls' turning behaviors.

Because we manipulated both the corner angle and the oncoming and current path widths, Experiment 2 utilized lower ID_C values than Experiment 1. As a result, the relationship between collision count and cornering time was less straightforward (Figure 46). For the most part, there were few collisions for 45° and 90° corners, across all ID_C values. The positive association between these two variables only becomes somewhat clear for 135° corners with an ID_C value of 0.87. Our findings in both experiments highlight that the relationship between cornering time and collision count is not so straightforward. The relationships among corner angle, path ratio, instruction method, and vehicle mechanics all play an important role in defining the relationship between cornering time and collision count. As we have shown in Experiment 2, corners with a lower task difficulty and corners that require fewer degrees of turning elicit a decreased likelihood of collision. However, we contend that the vehicle's maximum speed moderates this relationship. If the vehicle can travel at high speeds, the operator might be more likely to lose control of the vehicle and make a collision, regardless of turning angle and the path widths. Conversely, if the vehicle's maximum speed is quite low, the likelihood of making a collision could be reduced for more difficult turns. An important

caveat is that a slower vehicle speed could make the vehicle more likely to get stuck in a tight corner, as we noted in Experiment 1.

Figure 46

Cornering Time and Collision Count by ID_C Value and Corner Angle

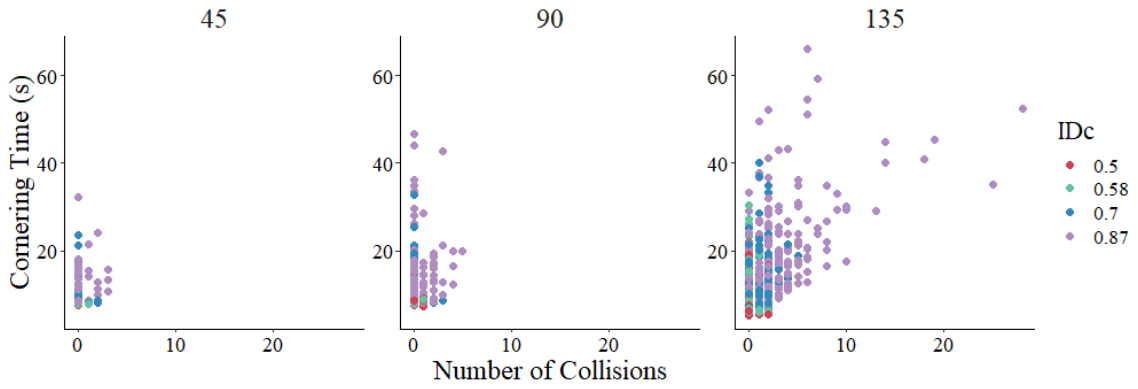

Like Experiment 1, we investigated collision locations. In general, we found that the majority of collisions occurred when the corner angle was 135° and that these collisions mostly occurred on the inside of the corner. The frequent collisions on the inside of the corner suggest that subjects were attempting to cut the corner, which is consistent with our review of the video recordings. As expected, collisions on the inside of the corner were the result of the sides or front of the vehicle colliding with the wall. The length of the vehicle likely contributed to the increased number of collisions on the inside of the corners vs. the outside of the corners. For instance, the length of the vehicle was more than 2.5 times the width of the vehicle, which could have made it more difficult for subjects to (initially) determine whether they could negotiate the corner without

collisions. For collisions that occurred on the two walls comprising the outside of the corner, there was difference in collision location on the vehicle depending on whether the collision was on the current path or the oncoming path. Collisions before the turn mostly occurred on the back or sides of the vehicle, which suggests that subjects reversed the vehicle to negotiate the corner and/or drove too close to the outer edge of the path when trying to take a wide turn. Collisions after the turn almost exclusively occurred at the front of the vehicle.

It was more difficult to assess a calibration effect in this experiment as each unique corner was only negotiated twice. However, looking at overall cornering times as a function of block order, corner angle, and ID_C value revealed that average cornering times for the 135° corners were faster when these corners were negotiated last. This could suggest that subjects, to some degree, improved over time, which is consistent with previous studies (Armstrong et al., 2014, 2015; Helton et al., 2014; Schmidlin & Jones, 2016). Like Experiment 1, subjects completed the NASA-TLX after each block. Unlike Experiment 1, blocks were sectioned by corner angle as opposed to ID_C value. This allowed us to assess changes in perceived workload by corner angle. In general, perceived workload increased as the corner angle increased, but the increase was statistically significant for all six scales between 45° corners and 135° corners. Again, these results are consistent with findings that perceived workload increases as the task demands increase (Shao et al., 2020).

One of the main goals of Experiment 2 was to test the efficacy of the cornering law. We wanted to determine whether the cornering law could account for differences in

corner angle and path ratios. Given the significant differences in cornering time depending on the angle of the negotiating corner, it was expected that we would need to adapt the equation for quantifying the task difficulty. First, to evaluate how well the ID_C could predict cornering time, according to Pastel et al.'s (2007) cornering law, we aggregated the data by ID_C value. We found that the data fit the model well, despite being aggregated across the various corner angles and path ratios. Consistent with our findings from Experiment 1, we discovered that adding the quadratic ID_C term to the model improved the model fit. The findings were similar when split by corner angle. Overall, our results indicated that for each ID_C value, cornering times varied depending on the corner angle, and fitting the models separately for each corner angle sufficiently captured average cornering time performance. We maintain, however, that the relationship between cornering time and the ID_C value is likely quadratic; this becomes more evident as the corner angle increases (see Figure 43).

Despite finding that the original cornering law equation could model cornering time for each corner angle separately, we investigated further how the ID_C equation could be adapted so that the aggregated cornering times could be fit to a single model. Our findings revealed that the distance travelled varied drastically for 135° corners. When the path widths were wider, subjects were able to cut off more than 10 meters of the corner's amplitude, resulting in a significant reduction in cornering times. When the path widths were narrower, subjects were unable to negotiate the corner with a single turning movement, resulting in longer cornering times. Although all corner amplitudes were the same, subjects travelled much shorter distances by cutting the corners for wider paths and

much longer distances by reversing and repositioning the vehicle for narrower paths. For the 45° and 90 corners, there was much less cutting off of the corner. To adapt the ID_C equation, we incorporated the amplitude of the corner, with an adjustment specifically for corners greater than 90° that includes the effective amplitude of the corner. This value decreases when the subject cuts off the corner and increases when the subject makes corrective movements to negotiate the corner. Ultimately, we were able to adapt the ID_C equation to incorporate changes in corner angle and path width. While our adapted ID_C fit our data well, it is unclear the extent to which the equation will generalize to other datasets.

Experiment 2 tested several assumptions of Pastel et al.'s (2007) cornering law. We found that corner angle, path ratio, and ID_C value influenced cornering time and cornering success. Although we found that the cornering law could account for these differences to some extent, we developed a new method for quantifying the ID_C that captures differences in path widths and corner angles without the need to fit separate models. In conclusion, we demonstrated that numerous factors that influence teleoperation performance and that the relationship between cornering time and the number of collisions is not clear cut.

CHAPTER IV

GENERAL DISCUSSION

Previously, researchers have shown that cornering time could be modeled as a function of an index of difficulty specifically for corners (e.g., Pastel et al., 2007). This relationship is referred to as the cornering law and is similar to Fitts' law. The cornering index of difficulty, denoted ID_C, is based on information theory and has been shown to adequately model average cornering times under various conditions, such as time delays and lighting conditions (Cross et al., 2018). Given the cornering law's recent development, there exist various gaps in our understanding of how outside factors might contribute to an operator's cornering performance.

In Experiment 1, cornering performance (i.e., cornering time and probability of successful cornering) was evaluated as a function of instruction method. We aimed to understand the relationship among instruction method, cornering time, and collision frequency. Results indicated that as the ID_C value increased, cornering time increased, and the probability of negotiating the corner without collision decreased. Furthermore, we found that subjects instructed to focus on accuracy had longer cornering times and fewer collisions than subjects instructed to focus on speed.

In Experiment 2, cornering performance was evaluated for different corner angles and path ratios. Up until now, the cornering law had only been tested for 90° corners and for corners whose current path width and oncoming path width were equivalent. Therefore, the aim of Experiment 2 was to evaluate how well the cornering law could model cornering time for various changes in the corner's geometry. Results indicated that

as the ID_C value increased, cornering time increased, and the probability of negotiating the corner without collision decreased. Additionally, cornering time and collision count increased as the corner angle increased and as the path ratio decreased.

Contributions

Teleoperation continues to be widely leveraged across a variety of domains spanning from USAR to entertainment and gaming. We believe the present experiments provide additional context for understanding how teleoperation performance is influenced by instruction method, corner angle, and the path widths of a given corner. In Experiment 1, we not only showed how teleoperation performance differs depending on instruction method, but we also provided a method for applying the ID_e to a cornering task. To our knowledge, this is the first study to do so. In Experiment 2, we showed that corner angle and path ratio are relevant factors of corner geometry that have significant impacts on teleoperation performance.

Across both experiments, we provided additional support for the cornering law. We demonstrated that average cornering time can be modeled as a function of the ID_C, even when the data are aggregated across instruction method, corner angle, and path ratio. In other words, the cornering law sufficiently quantifies average cornering time for corners of varying geometries. To appropriately model cornering time for the different corner angles, a separate model can be fit for each corner angle. To plot the average cornering times for each path ratio and corner angle combination using a single model, we developed a new method for quantifying the ID_C (see Equations 9 and 12). Results

indicated that the models for both equations fit the data well, accounting for over 95% of the variance in aggregated cornering times.

Consistent with much of the previous literature (Helton et al., 2014; Schmidlin & Jones, 2016), both experiments yielded some evidence of a calibration effect, showing that teleoperation performance does improve with time. In addition to cornering time, we also evaluated the probability of successful cornering. Consistent with previous findings (Chan et al., 2019; Pastel et al., 2007), we found that collisions were much more likely to occur as the ID_C value increased. We also noted that there were nearly three times the number of unique collisions in the speed condition compared to the accuracy condition. It was not surprising, therefore, that the probability of successful cornering was significantly greater when subjects were told to focus on accuracy. As expected, we found the subjects were more likely to negotiate 45° corners successfully than 90° and 135° corners.

One of the main contributions provided in this series of experiments is the empirical evaluation of collision locations. In both experiments, the majority of collisions occurred on the inside of the corner, indicating that subjects frequently attempted to cut the corner. This was a consistent trend across the different instruction methods, corner angles, and path ratios. The extent to which subjects could cut the corner increased as the corner angle increased. Therefore, there was much more of the corner to cut off for 135° corners than for 45° corners. This explains why for the widest turns, cornering times were, on average, much shorter for the 135° corners than for the 45° corners. There were also several instances where the back of the virtual vehicle collided with the outside of

the corner; this was most evident for 135° corners. This type of collision suggests that subjects reversed the vehicle to make corrective movements.

As expected, we found that perceived workload increased as the ID_C value increased and as the corner angle increased. For scenarios where operators may be negotiating these more difficult corners, it may be beneficial to utilize more autonomous robots that may be able to alleviate some of the cognitive burden associated with teleoperation.

Teleoperation Design Recommendations

From both experiments, we were able to highlight aspects of the teleoperation experience that worked well and those that could be improved. For instance, we provided various information about the vehicle in a directly perceivable manner. Placement of the camera above the vehicle, with the vehicle's hood in view, allowed subjects to perceive the width of the vehicle. Additionally, the textured walls allowed subjects to leverage optic flow in the environment, thus allowing them to perceive their rate of self-motion and heading direction. Despite being able to view the hood of the vehicle and environment periphery, subjects struggled to perceive the length of the vehicle, as evident in the frequent collisions that occurred on the sides of the vehicle. Therefore, providing an additional perspective such as a rear-facing camera or overhead camera may be beneficial to collision avoidance. In addition to the initial practice phase, where subjects were provided the opportunity to calibrate to the vehicle dimensions and maneuverability, subjects were also provided auditory feedback when a collision occurred. We believe these two factors helped mitigate the total number of collisions. Based on our findings,

we derived recommendations for the development and use of teleoperated robots and their respective input devices These recommendations can be found in Table 21.

Table 21

Teleoperation Recommendations

Teleoperation Factor	Recommendation(s)
Camera	• Place camera so hood of the vehicle is in view • Provide an additional rear camera viewpoint and/or an overhead viewpoint • Place camera above ground level (i.e., closer to one's eye-height) *Note: Providing too many viewpoints may yield cognitive tunneling*
Field of View	• Provide a wide field of view that allows the operator to perceive the optic flow in the periphery
Collision Feedback	• Provide feedback when a collision occurs
Latency & Time Delays	• Minimize any latency or time delay where possible • Provide operators the opportunity to calibrate to latency and/or time delays
Operator Experience	• Provide operator the opportunity to calibrate to the vehicle dimensions, the vehicle's maneuverability, the video feed quality, and the input device (i.e., let operators practice)

Future Research

The studies presented here provide a thorough investigation of how instruction method and corner geometry influence teleoperation performance. Throughout the process of data collection and analysis, we identified various avenues for additional research. First, we believe that future research should evaluate cornering time for more ID_C values to understand better the relationship. As we highlighted here, there was some

evidence to suggest that the relationship between task difficulty and cornering time is quadratic. Future research should be aimed at disentangling this relationship.

In Experiment 2, we manipulated the path ratio by changing the width of the current path width for a given oncoming path width. We found that cornering times were shorter when the current path was wider than the oncoming path (i.e., when turning onto a narrower path). While we believe this to be because the wider current path afforded more space for a larger turning radius, future research should further evaluate the effect of path ratio by manipulating the width of the oncoming path width. This will help increase our understanding of how the relationship between the current and oncoming path widths influences teleoperation performance.

Across both experiments, we noted that the relationship between cornering time and collision count was somewhat ambiguous. We believe this to be in large part because of the virtual vehicle's mechanics and maneuverability. If the vehicle travels at a slower speed, particularly if it can only travel at a slow speed, it is less likely for the vehicle to crash. If the vehicle's maximum speed is extremely high, then there may be more opportunities for a collision. Other relevant vehicle factors are the vehicle's dimensions, its weight, and its turning radius, as mentioned above. While we did not manipulate any of these variables, we believe they are relevant to an operator's teleoperation performance. Additional research should empirically test how these various factors influence both cornering time and collision frequency so that we can understand better how these two variables interact.

Furthermore, the effect of gaming experience was weak and somewhat ambiguous in both experiments. While it is possible that gaming experience is not strongly associated with teleoperation performance, it is also possible that our quantification of gaming experience was flawed. Perhaps a better method for quantifying gaming experience would be whether individuals had any experience instead of whether they had limited or moderate experience. In other words, it is likely that any amount of gaming experience is associated with improved teleoperation performance relative to zero gaming experience. It might be useful for future research to better quantify subjects' gaming experience and investigate differences between novice and expert video gamers.

Lastly, we believe that further research is needed to evaluate teleoperation performance under a variety of environmental conditions. Although conducting these two experiments virtually allowed us to easily track cornering time, collision count, collision locations, and collision durations, there was minimal ecological validity. The two experiments presented above were more akin to gaming than to USAR. As such, we believe future research should evaluate the cornering law under more realistic settings and quantify the effects of fog, rain, uneven terrain, and so forth on teleoperation performance. In addition, future research should quantify how contextual variables (e.g., sleep deprivation, adrenaline) influence teleoperation performance on cornering tasks.

Conclusion

The findings from these experiments highlight how teleoperation performance is impacted by instruction method and corner geometry. We showed that despite differences in cornering times across the various experimental conditions, Pastel et al.'s (2007)

cornering law could adequately model cornering time as a function of ID_C value. We also demonstrated that the ID_e could be applied to a cornering task, which has not been done prior to this work. Ultimately, the results from the experiments presented here emphasize that operator's ability to perform successfully in a teleoperation setting depends on variety of factors, and we present a new equation for computing the ID_C that can capture the influence of path ratio and corner angle.

APPENDIX A

Rating Scale Definitions for NASA-TLX

Title	**Endpoints**	**Description**
Mental Demand	Low/High	How much mental and perceptual activity was required (e.g., thinking, deciding, calculating, remembering, looking, searching, etc.)? Was the task easy or demanding, simple or complex, exacting or forgiving?
Physical Demand	Low/High	How much physical activity was required (e.g., pushing, pulling, turning, controlling, activating, etc.)? Was the task easy or demanding, slow or brisk, slack or strenuous, restful or laborious?
Temporal Demand	Low/High	How much time pressure did you feel due to the rate or pace at which the tasks or task elements occurred? Was the pace slow and leisurely or rapid and frantic?
Effort	Low/High	How hard did you have to work (mentally and physically) to accomplish your level of performance?
Performance	Good/Poor	How successful do you think you were in accomplishing the goals of the task set by the experimenter (or yourself)? How satisfied were you with your performance in accomplishing these goals?
Frustration Level	Low/High	How insecure, discouraged, irritated, stressed and annoyed versus secure, gratified, content, relaxed and complacent did you feel during the task?

APPENDIX B

NASA-TLX Scale

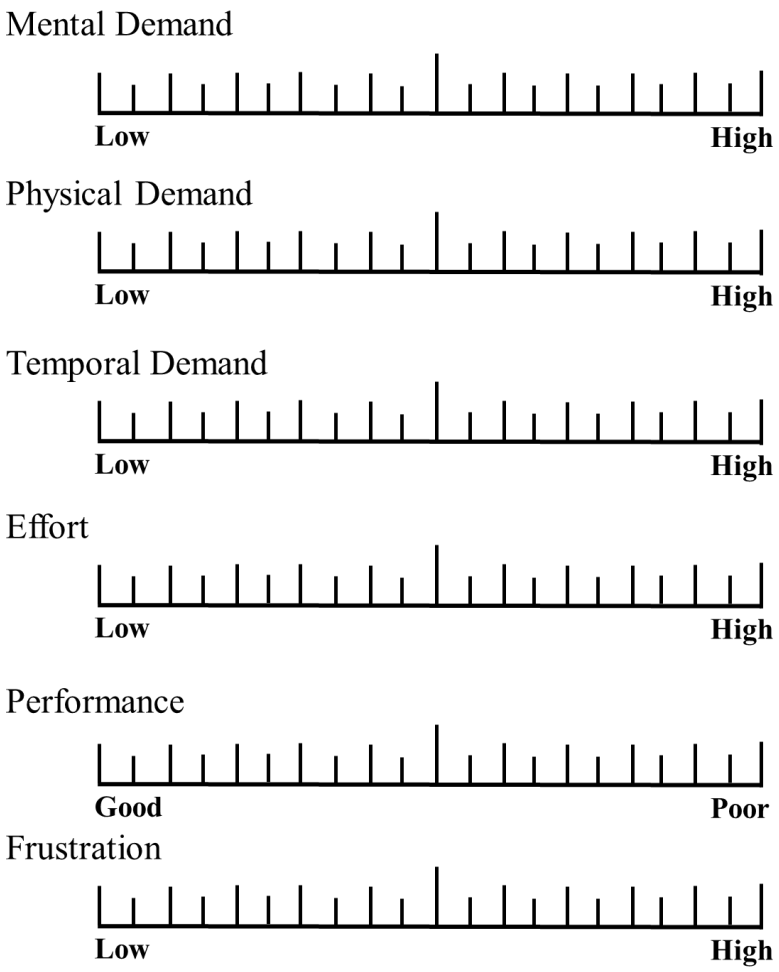

APPENDIX C

Post-Experiment Questions

1. How often do you play video games (via console, PC)?
   - ○ Very often (5-7 times a week)
   - ○ Fairly often (3-4 times a week)
   - ○ Often (1-2 times a week)
   - ○ Not very often (1-2 times a month)
   - ○ Almost never (Less than 1 time per month)
   - ○ Never

2. Gender
   - ○ Male
   - ○ Female
   - ○ Non-binary
   - ○ Prefer to self-describe:_____

3. Age
   _____

4. What do you think this experiment was testing?
   _____

5. Was there anything in particular you really liked or disliked about this experiment?
   _____

6. Do you have any other questions/comments?
   _____

APPENDIX D

Virtual Driving Courses

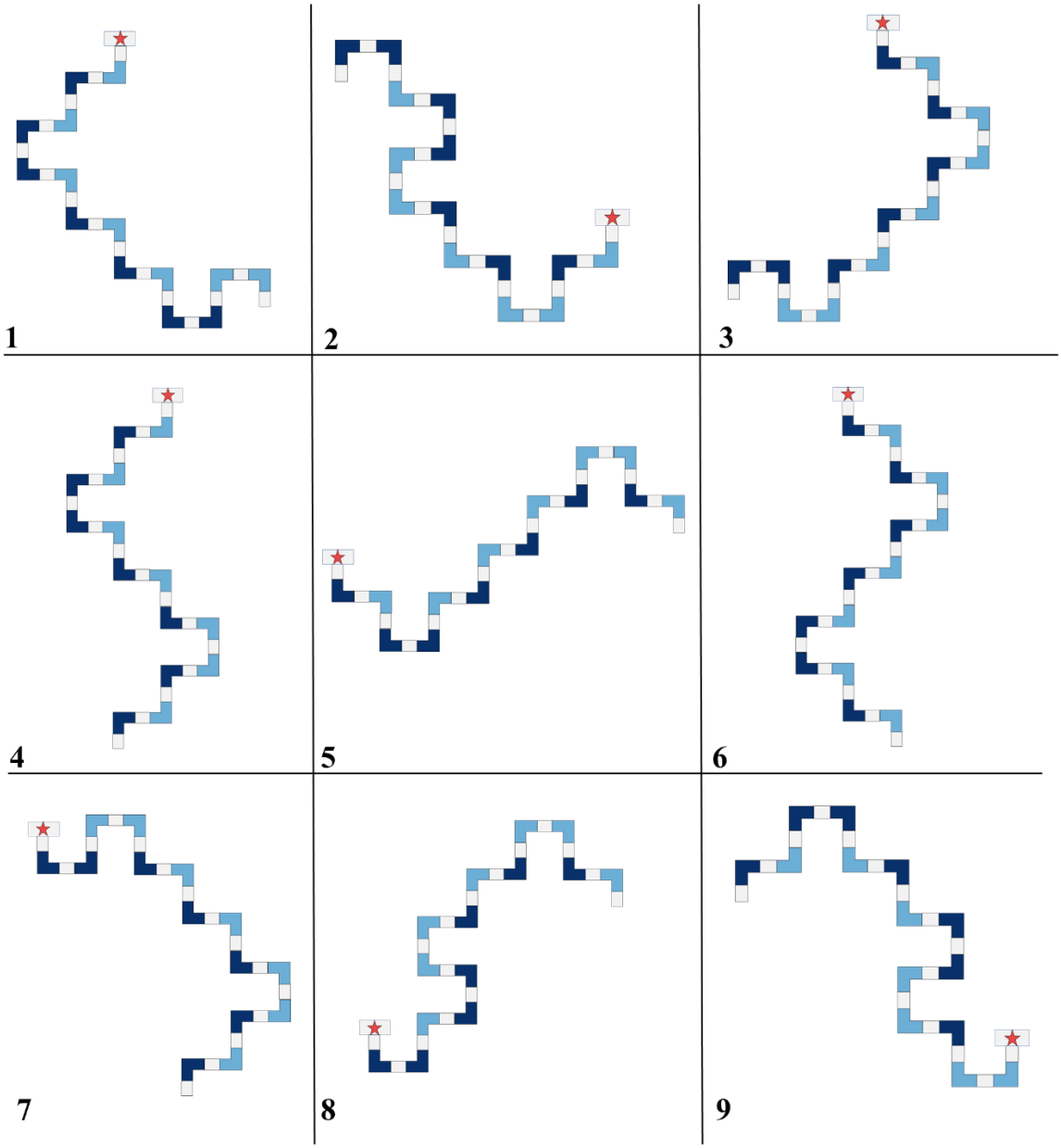

Note: Light blue corners correspond to left turns, and dark blue corners correspond to right turns. The star represents the end of the driving course where the virtual alarm system was located.

REFERENCES

Agresti, A. (2018). An introduction to categorical data analysis. John Wiley & Sons.

Ambrose, R. O., Aldridge, H., Askew, R. S., Burridge, R. R., Bluethmann, W., Diftler, M., Lovchik, C., Magruder, D., & Rehnmark, F. (2000). Robonaut: NASA's space humanoid. *IEEE Intelligent Systems and Their Applications*, *15*(4), 57–63. https://doi.org/10.1109/5254.867913

Armstrong, M. E., Jones, K. S., & Schmidlin, E. A. (2014). Tele-operation training: The effect of exploration on driveability judgments. *Proceedings of the Human Factors and Ergonomics Society Annual Meeting*, *58*(1), 1676–1680. https://doi.org/10.1177/1541931214581350

Armstrong, M. E., Jones, K. S., & Schmidlin, E. A. (2015). Tele-operating USAR robots: Does driving performance increase with aperture width or practice? *Proceedings of the Human Factors and Ergonomics Society Annual Meeting*, *59*(1), 1372–1376. https://doi.org/10.1177/1541931215591229

Babu, S., Tsai, M.-H., Hsu, T.-W., & Chuang, J.-H. (2020). An evaluation of the efficiency of popular personal space pointing versus controller based spatial selection in VR. *ACM Symposium on Applied Perception 2020*, 1–10. https://doi.org/10.1145/3385955.3407939

Banton, T., Stefanucci, J., Durgin, F., Fass, A., & Proffitt, D. (2005). The perception of walking speed in a virtual environment. *Presence: Teleoperators and Virtual Environments*, *14*(4), 394–406. https://doi.org/10.1162/105474605774785262

Barton, K. (2009). MuMIn: multi-model inference. R package version 1. 0. 0. *http://r-forge. r-project. org/projects/mumin/*.

Bateman, S., Doucette, A., Xiao, R., Gutwin, C., Mandryk, R. L., & Cockburn, A. (2011, May). Effects of view, input device, and track width on video game driving. In *Graphics Interface, 2011*, 207-214.

Beer, J. M., Fisk, A. D., & Rogers, W. A. (2014). Toward a framework for levels of robot autonomy in human-robot interaction. *Journal of Human-Robot Interaction*, *3*(2), 74. https://doi.org/10.5898/JHRI.3.2.Beer

Bengel, M., Pfeiffer, K., Graf, B., Bubeck, A., & Verl, A. (2009, October). Mobile robots for offshore inspection and manipulation. In *2009 IEEE/RSJ International Conference on Intelligent Robots and Systems* (pp. 3317-3322). IEEE.

Bhargava, A., Solini, H., Lucaites, K., Bertrand, J. W., Robb, A., Pagano, C. C., & Babu, S. V. (2020, March). Comparative evaluation of viewing and self-representation on passability affordances to a realistic sliding doorway in real and immersive virtual environments. In *2020 IEEE Conference on Virtual Reality and 3D User Interfaces (VR)* (pp. 519-528). IEEE.

Bingham, G. P., & Pagano, C. C. (1998). The necessity of a perception-action approach to definite distance perception: monocular distance perception to guide reaching. *Journal of Experimental Psychology: Human Perception and Performance*, *24*(1), 24.

Blau, J. J., & Wagman, J. B. (2022). *Introduction to Ecological Psychology: A lawful approach to perceiving, acting, and cognizing*. New York: Routledge.

Bouloubasis, A., McKee, G., & Tolson, P. (2007). Novel concepts for a planetary surface exploration rover. *Industrial Robot: An International Journal*, *34*(2), 116–121. https://doi.org/10.1108/01439910710727450

Box, G. E., & Cox, D. R. (1964). An analysis of transformations. *Journal of the Royal Statistical Society: Series B (Methodological)*, *26*(2), 211-243.

Brickler, D., Teather, R. J., Duchowski, A. T., & Babu, S. V. (2020). A Fitts' law evaluation of visuo-haptic fidelity and sensory mismatch on user performance in a near-field disc transfer task in Virtual Reality. *ACM Transactions on Applied Perception*, *17*(4), 1–20. https://doi.org/10.1145/3419986

Bruemmer, D. J., Few, D. A., Boring, R. L., Marble, J. L., Walton, M. C., & Nielsen, C. W. (2005). Shared understanding for collaborative control. *IEEE Transactions on Systems, Man, and Cybernetics - Part A: Systems and Humans*, *35*(4), 494–504. https://doi.org/10.1109/TSMCA.2005.850599

Casper, J. L., Micire, M., & Murphy, R. R. (2000, July). Issues in intelligent robots for search and rescue. In *Unmanned ground vehicle technology II* (Vol. 4024, pp. 292-302). International Society for Optics and Photonics.

Casper, J., & Murphy, R. R. (2003). Human-robot interactions during the robot-assisted urban search and rescue response at the World Trade Center. *IEEE Transactions on Systems, Man, and Cybernetics, Part B (Cybernetics)*, *33*(3), 367–385. https://doi.org/10.1109/TSMCB.2003.811794

Chan, A. H. S., Hoffmann, E. R., & Ho, J. C. H. (2019). Movement time and guidance accuracy in teleoperation of robotic vehicles. *Ergonomics*, *62*(5), 706–720. https://doi.org/10.1080/00140139.2019.1571246

Chen, J. Y. C., Haas, E. C., & Barnes, M. J. (2007). Human performance issues and user interface design for teleoperated robots. *IEEE Transactions on Systems, Man and Cybernetics, Part C (Applications and Reviews)*, *37*(6), 1231–1245. https://doi.org/10.1109/TSMCC.2007.905819

Cross, M., McIsaac, K. A., Dudley, B., & Choi, W. (2018). Negotiating corners with teleoperated mobile robots with time delay. *IEEE Transactions on Human-Machine Systems*, *48*(6), 682–690. https://doi.org/10.1109/THMS.2018.2849024

Day, B., Ebrahimi, E., Hartman, L. S., Pagano, C. C., & Babu, S. V. (2017). Calibration to tool use during visually-guided reaching. *Acta Psychologica*, *181*, 27–39. https://doi.org/10.1016/j.actpsy.2017.09.014

Dede, M., & Tosunoglu, S. (2006). Fault-tolerant teleoperation systems design. *Industrial Robot: An International Journal*, *33*(5), 365–372. https://doi.org/10.1108/01439910610685034

Di Paola, D., Milella, A., Cicirelli, G., & Distante, A. (2010). An autonomous mobile robotic system for surveillance of indoor environments. *International Journal of Advanced Robotic Systems*, *7*(1), 8. https://doi.org/10.5772/7254

Duchon, A. P., & Warren, W. H. (2002). A visual equalization strategy for locomotor control: Of honeybees, robots, and humans. *Psychological Science*, *13*(3), 272–278. https://doi.org/10.1111/1467-9280.00450

Dye, M. W., Green, C. S., & Bavelier, D. (2009). Increasing speed of processing with action video games. *Current directions in psychological science*, *18*(6), 321-326.

Fajen, B. R. (2007). Affordance-based control of visually guided action. *Ecological Psychology*, *19*(4), 383-410.

Fajen, B., & Warren, W. (2003). Behavioral dynamics of steering, obstacle avoidance, and route selection. *Journal of Experimental Psychology: Human Perception and Performance*, *29*(2), 343–362. https://doi.org/10.1167/1.3.184

Gao, Y., & Chien, S. (2017). Review on space robotics: Towards top-level science through space exploration. *Science Robotics*, *2*(7), 19.

Geuss, M. N., Stefanucci, J. K., Creem-Regehr, S. H., & Thompson, W. B. (2012). Effect of viewing plane on perceived distances in real and virtual environments. *Journal of Experimental Psychology: Human Perception and Performance*, *38*(5), 1242–1253. https://doi.org/10.1037/a0027524

Gibson, E. J. (1969). *Principles of perceptual learning and development*. Appleton-Century-Crofts.

Gibson, J. J. (1958). Visually controlled locomotion and visual orientation in animals*. *British Journal of Psychology*, *49*(3), 182–194. https://doi.org/10.1111/j.2044-8295.1958.tb00656.x

Gibson, J. J. (1979). *The ecological approach to visual perception*. Houghton Mifflin.

Gibson, J. J., & Gibson, E. J. (1995). Perceptual learning: Differentiation or enrichment? *Psychological Review*, *62*(1), 32–41.

Gomer, J. A., Dash, C. H., Moore, K. S., & Pagano, C. C. (2009). Using radial outflow to provide depth information during teleoperation. *Presence: Teleoperators and Virtual Environments*, *18*(4), 304–320. https://doi.org/10.1162/pres.18.4.304

Green, P., & MacLeod, C. J. (2016). SIMR: An R package for power analysis of generalized linear mixed models by simulation. *Methods in Ecology and Evolution*, *7*(4), 493–498. https://doi.org/10.1111/2041-210X.12504

Hart, S. G., & Staveland, L. E. (1988). Development of NASA-TLX (Task Load Index): Results of empirical and theoretical research. In *Advances in Psychology* (Vol. 52, pp. 139–183). Elsevier. https://doi.org/10.1016/S0166-4115(08)62386-9

Helton, W. S., Head, J., & Blaschke, B. A. (2014). Cornering law: The difficulty of negotiating corners with an unmanned ground vehicle. *Human Factors: The Journal of the Human Factors and Ergonomics Society*, *56*(2), 392–402. https://doi.org/10.1177/0018720813490952

Hofmann, D. A. (1997). An overview of the logic and rationale of hierarchical linear models. *Journal of management*, *23*(6), 723-744.

Interrante, V., Ries, B., & Anderson, L. (2006). Distance perception in immersive virtual environments, revisited. *IEEE Virtual Reality Conference (VR 2006)*, 3–10. https://doi.org/10.1109/VR.2006.52

Katrasnik, J., Pernus, F., & Likar, B. (2010). A survey of mobile robots for distribution power line inspection. *IEEE Transactions on Power Delivery*, *25*(1), 485–493. https://doi.org/10.1109/TPWRD.2009.2035427

Kelly, J. W., Donaldson, L. S., Sjolund, L. A., & Freiberg, J. B. (2013). More than just perception–action recalibration: Walking through a virtual environment causes rescaling of perceived space. *Attention, Perception, & Psychophysics*, *75*(7), 1473–1485. https://doi.org/10.3758/s13414-013-0503-4

Kelly, J. W., Hammel, W. W., Siegel, Z. D., & Sjolund, L. A. (2014). Recalibration of perceived distance in virtual environments occurs rapidly and transfers asymmetrically across scale. *IEEE Transactions on Visualization and Computer Graphics*, *20*(4), 588–595. https://doi.org/10.1109/TVCG.2014.36

Knief, U., & Forstmeier, W. (2021). Violating the normality assumption may be the lesser of two evils. *Behavior Research Methods, 53*(6), 2576-2590

Komsta, L., & Novomestky, F. (2015). Moments, cumulants, skewness, kurtosis and related tests. *R package version, 14*.

Lathan, C. E., & Tracey, M. (2002). The effects of operator spatial perception and sensory feedback on human-robot teleoperation performance. *Presence*, *11*(4), 368-377.

Lee, David N, Bootsma, R. J., Land, M., Regan, D., & Gray, R. (2009). Lee's 1976 paper. *Perception*, *38*(6), 837–858. https://doi.org/10.1068/pmklee

Lee, David N., & Reddish, P. E. (1981). Plummeting gannets: A paradigm of ecological optics. *Nature*, *293*(5830), 293–294. https://doi.org/10.1038/293293a0

Lee, D.N. (1976). A theory of visual control of braking based on information about time-to-collision. *Perception*, *5*(4), 437–459.

Long, L., Gomer, J., Wong, J., & Pagano, C. (2011). Visual spatial abilities in uninhabited ground vehicle task performance during teleoperation and direct line of sight. *Presence Teleoperators & Virtual Environments*, *20*, 466–479.

Loomis, J. M., & Knapp, J. M. (2003). Visual perception of egocentric distance in real and virtual environments. In *Virtual and Adaptive Environments: Applications, Implications, and Human Performance Issues* (Vol. 11, pp. 21–46).

Low, S. C., & Phee, L. (2006). A review of master–slave robotic systems for surgery. *International Journal of Humanoid Robotics*, *3*(04), 547-567.

Lucaites, K., (2021). Visually guided action for the person-plus-object system: Generalizing the optic flow equalization control law to asymmetrical bodies. *All Dissertations*. 2796. https://tigerprints.clemson.edu/all_dissertations/2796

Lucaites, K. M., Venkatakrishnan, R., Venkatakrishnan, R., Bhargava, A., & Pagano, C. C. (2020). Predictability and variability of a dynamic environment impact affordance judgments. *Ecological Psychology*, *32*(2–3), 95–114. https://doi.org/10.1080/10407413.2020.1741323

Luk, B. L., Cooke, D. S., Galt, S., Collie, A. A., & Chen, S. (2005). Intelligent legged climbing service robot for remote maintenance applications in hazardous environments. *Robotics and Autonomous Systems*, *53*(2), 142–152. https://doi.org/10.1016/j.robot.2005.06.004

MacKenzie, I. S., & Isokoski, P. (2008). Fitts' throughput and the speed-accuracy tradeoff. *Proceeding of the Twenty-Sixth Annual CHI Conference on Human*

Factors in Computing Systems - CHI '08, 1633. https://doi.org/10.1145/1357054.1357308

Mantel, B., Hoppenot, P., & Colle, E. (2012). Perceiving for acting with teleoperated robots: Ecological principles to human–robot interaction design. *IEEE Transactions on Systems, Man, and Cybernetics - Part A: Systems and Humans*, *42*(6), 1460–1475. https://doi.org/10.1109/TSMCA.2012.2190400

Marble, J. L., Bruemmer, D. J., & Few, D. A. (2003). Lessons learned from usability tests with a collaborative cognitive workspace for human-robot teams. *SMC'03 Conference Proceedings. 2003 IEEE International Conference on Systems, Man and Cybernetics. Conference Theme - System Security and Assurance (Cat. No.03CH37483), 1*, 448–453 vol.1. https://doi.org/10.1109/ICSMC.2003.1243856

Milella, A., Cicirelli, G., & Distante, A. (2008). RFID-assisted mobile robot system for mapping and surveillance of indoor environments. *Industrial Robot: An International Journal*, *35*(2), 143–152. https://doi.org/10.1108/01439910810854638

Milgram, P., Rastogi, A., & Grodski, J. J. (1995). Telerobotic control using augmented reality. *Proceedings 4th IEEE International Workshop on Robot and Human Communication*, 21–29. https://doi.org/10.1109/ROMAN.1995.531930

Moore, S., Gomer, J. A., Pagano, C. C., & Moore, D. D. (2009). Perception of robot passability with direct line of sight and teleoperation. *Human Factors: The Journal of the Human Factors and Ergonomics Society*, *51*(4), 557–570. https://doi.org/10.1177/0018720809341959

Moore, K.S., & Pagano, C. C. (2006). *Can humans perceive affordances for teleoperated robots* [Poster]. The North American Meeting of the International Society for Ecological Psychology.

Murphy, R. R. (2004). Human–robot interaction in rescue robotics. *IEEE Transactions on Systems, Man and Cybernetics, Part C (Applications and Reviews)*, *34*(2), 138–153. https://doi.org/10.1109/TSMCC.2004.826267

Nenna, F., & Gamberini, L. (2022, March). The influence of gaming experience, gender and other individual factors on robot teleoperations in VR. *Proceedings of the 2022 ACM/IEEE International Conference on Human-Robot Interaction,* 945-949.

Osborne, J. W. (2000). Advantages of hierarchical linear modeling. *Practical Assessment, Research, and Evaluation, 7*(1), 1.

Pastel, R. (2006). Measuring the difficulty of steering through corners. *Proceedings of the SIGCHI Conference on Human Factors in Computing Systems - CHI '06*, 1087. https://doi.org/10.1145/1124772.1124934

Pastel, R., Champlin, J., Harper, M., Paul, N., Helton, W., Schedlbauer, M., & Heines, J. (2007). The difficulty of remotely negotiating corners. *Proceedings of the Human Factors and Ergonomics Society Annual Meeting*, 489–493.

Rahmaniar, W., & Wicaksono, A. (2020). Design and implementation of a mobile robot for carbon monoxide monitoring. *Journal of Robotics and Control (JRC)*, *2*(1). https://doi.org/10.18196/jrc.2143

Raudenbush, S. W., & Bryk, A. S. (1992). *Hierarchical linear models: Applications and data analysis methods*. Sage Publications, Inc.

Sabater, J. M., Saltarén, R. J., Aracil, R., Yime, E., & Azorín, J. M. (2006). Teleoperated parallel climbing robots in nuclear installations. *Industrial Robot: An International Journal*, *33*(5), 381–386. https://doi.org/10.1108/01439910610685052

Sahm, C. S., Creem-Regehr, S. H., Thompson, W. B., & Willemsen, P. (2005). Throwing versus walking as indicators of distance perception in similar real and virtual environments. *ACM Transactions on Applied Perception*, *2*(1), 35–45. https://doi.org/10.1145/1048687.1048690

Sanders, D. (2009). Comparing speed to complete progressively more difficult mobile robot paths between human tele-operators and humans with sensor-systems to assist. *Assembly Automation*, *29*(3), 230–248. https://doi.org/10.1108/01445150910972912

Schmidlin, E. A., & Jones, K. S. (2016). Do tele-operators learn to better judge whether a robot can pass through an aperture? *Human Factors: The Journal of the Human Factors and Ergonomics Society*, *58*(2), 360–369. https://doi.org/10.1177/0018720815617849

Schmidt, A. F., & Finan, C. (2018). Linear regression and the normality assumption. *Journal of clinical epidemiology*, *98*, 146-151.

Shah, B., & Choset, H. (2004). Survey on urban search and rescue robots. *Journal of the Robotics Society of Japan*, *22*(5), 582–586.

Shao, S., Zhou, Q., & Liu, Z. (2021). Study of mental workload imposed by different tasks based on teleoperation. *International Journal of Occupational Safety and Ergonomics*, *27*(4), 979-989.

Shaw, R. E., Flascher, O. M., & Kadar, E. E. (1995). Dimensionless invariants for intentional systems: Measuring the fit of vehicular activities to environmental layout,. In J. M. Flach, P. A. Hancock, J. Caird, & K. J. Vicente (Eds.), *Global Perspectives on the Ecology of Human–Machine Systems* (pp. 293–358). LEA.

Shin, J., Zhong, Y., & Gu, C. (2017). Master-slave robotic system for needle indentation and insertion. *Computer Assisted Surgery*, *22*(sup1), 100–105. https://doi.org/10.1080/24699322.2017.1379236

Solini, H., & Andre, J. (2020). Time-to-arrival estimations to simulated pedestrians. *Accident Analysis & Prevention*, *146*, 105739. https://doi.org/10.1016/j.aap.2020.105739

Solini, H. M., Bhargava, A., & Pagano, C. C. (2021). The effects of testing environment, experimental design, and ankle loading on calibration to perturbed optic flow during locomotion. *Attention, Perception, & Psychophysics*, *83*(1), 497-511.

Srinivasan, M. V., Lehrer, M., Kirchner, W. H., & Zhang, S. W. (1991). Range perception through apparent image speed in freely flying honeybees. *Visual Neuroscience*, *6*(5), 519–535. https://doi.org/10.1017/S095252380000136X

Thomas, L. C., & Wickens, C. D. (2001). Visual displays and cognitive tunneling: Frames of reference effects on spatial judgments and change detection.

Proceedings of the Human Factors and Ergonomics Society Annual Meeting, *45*(4), 336–340. https://doi.org/10.1177/154193120104500415

Thompson, W. B., Creem-Regehr, S., Pick, H. L., Warren, W., Rieser, J. J., & Willemsen, P. (2004). Visual motion influences locomotion in a treadmill virtual environment. *Proceedings of the 1st Symposium on Applied Perception in Graphics and Visualization - APGV '04*, 19. https://doi.org/10.1145/1012551.1012554

Thrun, S. (2004). Toward a framework for human-robot interaction. *Human-Computer Interaction*, *19*(1–2), 9–24.

Tittle, J. S., Roesler, A., & Woods, D. D. (2002). The remote perception problem. *Proceedings of the Human Factors and Ergonomics Society Annual Meeting*, *46*(3), 260–264. https://doi.org/10.1177/154193120204600309

Tresilian, J. R. (1999). Visually timed action: Time-out for "tau"? *Trends in Cognitive Sciences*, *3*(8), 301–310.

Warren, W. H. (1988). Chapter 14 action modes and laws of control for the visual guidance of action. In *Advances in Psychology* (Vol. 50, pp. 339–379). Elsevier. https://doi.org/10.1016/S0166-4115(08)62564-9

Warren, W. H., & Whang, S. (1987). Visual guidance of walking through apertures: Body-scaled information for affordances. *Journal of Experimental Psychology: Human Perception and Performance*, *13*(7), 371–383. Withagen, R., & Michaels, C. F. (2005). The role of feedback information for calibration and attunement in

perceiving length by dynamic touch. *Journal of Experimental Psychology: Human Perception and Performance*, *31*(6), 1379.

Witmer, B. G., & Kline, P. B. (1998). Judging perceived and traversed distance in virtual environments. *Presence: Teleoperators and Virtual Environments, 7*(2), 144–167. https://doi.org/10.1162/105474698565640

Witmer, B. G., & Sadowski, W. J. (1998). Nonvisually guided locomotion to a previously viewed target in real and virtual environments. *Human Factors: The Journal of the Human Factors and Ergonomics Society*, *40*(3), 478–488. https://doi.org/10.1518/001872098779591340

Woltman, H., Feldstain, A., MacKay, J. C., & Rocchi, M. (2012). An introduction to hierarchical linear modeling. *Tutorials in Quantitative Methods for Psychology*, *8*(1), 52–69. https://doi.org/10.20982/tqmp.08.1.p052

Wynn, M. L., Clemente, C., Nasir, A. F. A. A., & Wilson, R. S. (2015). Running faster causes disaster: trade-offs between speed, manoeuvrability and motor control when running around corners in northern quolls (Dasyurus hallucatus). *Journal of Experimental Biology*, *218*(3), 433-439.